The Phenomenology of Beyond the Standard Model Scalars due to Extended Symmetries with New Fermions

By

SOUMYA SADHUKHAN

PHYS10201005007

The Institute of Mathematical Sciences, Chennai

A thesis submitted to the

Board of Studies in Physical Sciences

In partial fulfilment of requirements

For the Degree of

DOCTOR OF PHILOSOPHY

of

HOMI BHABHA NATIONAL INSTITUTE

October, 2016

Homi Bhabha National Institute

Recommendations of the Viva Voce Board

As members of the Viva Voce Board, we certify that we have read the dissertation prepared by **Soumya Sadhukhan** entitled **"The Phenomenology of Beyond the Standard Model Scalars due to Extended Symmetries with New Fermions"** and recommend that it maybe accepted as fulfilling the dissertation requirement for the Degree of Doctor of Philosophy.

_____ Date:

Guide - Prof. Shrihari Gopalakrishna

_____ Date:

Chairman - Prof. V. Ravindran

_____ Date:

Member 1 - Prof. Rahul Sinha

_____ Date:

Member 2 - Prof. Balachandran Sathiapalan

_____ Date:

External examiner - Prof. Sudhir Vempati

Final approval and acceptance of this dissertation is contingent upon the candidate's submission of the final copies of the dissertation to HBNI.

I hereby certify that I have read this dissertation prepared under my direction and recommend that it may be accepted as fulfilling the dissertation requirement.

Date: Guide: _____

Place: (Prof. Shrihari Gopalakrishna)

STATEMENT BY AUTHOR

This dissertation has been submitted in partial fulfillment of requirements for an advanced degree at Homi Bhabha National Institute (HBNI) and is deposited in the Library to be made available to borrowers under rules of the HBNI.

Brief quotations from this dissertation are allowable without special permission, provided that accurate acknowledgement of source is made. Requests for permission for extended quotation from or reproduction of this manuscript in whole or in part may be granted by the Competent Authority of HBNI when in his or her judgment the proposed use of the material is in the interests of scholarship. In all other instances, however, permission must be obtained from the author.

Soumya Sadhukhan

DECLARATION

I, hereby declare that the investigation presented in the thesis has been carried out by me. The work is original and has not been submitted earlier as a whole or in part for a degree/diploma at this or any other Institute/University.

Soumya Sadhukhan

ACKNOWLEDGEMENTS

First of all I would like to thank my supervisor Dr. Shrihari Gopalakrishna for his guidance and constant help throughout the rigorous journey of my Ph.D. He introduced me to the area of beyond the Standard Model and the LHC phenomenology, and is extraordinarily patient in explaining every detail of many physics/non-physics issue. He has always tried to make me as independent as possible in research and I am fortunate to have such a nice person as my Ph.D. guide.

I would like to thank my collaborator and friend Dr. Sayantan Choudhury for innumerous academic discussions. I am also thankful to my collaborator and friend Dr. Rahul Srivastava for his help in learning various topics of particle physics and his guidance to proceed in various research projects. I would like to convey my thanks to my collaborators Dr. Tanmoy Modak and Manibrata Sen. I am thankful to Prof. Rahul Sinha, Prof. V. Ravindran, Prof. Romesh Kaul and other faculties in high energy physics at IMSc for teaching me beautiful courses and helping me with academic discussion on different topics.

I express my deepest gratitude to my parents and family for their unconditional love and affection. Without them it would have never been possible for me to become what I am today and to them I owe a debt that can never be repaid.

Finally I thank IMSc for providing me with financial support and an excellent working environment during the whole period of my Ph.D. work.

My Publications

The thesis is based on the papers marked with "$*$" .

Published and on the arXiv

1. **CP-odd scalar with vector-like fermions at the LHC.**

   Shrihari Gopalakrishna, Tuhin Subhra Mukherjee, Soumya Sadhukhan.

   Physical Review D 93, no. 5, 055004 (2016)

   arXiv:1504.01074 [hep-ph]

2. $*$ **Status and Prospects of the Two-Higgs-Doublet SU(6)/Sp(6) little-Higgs Model and the Alignment Limit.**

   Shrihari Gopalakrishna, Tuhin Subhra Mukherjee, Soumya Sadhukhan.

   Physical Review D 94, no.1, 015034 (2016)

   arXiv:1512.05731 [hep-ph]

3. $*$ 750 **GeV Diphoton excess from Gauged** $B - L$ **Symmetry.**

   Tanmoy Modak, Soumya Sadhukhan and Rahul Srivastava.

   Physical Letters B 756, 405-412 (2016).

   arXiv:1601.00836 [hep-ph].

4. **Can Dark Matter be an artifact of extended theories of gravity?**

   Sayantan Choudhury, Manibrata Sen and Soumya Sadhukhan.

   European Physical Journal C 76, no.9, 494 (2016)

   arXiv:1512.08176 [hep-ph]

5. **Collider constraints on Gauss-Bonnet coupling in warped geometry model.**

Sayantan Choudhury, Soumya Sadhukhan and Soumitra SenGupta,

arXiv:1308.1477 [hep-ph]

Communicated to Journal.

Conference proceedings

6. **Warped Extra Dimensional Benchmarks for Snowmass 2013.**

   Kaustubh Agashe *et. al.* (Snowmass 2013 Proceedings)

   arXiv:1309.7847 [hep-ph].

7. **From Extended theories of Gravity to Dark Matter.**

   Sayantan Choudhury, Manibrata Sen and Soumya Sadhukhan,

   Conference: C16-02-14

   arXiv:1605.04043 [hep-ph]

Contents

List of Figures

List of Tables

Chapter 1

Introduction

The Standard Model (SM) of particle physics is a very successful theory in describing the physics of elementary particles. All the experimental results so far indicate that the SM is the consistent effective theory of elementary particles for energies up to a few hundred GeV scale. All the fundamental particles predicted by the SM including the Higgs boson have been found in different experiments. A significant development is that the Large Hadron Collider (LHC) at CERN has announced the discovery [1, 2] of the Higgs at a mass around 125 GeV. The couplings of the scalar observed at the LHC are also measured to be consistent with those of the SM Higgs. However, despite the excellent agreement with experiments, there are some shortcomings that cannot be addressed within the SM.

The gauge hierarchy problem is one of the main theoretical problems that the SM cannot address. The fundamental Planck scale ($M_{Pl} \sim 10^{19}$ GeV) is 16 orders of magnitude larger than the scale of electroweak symmetry breaking (EWSB) ($\sim 10^3$ GeV). If the SM is valid up to the Planck scale, a severe fine-tuning is necessary in order to keep the Higgs mass light in the presence of quantum corrections. This is elaborated upon next. The renormalized physical Higgs mass (m_h) is given by

$$m_h^2 = m_0^2 + \delta m_h^2, \tag{1.1}$$

where m_0 is the bare Higgs mass. The quantity δm_h^2 is the one-loop Higgs self energy

correction with the dominant contribution coming from the top loop which can be expressed as $\delta m_h^2 = ({y_t}^2/16\pi^2)\Lambda^2$; where y_t (~ 1) is the top Yukawa coupling and Λ is the cut-off scale. The quadratically divergent quantum correction to the Higgs mass lifts it to the largest scale in the theory making the Higgs mass of the order of the cut-off scale. One statement of the naturalness principle [3] is that the quantum correction of a quantity should be of the same order as (or smaller than) its tree level value, for that quantity to be natural. When the quantum correction is much larger than the tree level value, the bare value and the quantum correction will have to have an unexpectedly precise cancellation to give a result that is much smaller than either components. This will make the scalar mass unnatural, as for instance is the case for the Higgs boson which was discovered at the LHC at a relatively light mass of around 125 GeV. In order to keep the physical Higgs mass (m_h) at the scale of the observed particle, an enormous amount of fine-tuning (cancellation up to 30 decimal places for a cut-off scale $\Lambda \sim M_{Pl}$) between the bare Higgs mass and Higgs self energy corrections is required. This unusual "fine-tuning" is not addressed in the SM. The requirement of $\delta m_h^2 \sim m_h^2$, for the electroweak theory to be natural, leads to the cut-off scale of the theory around one TeV. If a fine tuning is to be avoided, some new physics has to be present near the TeV scale. This is one of the main motivations to extend the SM around the TeV scale. A detailed discussion on naturalness and the appearance of new physics at the TeV scale can be found in Ref. [4, 5].

In addition to the gauge hierarchy problem, the SM also cannot explain the large hierarchy of fermion masses. For instance, the mass of a top quark (≈ 173 GeV) is 6 and 12 orders of magnitude larger than the mass of an electron (≈ 0.5 MeV) and the mass of neutrinos ($\approx 1eV$) respectively. Although this flavor hierarchy is technically natural [3], it still leaves a question on whether there is some underlying physics that sets the disparate masses of the SM fermions.

In addition to the above theoretical arguments for BSM physics, there are some observed facts such as the nonzero neutrino mass, existence of dark matter and baryon asymmetry of the universe that strongly indicate that one may have to go beyond the SM

to explain them. These are discussed briefly below.

Neutrino mass: The nature of neutrinos is not very well understood. Whether neutrinos are of Dirac (particle and anti-particle are different) or Majorana (anti-particle is same as the particle) type, may be resolved from the neutrinoless double beta decay experiments. No sign of neutrinoless double beta decay is observed yet. So, still there is a possibility of neutrinos being either Dirac or Majorana types. Neutrinos are also massless in the SM as constructed earlier. However, neutrino oscillation experiments have shown that neutrinos do have mass. Neutrino mass can be generated in different ways. One of the simplest ways to generate a Dirac neutrino mass is by adding BSM right handed neutrinos to the SM, which can lead to the requirement of extraordinary small Yukawa couplings to provide a small mass to neutrinos, which is of the order of eV. For Majorana type neutrinos, the simplest way to generate a tiny mass term is through a seesaw mechanism [6], adding a heavy Majorana neutrino to the SM. A BSM theory where a tiny Dirac neutrino mass is possible is discussed in this thesis.

Dark matter: Although dark matter is not observed directly, there is evidence from its gravitational effects on visible matter and radiation such as the rotation curves of galaxies, gravitational lensing of background radiation and baryon acoustic oscillation experiments. These effects also have experimental evidence, which clearly suggest that dark matter exists. Many BSM models have been proposed to present a dark matter candidate. As an example, widely discussed models of dark matter are assumed to be composed of weakly interacting massive particles (WIMP). A WIMP with a mass around the TeV scale interacts with EW strength and can provide the correct relic abundance to account for the dark matter in the universe.

Baryon asymmetry: If the Big Bang had created equal amounts of matter and antimatter in the early universe, the baryon asymmetry of the Universe should be zero. Observations at the current time indicate that our universe is almost entirely made up of matter with very little anti-matter. To explain the observed matter-antimatter imbalance, large CP violating effects are required. The CP violation in the SM is orders of magnitude

too small to account for the observed baryon asymmetry [7].

Furthermore, the fact that the weak coupling constants for quarks and leptons are the same, flavor universality of quarks and leptons etc. could have origins in beyond the SM physics. In the last few decades, enormous effort has been made to construct and test the bigger theory which will address some of the unanswered questions of the SM. Supersymmetric (SUSY) theories, models with extra spatial dimension, dynamical models of EWSB such as technicolor, little-Higgs models etc. are some well-known examples of these BSM theories. Till now there is no concrete experimental evidence of the presence of BSM physics. In the recent past, an excess was reported by CMS and ATLAS in the $\gamma\gamma$ channel at the 13 TeV run of the LHC [8, 9]. It was a hint (confidence level $\sim 3\sigma$) of a new scalar resonance with a mass around 750 GeV. As more LHC data was analyzed and reported at the ICHEP conference [10, 11], the diphoton excess appears to have been a statistical fluctuation.

The focus of this PhD work is to explore some of the BSM models which have larger symmetries than the SM to provide solutions to some of the problems stated above. These models have bigger gauge or global symmetries which are usually broken at a higher scale and broken explicitly by a small amount to retain the SM symmetries at the TeV scale. Another feature of many of these BSM models is the presence of new heavy scalars apart from the 125 GeV Higgs. These extra scalars can come as $SU(2)$ singlets, doublets in a way similar to the two Higgs Doublet model (2HDM) and even as triplets. To either address gauge hierarchy or neutrino mass generation issues of the SM, the models with extended symmetry also require extra new fermions to be present. The main focus of this thesis is to study the LHC phenomenology of such heavy scalars in two types of models with extended symmetries namely the $SU(6)/Sp(6)$ little-Higgs model and the gauged $U(1)_{B-L}$ model, based on Ref. [12] and Ref. [13] respectively.

The little-Higgs models are one class of the BSM theories which address the hierarchy problem as the Higgs mass does not receive any quadratically divergent correction at one loop. In these models, the Higgs boson and the new scalars are pseudo Nambu-Goldstone

bosons. The 2HDM like structure is present in a number of little-Higgs models at the TeV scale. The $SU(6)/Sp(6)$ little-Higgs model is one such example, which manifest a 2HDM structure along with one extra complex scalar and BSM gauge bosons. The extra fermions are required in these models to cancel the quadratic divergence at one-loop. It is interesting to study the phenomenology of the BSM scalars at the LHC, quantifying the effects of BSM fermions on those heavy scalars.

Previously, the probable observation of an excess at the $\gamma\gamma$ channel with mass around 750 GeV, hinted at the presence of a BSM scalar. Although it is not observed in further searches,our study can be useful in searching for a BSM scalar in the diphoton channel, and can aid future searches at the LHC. Another model with its symmetry extended beyond the SM by a $U(1)$ $B-L$ symmetry is also explored in this context. These models with an extra $U(1)_{B-L}$ can explain the smallness of the Dirac or Majorana neutrino mass and may present a scalar dark matter (DM) candidate with the help of a symmetry that stabilizes the DM, preventing its decay. This model also contains two additional BSM scalars; one of which is proposed to be a 750 GeV resonance. In this thesis, the LHC phenomenology of a heavy scalar is discussed in a gauged $B-L$ model, where Dirac mass terms for neutrinos are generated.

Some models with their symmetries extended beyond the SM include models with grand unified theory (GUT) [14–16], little-Higgs models [17–19], Left-Right symmetric models [20–22], 3-3-1 models [23–25], 3-3-1-1 model [26], models with SM gauge group extended by one abelian symmetry [27–30] etc. One part of this thesis is on studying the phenomenology of a BSM theory with an extended symmetry namely the $SU(6)/Sp(6)$ little-Higgs model, introduced in Ref. [31]. Various other little-Higgs models are also studied in the literature, where the symmetries are extended beyond the SM. A detailed description of different kinds of little-Higgs models can be obtained from Refs. [18, 19]. The littlest Higgs model, the simplest construction of the little-Higgs model family is described in Refs. [19, 32]. Various aspects of the littlest Higgs model with extra symmetry (T-parity) are discussed in Refs. [33, 34]. A littlest Higgs model with custodial symmetry

is described in Ref. [35]. Construction of several other little-Higgs models are described in Refs. [33, 36, 37]. The constraints and the compatibility of the little-Higgs models with the properties of the 125 GeV state observed at the LHC are discussed in Refs. [38–45]. Some other studies investigating phenomenological and collider aspects of different little-Higgs models are given in Refs. [46–48].

Another aim of the thesis is to study the phenomenology of a heavy ($\sim$ 750 GeV) BSM scalar in the gauged $B-L$ model discussed in Ref. [49, 50]. Different procedures of neutrino mass generation in the gauged $B-L$ model are described in Refs. [50–53]. Other phenomenological issues and collider signatures related to the gauged $B-L$ model are presented in Refs. [54–56].

This thesis is structured as follows. In Chapter 2 of the thesis, the Low-Skiba-Smith (LSS) model i.e. the $SU(6)/Sp(6)$ little-Higgs model is studied in detail along with a brief discussion on various little-Higgs models, which include the littlest Higgs model, minimal-moose model etc. The gauge and Yukawa sector of the LSS model are described, pointing out the presence of a 2HDM structure with VLFs there. In Chapter 3, the properties of the 2HDM scalar potential of the LSS model are studied. The parameter space of the LSS model after imposing the 8 TeV LHC constraints is also presented in this chapter. The production and decay modes of the neutral and charged BSM scalars of the LSS model are studied in detail.

It is shown in Chapter 4, how the gauged $B-L$ model where the SM is extended by one $U(1)$ $B-L$ symmetry, can generate the observed tiny neutrino mass and present a dark matter candidate. The new particles that are introduced in the model for neutrino mass generation, are also listed. In Chapter 5, one heavy scalar of the gauged $B-L$ model with mass of 750 GeV is chosen to be studied, following the earlier hint of a diphoton excess at the LHC. The phenomenology of that scalar is discussed, explaining the enhanced cross section of the scalar at the diphoton channel. Non-observation of any excess in the other channels and the decay width of the scalar are also discussed. In Chapter 6, all the main results of the thesis are summarized, providing a phenomenological overview of the models

with extended symmetries.

Chapter 2

Little-Higgs Models

After the observation of other SM particles in a long series of previous experiments, the Large Hadron Collider (LHC) discovery of the Higgs boson at a mass of about 125 GeV has finally confirmed the standard model (SM) to be the consistent description of particle physics up to the electroweak (EW) ($\sim$ TeV) scale. The quadratic divergent corrections to the Higgs mass drives the EW scale mass to very high values resulting in the hierarchy problem of the SM. This can be a hint that some new particles beyond the standard model (BSM) may be around the EW scale to cancel the one-loop divergences, making the Higgs mass naturally stable against quantum corrections at the TeV scale.

Among the probable candidates of BSM physics that make the small Higgs mass natural at the EW scale, there are models where the SM Higgs is a pseudo-Nambu-Goldstone boson (pNGB). In some of these models, pNGBs apart from the Goldstone bosons appear as extra physical scalars. Concrete realizations of this idea, for example, are in models of little-Higgs, composite-Higgs and extra dimensions (for reviews see Refs. [18,19,57,58]). In little-Higgs models, in addition to the CP-even Higgs boson, new CP-odd (A) and CP-even (H) scalars can be present. Those extra scalars are also pNGBs due to which their mass can be much lower than the cut-off scale. Also, extra heavy vector-like fermions (VLF) are usually introduced which, along with the SM fermions, complete some representation of a bigger gauge group containing $SU(2) \otimes U(1)$. Apart from solving the hierarchy problem,

little-Higgs models can provide interesting phenomenology of the new scalar and fermions that is to be explored in detail. In our work [12], the phenomenology of BSM particles is discussed in the $SU(6)/Sp(6)$ little-Higgs model.

This chapter is organized as follows: In the first section, different little-Higgs models which contain extra scalars and fermions due to the extended symmetry of the theory, are described. In these little-Higgs models, the BSM scalars come as part of an extra scalar doublet like the 2HDM. Some new fermions are also required, which are usually taken as vector-like fermions. Therefore, to have a better understanding of the little-Higgs models, a brief description of the 2HDM and VLFs are given in the next section. In the last section, the $SU(6)/Sp(6)$ little-Higgs (LSS) model is described, with a detailed discussion on the scalar and Yukawa sectors, showing how a 2HDM structure with VLFs appears there. The LSS model is described here, following Refs. [12, 31].

2.1 Little-Higgs Models

In the SM, the Higgs mass squared parameter receives quadratically divergent one-loop radiative corrections sensitive to the cut-off scale of the theory. To naturally stabilize the electroweak (EW) scale i.e. to keep the fine tuning as small as possible, new physics is expected at around one TeV. The little-Higgs model [17] is an interesting BSM possibility that can stabilize the electroweak scale by preventing the Higgs mass from receiving quadratically divergent corrections at the one-loop level. This is arranged by making the Higgs a pseudo-Nambu-Goldstone boson (pNGB) (different models with this idea are reviewed in Refs. [18, 19]).

In the general construction of the little-Higgs models, a global symmetry ($\mathcal{G}$) of the Lagrangian is spontaneously broken to a subgroup $\mathcal{H}$ giving rise to Nambu-Goldstone bosons (NGB) which are massless at the tree-level and live in the coset $\mathcal{G}/\mathcal{H}$. The Higgs boson is taken to be one such NGB in the little-Higgs framework. Some of the other NGBs of the model emerge as the new physical scalars beyond the SM. As an example, one

simple little-Higgs model can be constructed with a global symmetry group $SU(3)$ which is spontaneously broken to $SU(2)$ at a breaking scale f (~ 1 TeV). The Higgs consists of four of the resulting Goldstone bosons due to this breaking and transforms as a doublet under the unbroken $SU(2)$. The other among the five NGBs is an $SU(2)$ singlet. Here, the Higgs is massless and has no Yukawa and gauge interactions.

The global symmetry ($\mathcal{G}$) in these models is broken explicitly by the gauge and Yukawa interactions to a subgroup. Due to this explicit breaking, the Higgs boson pick up masses at the loop-level making the Higgs a pseudo Nambu-Goldstone boson (pNGB). Other scalars, excluding those which are eaten as the longitudinal component of the gauge bosons, can also get mass in this way. This breaking is specially arranged to ensure that the mass picked up by the scalars remain finite at one-loop.

To ensure that the scalars are light, the Higgs multiplet is in a representation of the global symmetry group, containing the additional scalars. Similarly, extra fermion states beyond the SM are also introduced to fill up a representation of some bigger symmetry group, and to have sufficient symmetries to prevent quadratic divergence at one-loop. The beyond the standard model (BSM) fermions are made relatively heavier by making them vector-like with respect to the SM gauge group. The extra scalar states can typically be singlets, doublets, or triplets under the SM $SU(2)$. The vector-like fermions can also appear as the part of different $SU(2)$ multiplets. Depending on the nature of the symmetry groups $\mathcal{G}$ and $\mathcal{H}$, and how the global symmetries are broken, these extra scalar states can be much lighter than the global symmetry breaking scale f. Precision electroweak measurements impose tight constraints on little-Higgs models, typically resulting in a large fine-tuning. A discrete symmetry, the T-parity, can be incorporated to alleviate this problem as is shown in Ref. [59].

The "minimal-moose" [60] and the "littlest-Higgs" [32] models are some well-studied little-Higgs models. Some variants of these little-Higgs models are described below:

- **The minimal-moose with T-parity**:

  The minimal moose model is a two site model based on an $SU(3)$ global symmetry.

Unlike the original minimal-moose with gauged $SU(3) \times SU(2) \times U(1)$, in a minimal-moose model with T-parity (Ref. [33]), a Z_2 reflection symmetry is realized when the $[SU(2) \times U(1)]$ group within each of the $SU(3)$ are gauged. The unbroken diagonal sub-group is identified with the SM gauge group. The low-energy effective theory much below the scale f is a 2HDM. In the fermionic sector, this model contains new $SU(2)$ singlet colored vector-like Weyl fermion pair (u', $u^{c\prime}$) that cancel the divergent radiative correction from the SM top quark.

- Another minimal-moose model with T-parity (Ref. [59]) can be thought of as a UV completion of the model described above. The $SU(3)$ global symmetry structure at each site of the minimal moose is enlarged to $SO(5)$ so that the global symmetry contain the custodial symmetry group $SU(2)_C$ which further keeps the T-parameter under control. Here, to incorporate geometric reflection symmetry, an additional site is introduced under which mirror fermions are charged and couple with BSM fermions and makes them massive. The gauge structure is identical to the previous model, with the low energy effective theory again being a 2HDM. The fermion sector now include doublets and singlets, replicating the fermionic structure of the SM with new vector-like quarks and leptons.

- **The Littlest Higgs**:

  This theory is a simple extension of the SM, which contains a naturally light Higgs, free from quadratic divergences at the one-loop level. The EW sector of the SM is embedded into the $SU(5)/SO(5)$ non-linear sigma model where the Higgs is a pseudo Nambu-Goldstone boson. The symmetry breaking scale f is around a TeV, with the cut-off $\Lambda \leq 4\pi f \sim 10$ TeV. Gauging an $[SU(2) \times U(1)]^2$ subgroup of $SU(5)$ explicitly breaks the global symmetry. The Higgs quartic self-coupling is generated by the gauge and Yukawa interactions, while the top Yukawa coupling generates a negative mass squared term, triggering electroweak symmetry breaking. The new particle content at the TeV scale consists of one set of new vector bosons with

the same quantum numbers as the electroweak gauge bosons (W and Z), an EW singlet up-type vector-like quark, and an EW triplet scalar. These new particles through their interaction with the Higgs cancel the one-loop quadratically divergent corrections to the Higgs mass.

- **The Littlest Higgs with T parity**:

  The strongest Electroweak Precision constraints come from the tree level couplings of the SM fields to the new gauge bosons, as well as the vacuum expectation value (vev) of any $SU(2)$ scalar triplet which arises from its coupling to the SM Higgs. However, new particles are required to couple to the Higgs only at loop level to cancel the quadratic divergence. Therefore, it is possible to suppress the tree level contributions due to the new physics without upsetting the cancellation of the quardrant divergence. The natural way to implement this is to have a new symmetry acting on new TeV particles, while all the Standard Model fields are neutral under that new symmetry. The simplest choice for such a symmetry is a Z_2, under which the SM particles are *even* and the new ones are *odd*. This would automatically prevent mixing of SM electroweak gauge bosons with the new heavy ones. With this new symmetry, the little hierarchy problem can be solved consistently.

- In the littlest-Higgs with T-parity by Low (Ref. [34]), the group $SU(5)_l \times SO(5)_r / SO(5)_v$ is chosen among the two choices of $\mathcal{G}$ presented in that work. The low-energy effective theory is a 2HDM plus a singlet complex scalar. The mass of the extra doublet is controlled by the ϵ_1 parameter defined in the paper: both the Higgs doublets are light for $\epsilon_1 \ll 1$, while for $\epsilon_1 \sim 4\pi$, the extra scalar doublet mass is of the order of 10 TeV. The new fermions are one doublet and two singlet up-type (EM charge $+2/3$) vector-like quarks.

- In a little-Higgs model by Kaplan and Schmaltz (Ref. [37]), the global symmetry structure is $[SU(4)/SU(3)]^4$ with gauged $SU(4) \times U(1)$. The low-energy effective theory is a 2HDM. The new fermion is an up-type singlet (EM charge $+2/3$)

vector-like quark pair.

- **The Low-Skiba-Smith (LSS) Model**:

  A variant of the littlest-Higgs model is constructed by Low, Skiba and Smith (LSS, Ref. [31]) where the global symmetry structure is taken to be $SU(6)/Sp(6)$, in which $[SU(2)]^2$ is gauged whose diagonal sub-group is identified with the SM $SU(2)$ gauge-group. The $U(1)_Y$ is not contained in the $SU(6)$. The low-energy effective theory is a 2HDM. The new fermions are one vector-like quark doublet with $Y = 1/6$, and two vector-like quark singlets which are one up-type with EM charge $+2/3$ and one down-type with EM charge $-1/3$.

All these little-Higgs models have extra scalars with new fermions at the TeV scale. The vector-like fermions are essential in little-Higgs models. In Ref. [61] the phenomenology of BSM scalars is addressed in a model-independent setting, while some effective models with inclusion of vector-like fermions are studied also. In this thesis, the main focus is on the little-Higgs models that have a 2HDM structure. To give a better idea of the phenomenology of these models, the 2HDM and VLFs are briefly discussed in the next section.

2.2 General 2HDM & VLFs

In this section, the 2HDM extended scalar sector with VLFs also are discussed. To understand the phenomenology of the little-Higgs models where these structures appear, various features that are discussed here will be important.

Two Higgs Doublet Model (2HDM):

In the 2HDM there are two scalar doublets, Φ_1 with a hypercharge $+1/2$ and Φ_2 with a hypercharge $-1/2$, which can be parametrized as

$$\Phi_1 = \begin{pmatrix} \phi_1^+ \\ \frac{1}{\sqrt{2}}(v_1 + \rho_1 + i\eta_1) \end{pmatrix}, \qquad \Phi_2 = \begin{pmatrix} \frac{1}{\sqrt{2}}(v_2 + \rho_2 + i\eta_2) \\ \phi_2^- \end{pmatrix}, \tag{2.1}$$

with $v_1 = v\cos\beta$, $v_2 = v\sin\beta$ and $\tan\beta = v_2/v_1$. The Higgs Lagrangian is given by

$$\mathcal{L} \supset |D_\mu \Phi_1|^2 + |D_\mu \Phi_2|^2 - V(\Phi) \ , \tag{2.2}$$

where the general form of the 2HDM potential is written as

$$\begin{aligned} V(\Phi_1,\Phi_2) =& m_{11}^2|\Phi_1|^2 + m_{22}^2|\Phi_2|^2 - m_{12}^2(\Phi_1^T\cdot\Phi_2 + \text{h.c.}) + \lambda_1|\Phi_1|^4 + \lambda_2|\Phi_2|^4 + \\ & \lambda_3|\Phi_1|^2|\Phi_2|^2 + \lambda_4[(\Phi_1^T\cdot\Phi_2)(\Phi_2^T\cdot\Phi_1) + \text{h.c.}] + \frac{\lambda_5}{2}[(\Phi_1^T\cdot\Phi_2)^2 + \text{h.c.}] \ . \end{aligned} \tag{2.3}$$

Here, $\Phi_1^T\cdot\Phi_2 \equiv \Phi_1^T i\sigma^2\Phi_2$ is the antisymmetric product of the doublets. The m_{12}^2 term softly breaks the discrete Z_2 symmetry, under which $\Phi_1 \to -\Phi_1$, $d_R \to -d_R$ with all other fields unchanged. This symmetry is invoked as it saves the 2HDM from tree-level FCNCs [62]. The physical mass eigenstates in the 2HDM are the following: a heavy CP-even scalar $H = \rho_1\cos\alpha + \rho_2\sin\alpha$, a light CP-even scalar $h = \rho_1\sin\alpha - \rho_2\cos\alpha$, a CP-odd scalar $A = \eta_1\sin\beta + \eta_2\cos\beta$, and charged scalars $H^\pm = \phi_1^\pm\sin\beta + \phi_2^\pm\cos\beta$. The minima of potential are at $\langle\Phi_1\rangle = (0,\ v_1/\sqrt{2})^T$ and $\langle\Phi_2\rangle = (v_2/\sqrt{2},\ 0)^T$, with the constraint $v_1^2 + v_2^2 = v^2$. There remains seven free parameters in the 2HDM and those are taken as, m_A, m_h, m_H, $m_{H^\pm}$, $\tan\beta$, α and m_{12}^2, consistent with a notation commonly used in the literature (see for example Ref. [63]).

Our interest is in the case where the lighter CP-even scalar (h) is the observed 125 GeV Higgs boson. For this, the $\cos(\beta-\alpha) \approx 0$ is the most favored region [64]. It is also assumed that the "alignment limit" ($\beta - \alpha = \pi/2$) holds sufficiently accurately so that the h couplings are SM like to match with the properties of the observed 125 GeV state at the LHC as discussed in Ref. [65]. In this limit, the $H \to WW$ and $H \to ZZ$ decays do not give any significant constraints on the parameter space, which is evident from the LHC result of Ref. [66].

A comprehensive discussion on the theory and phenomenology of general 2HDMs is given in Refs. [63, 67] and references therein. Constraints on 2HDMs after the LHC Higgs discovery are discussed in Ref. [68]. The phenomenology of the neutral 2HDM BSM

scalars A, H is studied later in this thesis, in the context of a little-Higgs model.

Vector-like Fermions:

The SM fermions are chiral since their left and right chiralities belong to different representations of the SM gauge group. A fermion is defined to be vector-like if its left and right chiralities belong to conjugate representations of the gauge group of the theory. In a single Higgs doublet model, the presence of new chiral sequential fourth generation quarks are not favorable [69] from the Higgs production cross section and the electroweak precision tests (EWPT). As the chiral quarks couple to the Higgs boson with a strength proportional to its mass, the heavy chiral quarks do not decouple in the loop induced Higgs production and decay. On the other hand, heavy vector-like quarks which do not receive masses from the SM Yukawa-like couplings of the Higgs are less severely constrained by the recent Higgs-data [70]. This is because the vector-like quarks have a decoupling property. Although they are the key ingredients for many BSM theories, so far there is no experimental evidence of the existence of vector-like quarks. For example, vector-like quarks appear in extra-dimensional theories where higher excitations of the SM quarks are vector-like, composite Higgs models [71, 72], little-Higgs models [43, 46], some non-minimal supersymmetric extensions [73, 74] of the SM etc. For more details on the vector-like fermions see for example Refs. [75–77].

2.3 The LSS Model

The little-Higgs model by Low, Skiba and Smith (Ref. [31]), namely the LSS model has been introduced as an extension of the SM, with the Higgs as a pseudo-Goldstone boson. The LSS model is introduced and discussed in detail in Refs. [31], mainly emphasizing the construction of the model. The LSS model is also described briefly in our work Ref. [12], presenting the phenomenological analysis of the model. The main focus of discussion on the LSS model in this thesis will be on the aspects important to study the phenomenological side of the model. The BSM vector bosons are required to be somewhat

heavier in order to avoid precision electroweak constraints. The effective theory at the TeV scale is then a 2HDM with vector-like fermions and somewhat heavier vector bosons. Our main focus will be on the phenomenology of the scalars including the effect of vector-like fermions on them.

In this section, all relevant details necessary to our work is provided following the discussion in Ref. [12]. The global symmetry structure in the LSS model is $SU(6)/Sp(6)$. Depending on how the fermion condensate breaks the $SU(6) \to Sp(6)$ symmetry, different models can be formed and those are listed in Ref. [31]. Here, at a lower energy scale (~ 1 TeV) which is phenomenologically interesting at the LHC, the nonlinear sigma model describing $SU(6)/Sp(6)$ can provide all important information about the model. The $SU(6)$ has 35 generators and $Sp(6)$ has 21 generators. In this model, the global $SU(6)$ symmetry is spontaneously broken to $Sp(6)$, generating 14 Goldstone bosons. As the $SU(6) \to Sp(6)$ breaking also breaks $(SU(2) \otimes U(1))^2$ to the SM electroweak gauge group $SU(2)_L \otimes U(1)_Y$, there exist four BSM heavy gauge bosons. These four gauge bosons get their longitudinal components from four Goldstone bosons. Eight other Goldstone bosons form two $SU(2)_L$ scalar doublets that provide extra BSM scalars of the theory. So the extended symmetry gives rise to the BSM scalars here. The remaining two Goldstone bosons form a complex scalar singlet which is taken to be neutral. This scalar is not protected from quadratic divergences and therefore, is taken to be heavier than the other scalars (and at the cutoff scale). A set of massive gauge bosons are also present, but as discussed later, those bosons are taken to be heavier to evade the constraints from electroweak precision constraints. So, at the TeV scale, the model effectively becomes a two Higgs doublet model. The massive gauge bosons present in this model cancel the one loop divergences to the Higgs mass that originated from the SM gauge sector. Similarly, the neutral singlet plays an important role to soften the divergences arising from the Higgs quartic coupling of the SM. The divergent contribution due to the top quark does not get cancelled in the present set up. To eliminate the divergences related to the fermionic Yukawa couplings, extra colored vector-like fermions are added. Thus at the TeV scale

the LSS model is 2HDM with vector-like fermions.

Starting with a non-linear sigma model, its field Σ transforms under a global symmetry $SU(6)$ transformations. When the $SU(6)$ is broken down to $Sp(6)$ by an antisymmetric condensate, the pNGBs π^a are contained in the field as $\Sigma = e^{i\pi^a X^a/f}\langle\Sigma\rangle$ [12, 31], with the antisymmetric condensate

$$\langle\Sigma\rangle = \begin{pmatrix} 0 & -I_{3\times3} \\ I_{3\times3} & 0 \end{pmatrix} ,$$

where the X^a are the broken generators of $SU(6)$ and $I_{3\times3}$ is a 3×3 unit matrix. The breaking scale f sets the scale of the theory, which is used as an input to the effective theory. How f can be dynamically generated by the UV completion is not discussed here. The 2HDM fields are contained in the pNGB π^a that remain light after turning on the gauge and Yukawa couplings. Writing the pseudo-Goldstone states in term of representations of the $SU(2)_W$, the Σ field is defined through [12, 31]

$$\pi^a X^a \supset \begin{pmatrix} 0 & 0 & & 0 & s & \\ 0 & 0 & \phi_2 & -s & 0 & \phi_1 \\ & \phi_2^\dagger & 0 & & -\phi_1^T & 0 \\ 0 & -s^* & & 0 & 0 & \\ s^* & 0 & -\phi_1^* & 0 & 0 & \phi_2^* \\ & \phi_1^\dagger & 0 & & \phi_2^T & 0 \end{pmatrix} , \tag{2.4}$$

where the (light) pNGB two Higgs-doublets are presented as ϕ_1 and ϕ_2, with also the (heavy) singlet as s. Integrating-out the heavy s generates quartic couplings of the ϕ_1 and ϕ_2.

In the gauge sector of the LSS model collective symmetry breaking is ensured when $SU(2)_1 \otimes SU(2)_2$ with respective gauge couplings g_1 and g_2 is gauged. If either of the $SU(2)$ gauge couplings are turned off, the theory respects two different exact $SU(4)$ global symmetries. $\langle\Sigma\rangle$ breaks the $SU(2)_1 \otimes SU(2)_2$ gauge group to the electroweak $SU(2)_W$. The $SU(2)_1, SU(2)_2$ generators are taken as Q_1^a, Q_2^a with the Pauli matrices σ^a in the

uppermost and lowermost 2×2 block respectively and zeros elsewhere. The diagonal subgroup that is generated by unbroken linear combination of generators is identified with the SM $SU(2)$ with gauge coupling g. Some of the Goldstone bosons that are represented by the broken generators are eaten up to become longitudinal components of the BSM massive gauge bosons.

Both the abelian groups $U(1)$ with hypercharges Y_i are not contained in the $SU(6)$. The hypercharge transformation is denoted as $\Sigma \to e^{i\epsilon Y_1}\Sigma e^{-i\epsilon Y_2}$, with $Y_1 = \text{diag}(0,\ 1,\ 0,\ 0)$ and $Y_2 = \text{diag}(0,\ 0,\ 0,\ -1)$. The condensate $\langle\Sigma\rangle$ breaks $U(1)_1 \otimes U(1)_2$ with gauge couplings g_1' and g_2' down to the diagonal subgroup, which is identified with the SM $U(1)_Y$. This results in the hypercharge assignments $Y_{\phi_1} = +1/2$ and $Y_{\phi_2} = -1/2$ and makes the singlet s neutral. The light SU(2) and U(1) gauge bosons (massless before EWSB) are identified with the SM W_μ and B_μ respectively, and the corresponding heavy gauge bosons are presented as W_μ' and B_μ'. The gauge couplings are related as

$$\frac{1}{g^2} = \frac{1}{g_1^2} + \frac{1}{g_2^2}\ , \quad \frac{1}{g'^2} = \frac{1}{g_1'^2} + \frac{1}{g_2'^2}\ . \tag{2.5}$$

The fermion sector has to be constructed in a way that a large top Yukawa coupling can be there, without inducing a quadratic divergence. In this model, in addition to the third generation SM fermions Q, t^c, new vector-like Weyl fermion pairs are introduced. The new fermions are one vector-like quark doublet Weyl-fermion pair Q', Q'^c with $Y = 1/6$ and EM charge $2/3$, one vector-like pair of up-type quark singlets ψ_1, ψ_1^c with EM charge $\pm 2/3$, and one vector-like pair of down-type quark singlets ψ_2, ψ_2^c with EM charge $\mp 1/3$. The SU(2) structure of the fermions are expanded as $Q = (t, b)^T$, $Q' = (t', b')^T$ and $Q'^c = (-b'^c, t'^c)^T$. In the fermion sector also, collective symmetry breaking is ensured by a special structure of the Yukawa couplings [12, 31], where Σ couples to the fermionic

multiplets as

$$\mathcal{L}_{Yuk} = \lambda_1 f \begin{pmatrix} Q'^T & \psi_1 & (i\sigma^2 Q)^T & 0 \end{pmatrix} \Sigma^* \begin{pmatrix} 0 \\ t^c \end{pmatrix} + \lambda_2 f \begin{pmatrix} 0 & 0 & Q^T & 0 \end{pmatrix} \Sigma \begin{pmatrix} i\sigma^2 Q'^c \\ \psi_1^c \\ 0 \\ \psi_2^c \end{pmatrix} + \text{h.c.} \,. \tag{2.6}$$

Both of these terms respect a subgroup of the global symmetry group $SU(6)$ to protect the Higgs mass from one-loop quadratic divergent terms. With the expansion of the Yukawa couplings and inclusion of Dirac mass terms of the vector-like fermions, the Lagrangian looks like

$$\begin{aligned} \mathcal{L}^{\text{ferm}} \supset \quad & -\lambda_1 \left(f\psi_1 t^c - iQ'^T \phi_2^* t^c - iQ^T \cdot \phi_1 t^c \right) + \lambda_2 \left(f Q^T \cdot Q'^c + iQ^T \phi_1^* \psi_2^c + iQ^T \phi_2^* \psi_1^c \right) \\ & + \lambda_3 f Q'^T \cdot Q'^c + \lambda_4 f \psi_1^c \psi_1 + \lambda_5 f \psi_2^c \psi_2 + h.c. \,, \end{aligned} \tag{2.7}$$

where again, the "$\cdot$" represents the anti-symmetric combination of the SU(2) indices.

For generating the bottom mass, an SU(2) singlet field b^c is introduced with the Yukawa coupling as

$$\mathcal{L}^b_{Yuk} = -iy_1^b f \begin{pmatrix} 0 & 0 & Q^T & 0 \end{pmatrix} \Sigma \begin{pmatrix} 0 \\ 0 \\ 0 \\ b^c \end{pmatrix} + iy_2^b f \begin{pmatrix} 0 & 0 & (i\sigma_2 Q)^T & 0 \end{pmatrix} \Sigma^* \begin{pmatrix} 0 \\ b^c \\ 0 \\ 0 \end{pmatrix} + h.c. \,. \tag{2.8}$$

Expansion of the $\mathcal{L}^b_{Yuk}$ gives

$$\mathcal{L}^b_{Yuk} \supset y_1^b Q^T \phi_1^* b^c - y_2^b Q^T \cdot \phi_2 b^c + \text{h.c.} \,. \tag{2.9}$$

From Eq. (2.7) and Eq. (2.9), the fermion mass matrix can be constructed after the EWSB.

The EM charge $+2/3$ and $-1/3$ fermion mass matrices are [12]

$$\mathcal{L} \supset \begin{pmatrix} t & \psi_1 & t' \end{pmatrix} \begin{pmatrix} i\lambda_1 \frac{v_1}{\sqrt{2}} & i\lambda_2 \frac{v_2}{\sqrt{2}} & \lambda_2 f \\ -\lambda_1 f & \lambda_4 f & 0 \\ i\lambda_1 \frac{v_2}{\sqrt{2}} & 0 & \lambda_3 f \end{pmatrix} \begin{pmatrix} t^c \\ \psi_1^c \\ t'^c \end{pmatrix}$$
$$+ \begin{pmatrix} b & \psi_2 & b' \end{pmatrix} \begin{pmatrix} y_i^b \frac{v_i}{\sqrt{2}} & i\lambda_2 \frac{v_1}{\sqrt{2}} & \lambda_2 f \\ 0 & \lambda_5 f & 0 \\ 0 & 0 & \lambda_3 f \end{pmatrix} \begin{pmatrix} b^c \\ \psi_2^c \\ b'^c \end{pmatrix} + \text{h.c.} \,, \tag{2.10}$$

where $v_i = \{v_1, v_2\}$. To work out the couplings of the scalars to top-like fermions in the mass basis, the mass matrices in Eq. (2.10) are to be diagonalized. A two-step diagonalization process is implemented: first the f-dependent global symmetry breaking terms and then the $v_{1,2}$ dependent EWSB pieces are diagonalized. The transformations that diagonalize the f dependent terms in the top sector are,

$$\begin{pmatrix} t \\ \psi_1 \\ t' \end{pmatrix} = \begin{pmatrix} c_{23} & 0 & -s_{23} \\ 0 & i & 0 \\ s_{23} & 0 & c_{23} \end{pmatrix} \begin{pmatrix} t_0 \\ \psi_1' \\ t_1 \end{pmatrix} ; \quad \begin{pmatrix} t^c \\ \psi_1^c \\ t'^c \end{pmatrix} = \begin{pmatrix} ic_{14} & is_{14} & 0 \\ is_{14} & -ic_{14} & 0 \\ 0 & 0 & -1 \end{pmatrix} \begin{pmatrix} t_0^c \\ t_1^c \\ t_1'^{\,c} \end{pmatrix} . \tag{2.11}$$

The transformation in the bottom sector is given as,

$$\begin{pmatrix} b \\ \psi_2 \\ b' \end{pmatrix} = \begin{pmatrix} c_{23} & 0 & s_{23} \\ 0 & i & 0 \\ s_{23} & 0 & -c_{23} \end{pmatrix} \begin{pmatrix} b_0 \\ \psi_2' \\ b_1 \end{pmatrix} . \tag{2.12}$$

The ψ_2^c is transformed as $\psi_2^c \to -i\psi_2^c \equiv \psi_2'^c$. The rotation angles are given as, $s_{23} \equiv \sin\theta_{23} = \lambda_2/(\sqrt{\lambda_2^2 + \lambda_3^2})$, $c_{23} \equiv \cos\theta_{23} = -\lambda_3/(\sqrt{\lambda_2^2 + \lambda_3^2})$, and $s_{14} \equiv \sin\theta_{14} = \lambda_1/(\sqrt{\lambda_1^2 + \lambda_4^2})$.

After these rotations the mass matrices become

$$\mathcal{L}^{\rm mass} \supset \begin{pmatrix} t_0 & \psi_1' & t_1 \end{pmatrix} \begin{pmatrix} \mathcal{M}^t_{11} & \mathcal{M}^t_{12} & 0 \\ 0 & \mathcal{M}^t_{22} & 0 \\ \mathcal{M}^t_{31} & \mathcal{M}^t_{32} & \mathcal{M}^t_{33} \end{pmatrix} \begin{pmatrix} t_0^c \\ t_1^c \\ t_1'^c \end{pmatrix}$$
$$+ \begin{pmatrix} b_0 & \psi_2' & b_1 \end{pmatrix} \begin{pmatrix} \mathcal{M}^b_{11} & \mathcal{M}^b_{12} & 0 \\ 0 & \mathcal{M}^b_{22} & 0 \\ \mathcal{M}^b_{31} & \mathcal{M}^b_{32} & \mathcal{M}^b_{33} \end{pmatrix} \begin{pmatrix} b^c \\ \psi_2'^c \\ b'^c \end{pmatrix} + \text{h.c.} \,. \tag{2.13}$$

where $\sqrt{\lambda}_{14} \equiv \sqrt{\lambda_1^2 + \lambda_4^2}$, $\sqrt{\lambda}_{23} \equiv \sqrt{\lambda_2^2 + \lambda_3^2}$ and the elements of the mass matrix are given by [12]

$$\begin{aligned}
\mathcal{M}^t_{11} &= \frac{\lambda_1(\lambda_3\lambda_4 v_1 + \lambda_2\lambda_3 v_2 - \lambda_2\lambda_4 v_2)}{\sqrt{\lambda}_{14}\sqrt{\lambda}_{23}\sqrt{2}}\,, \qquad \mathcal{M}^t_{12} = \frac{(\lambda_1^2\lambda_3 v_1 - \lambda_2\lambda_3\lambda_4 v_2 - \lambda_1^2\lambda_2 v_2)}{\sqrt{\lambda}_{14}\sqrt{\lambda}_{23}\sqrt{2}}\,, \\
\mathcal{M}^t_{31} &= \frac{\lambda_1(\lambda_2\lambda_4 v_1 + \lambda_2^2 v_2 + \lambda_3\lambda_4 v_2)}{\sqrt{\lambda}_{14}\sqrt{\lambda}_{23}\sqrt{2}}\,, \qquad \mathcal{M}^t_{32} = \frac{(\lambda_1^2\lambda_2 v_1 - \lambda_2^2\lambda_4 v_2 + \lambda_1^2\lambda_3 v_2)}{\sqrt{\lambda}_{14}\sqrt{\lambda}_{23}\sqrt{2}}\,, \\
\mathcal{M}^t_{22} &= f\sqrt{\lambda}_{14}\,, \qquad \mathcal{M}^t_{33} = f\sqrt{\lambda}_{23}\,, \\
\mathcal{M}^b_{11} &= y^b_i \frac{v_i}{\sqrt{2}} c_{23}\,, \qquad \mathcal{M}^b_{12} = \lambda_2 \frac{v_1}{\sqrt{2}}\,, \qquad \mathcal{M}^b_{22} = \lambda_5 f\,, \\
\mathcal{M}^b_{31} &= y^b_i \frac{v_i}{\sqrt{2}} s_{23}\,, \qquad \mathcal{M}^b_{32} = -\lambda_2 \frac{v_2}{\sqrt{2}} s_{23}\,, \qquad \mathcal{M}^b_{33} = \sqrt{\lambda}_{23} f.
\end{aligned} \tag{2.14}$$

The top sector mass matrix $\mathcal{M}^t$ is to be diagonalized next. This asymmetric mass matrix diagonalization is done through a bi-orthogonal transformation of the fermionic states, given by U and V in the top sector as: $(t_0\ \psi_1'\ t_1)^T = U^T(\hat{t}_1\ \hat{t}_2\ \hat{t}_3)^T$ and $(t_0^c\ t_1^c\ t_1'^c)^T = V^T(\hat{t}_1^c\ \hat{t}_1^c\ \hat{t}_3^c)^T$, such that $U\mathcal{M}^t V^T \equiv \hat{\mathcal{M}}^t$ is diagonal. In the top quark sector the mass eigenstate fields are denoted as $\hat{t}_i, \hat{t}_i^c$ with $(\hat{t}_1, \hat{t}_1^c)$ being identified as the observed top-quark. The mass eigenvalues in the top sector are denoted as m_t, M_{t_2}, M_{t_3}. Analytical expressions of U, V are not given here as the diagonalization of the $v_{1,2}$ dependent part is done numerically in this thesis. In the bottom sector, the v_i proportional off-diagonal terms are numerically insignificant due to smallness of the Yukawa coupling y^b and can be ignored. The (b_0, b^c) are identified as the two Weyl fermions that constitute the observed bottom

quark. The mass eigenvalues in the bottom sector are presented as m_b, M_{b_2}, M_{b_3}.

Now the top quark Yukawa coupling y_{htt} is to be extracted using the rotation of the fermion fields defined above. In the flavor basis where the mass matrix is not diagonalized, the htt Yukawa coupling is written as,

$$\mathcal{L}_{htt} = \frac{i\,h}{\sqrt{2}} \begin{pmatrix} t & \psi_1 & t' \end{pmatrix} \begin{pmatrix} \lambda_1 c_\alpha & -\lambda_2 s_\alpha & 0 \\ 0 & 0 & 0 \\ -\lambda_1 s_\alpha & 0 & 0 \end{pmatrix} \begin{pmatrix} t^c \\ \psi_1^c \\ t'^c \end{pmatrix} + \text{h.c.}\ . \tag{2.15}$$

These can be rewritten in the basis where the f-terms are diagonal with the transformation of Eq. (2.11). Then the bi-orthogonal transformation U, V can provide the y_{htt} in the physical Higgs and top basis. Details of the BSM scalar Yukawa couplings are given in Chapter 3 where phenomenology of the BSM scalars are discussed.

The s-quark mass is generated in a fashion identical to how it is done in the bottom sector, with the replacement $y_b \to y_s$. To generate the c-quark mass an $SU(2)$ doublet field $Q_2 = (c, s)^T$ and an $SU(2)$ singlet field c^c are introduced with the Yukawa term that is similar to the Yukawa term of Eq. 2.8 with the replacements $y_i^b \to y_i^c, Q \to Q_2, b^c \to c^c$. Expanding the terms, the Lagrangian $\mathcal{L}_{Yuk}^c$ is obtained as:

$$\mathcal{L}_{Yuk}^c \supset y_1^c Q_2^T \cdot \phi_1 c^c + y_2^c Q_2^T \phi_2^* c^c + \text{h.c.}\ . \tag{2.16}$$

Similarly, for the τ lepton the Yukawa Lagrangian is obtained as,

$$\mathcal{L}_{Yuk}^\tau \supset y_1^\tau L^T \phi_1^* \tau^c - y_2^\tau L^T \cdot \phi_2 \tau^c + \text{h.c.}, \tag{2.17}$$

where L is the $SU(2)$ lepton doublet with $Y = -1/2$ and τ^c is the $SU(2)$ lepton singlet with $Y = 1$. Masses for the other light SM fermions can be generated in a similar way as shown above. This structure of $\mathcal{L}_{Yuk}^{b,c,s,\tau}$ and the other light fermions does not implement the little-Higgs mechanism. In the light fermionic sector, Yukawa couplings for these

fermions are all small enough in the phenomenologically acceptable small $\tan\beta$ region and the fine-tuning required to generate these masses is insignificant.

The effective theory which presents a 2HDM can be obtained integrating out the heavy BSM gauge bosons and the heavy scalar. The Higgs potential generated in this way at 1-loop in the LSS model is that of Eq. (3.1) [31] which is similar to that of Eq. (2.3) with some replacement and redefinition. Expressing the effective parameters of the model in terms of the input Lagrangian parameters the model is analyzed in detail. In particular, the $m_1^2 = \Sigma m_{1i}^2$, $m_2^2 = \Sigma m_{2i}^2$, b^2 and λ_5' are functions of the input Lagrangian parameters, as given below [12, 31]:

$$\begin{aligned}
\lambda_5' &= \frac{c g_1^2\,[g_2^2 + (c'/c)\lambda_2^2])}{g_1^2 + g_2^2 + (c'/c)\lambda_2^2}\ , \quad b^2 = \frac{3f^2}{8\pi^2}\lambda_1^2\lambda_2(\lambda_3 - \lambda_4)\log\frac{\Lambda^2}{M_f^2}\ , \\
m_{1\,f}^2 &= \frac{3f^2}{8\pi^2}(\lambda_1^2 - \lambda_2^2)(\lambda_3^2 - \lambda_4^2)\log\frac{\Lambda^2}{M_f^2}\ , \\
m_{2\,f}^2 &= \frac{3f^2}{8\pi^2}(\lambda_1^2\lambda_2^2 + \lambda_2^2\lambda_5^2 - \lambda_2^2\lambda_3^2 - \lambda_1^2\lambda_4^2)\log\frac{\Lambda^2}{M_f^2}\ , \\
m_{1g}^2 &= m_{2g}^2 = \frac{3}{64\pi^2}\left[3g^2M_g^2\log\frac{\Lambda^2}{M_g^2} + g'^2M_{g'}^2\log\frac{\Lambda^2}{M_{g'}^2}\right]\ , \\
m_{1s}^2 &= m_{2s}^2 = \frac{\lambda_5'}{16\pi^2}M_s^2\log\frac{\Lambda^2}{M_s^2}\ ,
\end{aligned} \tag{2.18}$$

where Λ is the cut-off which is taken to be $4\pi f$. M_f is the heavy vector-like fermion mass-scale. The heavy gauge-boson masses are $M_g = f\sqrt{(g_1^2 + g_2^2)/2}$ and $M_{g'} = f\sqrt{(g_1'^2 + g_2'^2)/2}$. The singlet scalar ($s$) mass is $M_s = f\sqrt{c(g_1^2 + g_2^2) + c'\lambda_2^2}$, where c and c' are $O(1)$ parameters that depend on the UV completion details as explained in Ref. [31].

The gauge and Yukawa coupling structure in the LSS model breaks the global SU(6) explicitly, allowing the Higgs to acquire a mass at the loop-level. The symmetry breaking for the little-Higgs model is collective which implies that any non-vanishing quantum correction to the Higgs mass must necessarily be proportional to a product of both the gauge coupling constants. In this case if either of the gauge couplings is turned off, there

is an exactly preserved global symmetry keeping the Higgs massless. Also for the two Yukawa couplings, if either of them is turned off the Higgs potential will have a new symmetry. Therefore as shown above, the loop generated Higgs potential terms should be proportional to a product of both the gauge couplings and similarly both the Yukawa couplings, which implies that the Higgs mass is finite at 1-loop.

Chapter 3

Phenomenology of the LSS model

As a concrete example of the phenomenology of new scalars and vector-like fermions in models with extended symmetry, one focus of this thesis is on the little Higgs model by Low, Skiba and Smith [31] (LSS), described in Chapter 2. The effective theory at the TeV scale is a 2HDM with heavy vector-like fermions and relatively heavier vector-bosons. Here, the scalar sector of the LSS little-Higgs model is studied in detail, and the lightest CP-even neutral scalar state of the model is matched with the 125 GeV state discovered at the LHC. Since the observed scalar properties measured at the LHC are very close to the SM Higgs values, it can constrain the parameter space of the model significantly. Probing the allowed regions of the parameter space that survive various theoretical and experimental constraints, is the main issue to be addressed here. This can have important effects on future LHC searches of extra scalars of various little-Higgs models, including the LSS model.

In this thesis, one focus is mainly on the phenomenology of the BSM *scalar* particles that arise in the LSS model as part of a 2HDM. For the other BSM particles i.e. the vector-like fermions and heavy vector-bosons in little-Higgs models, a detailed discussion of their LHC signatures are given in Refs. [19, 47, 48]. The LHC signatures of the t_2, t_3, b' will be similar to those studied in Refs. [75, 76]. The LHC phenomenology of LSS heavy vector bosons will be similar to those of Ref. [78–80].

In this Chapter, the heavy scalar phenomenology of the LSS model, described in Chapter. 2 is discussed following our work in Ref. [12]. In the first section, a 2HDM emerging in the LSS model is analysed to show some phenomenological correlation in the model. The goal of the next section is to scan the parameter space of the LSS model in order to find regions where the experimental constraints are all satisfied, and to study in these regions, the scalar, fermion and vector-boson sectors of the LSS model. The heavy scalars of the LSS model are studied in the last section, with a detailed analysis of their production and decay channels at the LHC, emphasizing the effects of vector-like fermions on BSM scalar production. BSM scalar Yukawa couplings with the SM and BSM fermions are also presented separately.

3.1 Effective 2HDM Analysis

In this section the effective 2HDM that arises in the LSS model is analyzed. The scalar potential of this model is given as [12, 31]:

$$\mathcal{V}_{LSS} = m_1^2|\phi_1|^2 + m_2^2|\phi_2|^2 + (b^2\phi_1^T \cdot \phi_2 + \text{h.c.}) + \lambda_5'|\phi_1^T \cdot \phi_2|^2 \ , \tag{3.1}$$

where ϕ_1 and ϕ_2 are the $SU(2)$ doublet scalars with hypercharge $+1/2$ and $-1/2$ respectively, and $\phi_1^T \cdot \phi_2 \equiv \phi_1^T i\sigma^2\phi_2$ is the antisymmetric product of the doublets. Here, the $\phi_{1,2}$ fields are same as the $\Phi_{1,2}$ fields defined in Eq. 2.1. This is the 2HDM potential of Eq. 2.3, with certain terms made zero and others redefined. As explained in detail in Chapter 2, this 2HDM structure is generated through loop contributions in the LSS model. In this effective 2HDM structure the coefficients of the scalar potential, m_1^2, m_2^2, b^2 and λ_5' are given in terms of free parameters in Eq. 2.18.

For the spontaneous breaking of the electroweak symmetry to electromagnetic $U(1)_{EM}$, the vacuum expectation values (VEV) of the ϕ_1 and ϕ_2 are required to be nonzero at the minimum of the LSS scalar potential, $\mathcal{V}_{LSS}$. From the expressions of Ref. [31], a sufficient condition for symmetry breaking is $m_{1,2}^2 > 0$ and $(m_1^2 m_2^2 - b^4) < 0$. The input Lagrangian

parameters must be such that these conditions are satisfied, in which case, the field VEVs at the minimum are written as $\langle\phi_1\rangle = (0\ v_1/\sqrt{2})^T$ and $\langle\phi_2\rangle = (v_2/\sqrt{2}\ 0)^T$. Using these in the minimization conditions results in,

$$\begin{aligned} \tan\beta \equiv v_1/v_2 &= \sqrt{m_2^2/m_1^2} \\ v \equiv \sqrt{v_1^2+v_2^2} &= \frac{2}{\lambda_5'}\frac{(1+\tan^2\beta)}{\tan\beta}\left(b^2 - m_1^2\tan\beta\right) \ . \end{aligned} \tag{3.2}$$

The vacuum expectation value of the doublet containing the Higgs is fixed at $v = 246$ GeV. Inside the doublet fields $\phi_{1,2}$, $\rho_{1,2}, \eta_{1,2}$ are the CP-even and CP-odd fields respectively. The linear combinations of $\eta_{1,2}$ (G) and $\phi^+_{1,2}, \phi^-_{1,2}$ (G^+, G^-) are massless Goldstone bosons and are eaten to become the longitudinal degrees of freedom of the Z_μ, W^+_μ, W^-_μ respectively. Four physical states, two (real) CP-even scalars (h, H), one (real) CP-odd scalar (A) and one (complex) charged scalar ($H^\pm$) are obtained. The fields are rotated as,

$$\begin{pmatrix}\rho_1\\ \rho_2\end{pmatrix} = \begin{pmatrix} c_\alpha & s_\alpha \\ -s_\alpha & c_\alpha\end{pmatrix}\begin{pmatrix} h \\ H\end{pmatrix} \ ; \qquad \begin{pmatrix}\eta_1\\ \eta_2\end{pmatrix} = -\begin{pmatrix} c_\beta & -s_\beta \\ s_\beta & c_\beta\end{pmatrix}\begin{pmatrix} A \\ G\end{pmatrix} \ , \tag{3.3}$$

Charged scalars $(\phi_1^\pm, \phi_2^\pm)$ are rotated to the physical fields $(H^\pm, G^\pm)$, in a way similar to the CP-odd scalars. The rotation angles are determined from the potential as

$$\tan(2\alpha) = \frac{-2(b^2 - v_1 v_2\lambda_5')}{(m_2^2 + \lambda_5' v_1^2/2) - (m_1^2 + \lambda_5' v_2^2/2)} \ ; \quad \tan(2\beta) = \frac{-2b^2}{(m_2^2 + \lambda_5' v_1^2/2) - (m_1^2 + \lambda_5' v_2^2/2)} \ . \tag{3.4}$$

The α and β solutions of Eq. (3.4) are picked to ensure $m_h < m_H$ and $m_G = 0$. $c_\theta \equiv \cos\theta$, $s_\theta \equiv \sin\theta$ are definitions used for convenience. Here, α and β both differ from the α, β of Section 2.2 by a phase of $\pi/2$.

The mass eigenvalues are calculated as

$$\begin{aligned} m_A^2 &= 2b^2/\sin(2\beta) \\ m_{H^\pm}^2 &= m_A^2 - \lambda_5' v^2/2 \\ m_{H,h}^2 &= \frac{1}{2}\left[m_A^2 \pm \sqrt{m_A^4 - 4(m_A^2 - m_{H^\pm}^2)m_{H^\pm}^2 \sin^2(2\beta)}\right] \end{aligned} \tag{3.5}$$

which are in agreement with Ref. [31]. The lighter CP-even scalar state (h) is identified to be the 125 GeV resonance observed at the LHC.

The CP-even scalar couplings to W^+W^- are given by

$$\mathcal{L}_{hW^+W^-} = \frac{g^2 v}{2} W_\mu^+ W^{-\mu} \left[\sin(\beta-\alpha)h + \cos(\beta-\alpha)H\right] \ . \tag{3.6}$$

Similarly, the hZZ coupling is proportional to $\sin(\beta-\alpha)$, and HZZ coupling to $\cos(\beta-\alpha)$. The hhW^+W^- is exactly SM like. The hAZ, $W^\pm H^\pm h$ and Hhh couplings are given by

$$\begin{aligned} \mathcal{L}^{AZh} &= \frac{g}{2\cos\theta_W} c_{\beta-\alpha} \left(Z^\mu A \partial_\mu h - Z^\mu h \partial_\mu A\right), \\ \mathcal{L}^{W^\pm H^\pm h} &= -i\frac{g}{2} c_{\beta-\alpha} \left(W^{+\mu} h \partial_\mu H^- - W^{+\mu} H^- \partial_\mu h + h.c.\right), \\ \mathcal{L}^{Hhh} &= -\frac{\lambda_5' v}{2}\left(2c_{2\alpha}c_{\beta+\alpha} - s_{2\alpha}s_{\beta+\alpha}\right) hhH \ . \end{aligned} \tag{3.7}$$

The $H^\pm W_\mu^\mp A^\mu$, $H^\pm W_\mu^\mp Z^\mu$, $hA_\mu Z^\mu$, $HA_\mu Z^\mu$, $HZ_\mu h$ couplings are all zero.

In Fig. 3.1, the contours of λ_5', $\cos(\beta-\alpha)$ and $m_{H^\pm}$ are shown in the m_A-$\tan\beta$ plane. Two free parameters m_A and $\tan\beta$ are chosen to be varied after applying the constraints, $m_h = 125$ GeV and $v \approx 246$ GeV. Imposing the constraint that λ_5' must not be imaginary, the allowed region is shown as the shaded region in Fig. 3.1. The hWW and hZZ couplings are constrained by the LHC data to be SM-like, which implies $c_{\beta-\alpha} \approx 0$ from Eq. (3.6). In the middle one in Fig. 3.1, contours of $c_{\beta-\alpha}$ values are presented, showing the amount of deviation allowed from the alignment limit defined in Section 2.2. The charged Higgs mass of Eq. 3.5 remains almost constant for a particular m_A, because the variation of λ_5'

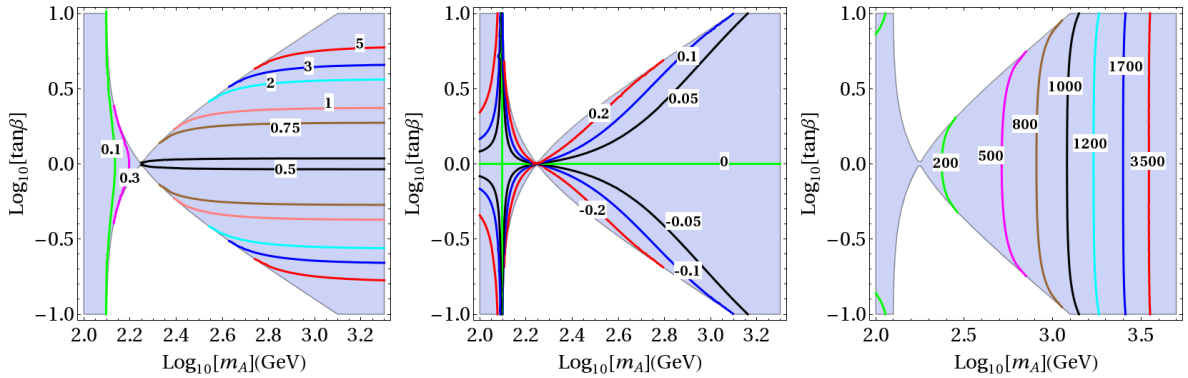

Figure 3.1: Contours of λ_5' (left), $\cos(\beta-\alpha)$ (middle) and $m_{H^\pm}$ (right) in GeV with $m_h = 125$ GeV. The part of the parameter space for which λ_5' is real is shown in the shaded (light-blue) region.

with $\tan\beta$ is really slow except near the funnel region.

Depending on how the fermions couple to Φ_1 and Φ_2, four types of 2HDM have been defined in the literature. Still, it is possible for the 2HDM structure in some models to have a different Yukawa structure altogether where y_{Htt} coupling gets accidentally suppressed. Consequently, as discussed later in the case of the $SU(6)/Sp(6)$ little Higgs model, the $BR(H, A \to t\bar{t})$ becomes small.

3.2 Constraints on the LSS model

In this section, the theoretical and experimental constraints on the LSS model are listed and how those constrain the LSS model parameter space is discussed. The LSS model has 12 free parameters, f, g_1, g_2, g_1', g_2', λ_1, λ_2, λ_3, λ_4, λ_5, c, c' in its Lagrangian. The symmetry breaking scale f is expressed in terms of $v = 246$ GeV and other free parameters using Eqs. (3.2) and (2.18). The gauge couplings g, g' defined in Eq. (2.5) are used to write the precisely measured $W^\pm, Z$ masses in the SM, with the vev fixed at 246 GeV. Among the four parameters g_i and g_i', g_2 and g_2' can be determined in terms of independent parameters g_1, g_1' and $W^\pm, Z$ masses, reducing the number of free parameters by two. The number of free input parameters at this point are reduced to nine, which are listed as g_1, g_1', λ_1, λ_2, λ_3, λ_4, λ_5, c, c'. The observables like the fermion and scalar masses are

Table 3.1: The experimental constraints at about the 2 to 3 σ level.

Quantity	Constraint	Reference
Top mass ($\overline{MS}$)	$158 < m_t^{\overline{MS}} < 168.7$ GeV	Ref. [81]
Higgs VEV	$v \equiv 246$ GeV	
Higgs mass	$123 < m_h < 127$ GeV	Ref. [82]
Higgs Yukawa	$0.63 < \lvert\kappa_{htt}\rvert < 1.2$	Table 15 of Ref. [83]
hW^+W^- coupling	$\lvert\cos(\beta-\alpha)\rvert < 0.4$	Table 15 of Ref. [83]
VLQ mass	$M_{t',b'} > 750$ GeV	Refs. [84], [85]

functions of multiple parameters in a complicated way. So replacing one free parameter directly in terms of other observables is analytically very difficult. Therefore a scan is done over the nine free parameters to find out the regions which satisfy the experimental constraints. How the scan is done and how the allowed points correlate the observable parameters are detailed later.

All the experimental constraints that are relevant for this analysis, along with the references of corresponding measurements are given in Table B.1. All the observable values are included with a statistical error range of 2 to 3 σ.

The top mass in the LSS model, obtained after a two step diagonalization of the mass matrix, is matched to the top mass shown in the Table B.1. The $(1,1)$ element of the diagonal matrix $U\mathcal{M}^tV^T$ is the physical top mass, with U, V being the two rotation matrices of the left and right handed fermion fields respectively. The top Yukawa coupling measured at the LHC so far approximately agree with that of the SM, within experimental error. The h Yukawa couplings in the basis with fields redefined to diagonalize f dependent terms (with v-terms not diagonalized) are

$$\mathcal{L}_h^{\text{Yuk}} \supset \frac{h}{\sqrt{2}}\left[y_{00}t_0t_0^c + y_{01}t_0t_1^c + y_{10}t_1t_0^c + y_{11}t_1t_1^c\right] + \text{h.c.}\,, \tag{3.8}$$

with $y_{00} \equiv (-\lambda_1 c_\alpha c_{14}c_{23} + \lambda_1 s_\alpha c_{14}s_{23} + \lambda_2 s_\alpha s_{14}c_{23})$, $y_{01} \equiv (-\lambda_1 c_\alpha s_{14}c_{23} + \lambda_1 s_\alpha s_{14}s_{23} - \lambda_2 s_\alpha c_{14}c_{23})$, $y_{10} \equiv (\lambda_1 c_\alpha c_{14}s_{23} + \lambda_1 s_\alpha c_{14}c_{23} - \lambda_2 s_\alpha s_{14}s_{23})$, $y_{11} \equiv (\lambda_1 c_\alpha s_{14}s_{23} + \lambda_1 s_\alpha s_{14}c_{23} + \lambda_2 s_\alpha c_{14}s_{23})$. Using the bi-orthogonal transformation involving U and V, the top Yukawa

coupling of the 125 GeV Higgs, y_{htt} in the model is given as

$$y_{htt} = [y_{00}U_{11}V_{11} + y_{01}U_{11}V_{12} + y_{10}U_{12}V_{11} + y_{11}U_{12}V_{12}] \ , \tag{3.9}$$

where $(U, V)_{ij}$ with $i, j = \{1, 2, 3\}$, are the (i, j) elements of the rotation matrices U, V. Relative magnitude of the top Yukawa coupling compared to the corresponding SM value is given as $\kappa_{htt} \equiv y_{htt}/y_{htt}^{SM}$.

In the 2HDM structure of the LSS model, the lighter CP-even state (h) is identified with the scalar state discovered at the LHC. LHC results indicate that the magnitude of the Higgs gauge couplings i.e. the hWW, hZZ vertex factors, almost match the SM values. From the h couplings of Eq. (3.6), it is evident that $|\sin(\beta - \alpha)| \approx 1$ i.e. $(\alpha - \beta) \approx \pm\pi/2$ is required to make the hWW, hZZ vertices exactly SM-like. This limit where one of the CP-even scalar of the 2HDM gets aligned with the SM Higgs is called the alignment limit [86,87]. The experimental data has not fixed the sign of the hVV coupling so far. In accordance to the SM convention, the positive signs of those couplings are usually taken. The $h \to WW, ZZ$ decays are not sensitive to the sign of hVV coupling as the tree-level amplitudes dominate these modes. But the $h \to \gamma\gamma$ decay, being at the loop-level with the interference between the gauge-boson and top-loop, is sensitive only to the relative sign between the hVV and htt couplings. Thus, to keep the Higgs observables independent of the sign of the couplings two possibilities exist: either hVV and htt both are positive, or alternately both are negative. Both these possibilities can be realized in the alignment limit; therefore when hVV is negative, htt is also taken negative. It will be important to find the collider observables that are sensitive to both the hff and hVV sign reversal and those can be probed in future. The hVV coupling constraint shown in Table B.1 is for the case when it is assumed that no new particles contribute in the hgg loop. This is a good approximation in the LSS model as the vector-like fermions that are usually very heavy, contribute minimally in the hgg loop. Therefore, use of the hVV coupling value chosen here will provide a more conservative bound. The deviations of the SM Higgs

couplings due to the presence of vector-like fermions at one-loop are discussed in Ref. [77]. The direct LHC limit on the vector-like quarks (VLQ) are given as $M_{t',b'} > 750$ GeV.

In the LSS model, after imposing the constraints of W^+, Z mass and v, there are nine free Lagrangian parameters. The nine dimensional parameter space is scanned to carve out the parameter region satisfying all the experimental constraints discussed above. In these allowed regions the LSS model BSM particles are studied with emphasis on the correlation of the masses of the LSS model scalars, fermions and vector bosons. Dividing the range of all the parameters in tiny steps and scanning over the nine dimensional parameter space to get the points which satisfy the constraints of the Table B.1 is computationally time consuming and challenging. An alternative method, where the points in the nine dimensional parameter space are randomly chosen, is adopted instead. Here a χ^2 function is defined to measure the deviation of various observables from their expected values as,

$$\chi^2 \equiv \frac{(m_h - \langle m_h \rangle)^2}{\sigma^2_{m_h}} + \frac{(m_t - \langle m_t \rangle)^2}{\sigma^2_{m_t}} + \frac{(|\kappa_{htt}| - \langle \kappa_{htt} \rangle)^2}{\sigma^2_{htt}} + \frac{(c_{\beta-\alpha} - \langle c_{\beta-\alpha} \rangle)^2}{\sigma^2_{c_{\beta-\alpha}}} \ , \qquad (3.10)$$

and this function is minimized implementing a method of steepest descent mechanism for each point in a randomly sampled parameter space. Here the chosen values are $\langle m_h \rangle = 125$ GeV, $\langle m_t \rangle = 163.3$ GeV, $\langle \kappa_{htt} \rangle = 1$, $\langle c_{\beta-\alpha} \rangle = 0$, with the corresponding standard deviations, $\sigma_{m_h} = 3$ GeV, $\sigma_{m_t} = 5.4$ GeV, $\sigma_{htt} = 0.25$, $\sigma_{c_{\beta-\alpha}} = 0.2$. In this method a random point is picked up as the starting point and the χ^2 function and its partial derivatives with respect to all of the nine parameters are computed at that point. From those computations, an infinitesimal step is taken around the starting point to reach the new point with a lower χ^2. This point is then made the new starting point and the same process is iterated till the local minimum of the χ^2 is reached. The point is retained if $\chi^2 < 10$, and discarded otherwise, triggering a search for a new random point. In this manner, a list of points is obtained in the nine dimensional space that have $\chi^2 < 10$. Additional constraints like the requirement of same sign κ_{htt} and $s_{\beta-\alpha}$ and vector-like quarks (t' and b') heavier than 750 GeV, are further imposed on this sample. The points

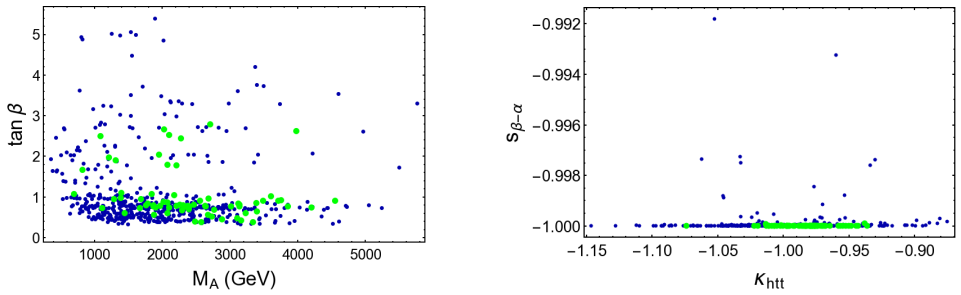

Figure 3.2: M_A vs $\tan\beta$ (left), κ_{htt} vs $s_{\beta-\alpha}$, the ratios of the htt and hVV couplings to the corresponding SM values, with $VV = \{W^+W^-, ZZ\}$. (right)

that satisfy all these criteria are shown as blue dots in all the plots that follow.

As this model does not contain any symmetry that prohibits the tree-level mixing of SM and BSM gauge bosons, electroweak precision constraints could be important here. The constraints on the LSS model coming from the S, T, U parameter bounds have been discussed in Refs. [36, 88, 89]. To get some idea of the constraints that precision tests can impose, the "near-oblique" limit discussed in Ref. [88] is considered here, with the additional requirement of the constraining equation $M_{W'} > 1800\ \text{GeV} \times (g_2^2 - 2g^2)/(g_2^2 - g^2)$ to be satisfied. Putting a model independent constraint due to the BSM abelian vector boson B' is difficult as its mass generation is more or less model dependent. As discussed in Ref. [88], B' can be made massive enough to avoid any significant constraint by invoking a new symmetry breaking scale. In the plots shown throughout this Chapter, the blue points represent the points that satisfy all the constraints discussed above except those from EW precision constraints. The points those are allowed after imposing the EW precision constraints with previous constraints also included, are indicated as green points. The LSS Lagrangian parameters and the resulting masses, couplings and other quantities for 9 sample points (the green dots) that satisfy direct and precision electroweak constraints are listed in App. B.

In Fig. 3.2, some 2HDM related relations are shown in the allowed parameter space. The left plot shows the correlation of $m_A - \tan\beta$ for the allowed points. The allowed $\tan\beta$ values are typically small, lying in the range of $(0.3, 5.4)$. The κ_{htt} and $s_{\beta-\alpha}$ are shown in Eq. (3.8) and Eq. (3.6), as the ratios of the htt and hVV couplings ($VV = \{W^+W^-, ZZ\}$)

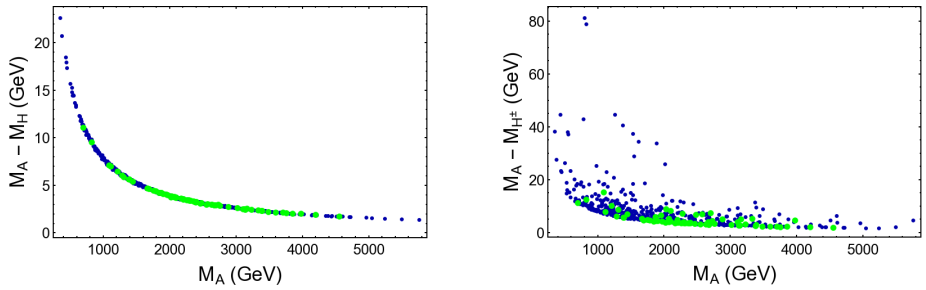

Figure 3.3: The relation of scalar masses of the LSS model for the points that satisfy the direct experimental constraints along with the precision electroweak constraints.

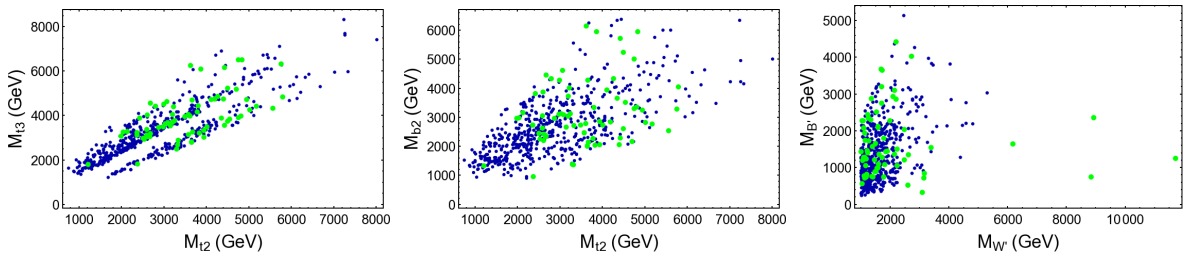

Figure 3.4: Correlation of the heavy vector-like fermion and vector-boson masses.

to their SM values respectively. In Fig. 3.2 (right), it is shown how κ_{htt} and $s_{\beta-\alpha}$ are correlated in the allowed parameter space. All the allowed points have $s_{\beta-\alpha}$ values almost -1, and therefore satisfy the alignment limit discussed in the beginning of this section very well. The κ_{htt} values are also very close to -1, making the top Yukawa coupling of the Higgs SM like in magnitude. Interestingly, the standard sign convention of the SM is reversed with both the hff and hVV signs negative, for all the points that satisfy the constraints.

In Fig. 3.3, the correlation of scalar masses, m_A, m_H and $m_{H^\pm}$ of the 2HDM in the LSS model is presented. From the Eq. (3.5), scalar masses are related as $m_A^2 - m_H^2 = m_h^2$ and $m_A^2 - m_{H^\pm}^2 = \lambda_5' v^2$. Since m_h is fixed to the experimentally measured value, $(m_A - m_H)$ falls smoothly like $1/m_A$. As λ_5 takes different values for allowed points, $(m_A - m_{H^\pm})$ falls with $1/m_A$ along with being scattered due to its dependence on λ_5. For the allowed points, m_h is kept fixed and λ_5 does not vary much, indicating the heavy scalar masses m_A, m_H and $m_{H^\pm}$ to be more degenerate with the increase of m_A.

In Fig. 3.4, the correlation of the heavy vector-boson and vector-like fermion masses are presented. Without imposing precision electroweak constraints, new top-like fermion

with mass M_{t2} can be as light as around 750 GeV and it can have good discovery potential at the LHC. Similarly for the bottom sector mass of $M_{b'} = 948$ GeV, precision electroweak constraints are satisfied along with other constraints and LHC discovery is possible. Expectedly, as shown by the green dots, precision electroweak constraints raises the mass scale of the BSM states. It is explored later if these vector-like fermions can contribute significantly to phenomenology of the LSS model at at the one-loop level. In another of our work in Ref. [61] presents a more general analysis on the effect of vector-like fermions on the scalar phenomenology. For the allowed points, the heavy abelian vector-boson mass $M_{B'}$ can be significantly lower than the heavy $SU(2)$ vector-boson mass $M_{W'}$. The B' mass is quite model dependent and can be made heavier if the electroweak precision constraints are imposed on it.

How the flavor sector observables can put constraints on the LSS model parameter space is briefly outlined here. Flavor-changing-neutral currents (FCNC) can play an important role in this aspect, depending on the Yukawa structure of the lighter fermions of the theory. In the LSS model, as evident from Eq. (2.7), the top-quark couples to both the scalar doublets ϕ_1 and ϕ_2. This resembles a Type III 2HDM flavor structure, which can be non-trivially constrained from the FCNCs involving the 3rd generation fermions. For the other fermions, if the Yukawa structure has $y_1^{b,\tau,c} \neq 0; y_2^{b,\tau,c} \neq 0$, non-trivial constraints will be placed from the $h \to bb, \tau\tau$ measurement at the LHC. Those constraints can be avoided either with the assumption, $y_1^{b,\tau,c} = 0; y_2^{b,\tau,c} \neq 0$ or with $y_1^{b,\tau,c} \neq 0; y_2^{b,\tau,c} = 0$. With these kind of assumption extended to all light fermions, a Type I 2HDM framework is achieved for the light fermion sector, with only the top quark breaking it. For the light fermions, one alternative Yukawa structure can be explored where $y_1 \neq 0, y_2 = 0$ for the up-type fermions, and $y_1 = 0, y_2 \neq 0$ for the down type ones. In that case the light fermion sector will be analogous to a Type II 2HDM, with again only the top sector resembling the Type III structure. A detailed analysis of these flavor issues is beyond the scope of this thesis. Ref. [90] and references therein, present a detailed analysis of flavor constraints in the Type III 2HDM.

3.3 Heavy BSM scalar Phenomenology

The phenomenology of the BSM scalars, heavy CP-even scalar H, CP-odd scalar A and charged scalar $H^{\pm}$, that are part of the 2HDM structure of the LSS model are studied in this thesis. To understand and calculate the dominant production and decay modes of BSM scalars, their couplings with the SM/BSM particles are important to know. All these couplings are presented here, following our work Ref. [12].

3.3.1 BSM Scalar Couplings

The gauge boson couplings of the heavy CP even scalar can be obtained from Eq. 3.6. The CP-odd scalar does not couple to the SM massive gauge bosons due to CP invariance. The self couplings between different scalars can be extracted from the 2HDM potential given in Eq. 3.1. The Yukawa couplings of these scalars are discussed below.

In the LSS model described in Chapter 2, the f dependent terms of the fermion mass matrices are diagonalized. The fields are redefined there in a way such that the fermion mass matrix entries become real. The H Yukawa couplings in that basis with v-terms not diagonalized are

$$\mathcal{L}_H^{\text{Yuk}} \supset \frac{H}{\sqrt{2}}\left[y_{00}^H t_0 t_0^c + y_{01}^H t_0 t_1^c + y_{10}^H t_1 t_0^c + y_{11}^H t_1 t_1^c\right] + \text{h.c.}\ , \tag{3.11}$$

with

$$\begin{aligned}
y_{00}^H &\equiv -\lambda_1 s_\alpha c_{14} c_{23} - \lambda_1 c_\alpha c_{14} s_{23} - \lambda_2 c_\alpha s_{14} c_{23},\\
y_{01}^H &\equiv -\lambda_1 s_\alpha s_{14} c_{23} - \lambda_1 c_\alpha s_{14} s_{23} + \lambda_2 c_\alpha c_{14} c_{23},\\
y_{10}^H &\equiv \lambda_1 s_\alpha c_{14} s_{23} - \lambda_1 c_\alpha c_{14} c_{23} + \lambda_2 c_\alpha s_{14} s_{23},\\
y_{11}^H &\equiv \lambda_1 s_\alpha s_{14} s_{23} - \lambda_1 c_\alpha s_{14} c_{23} - \lambda_2 c_\alpha c_{14} s_{23}.
\end{aligned} \tag{3.12}$$

How the bi-orthogonal rotations U, V can take us to the mass-basis diagonalizing the v dependent terms is also described in the section. Using those rotation angles, the

top Yukawa coupling of the heavy CP-even scalar, y_{Htt} in the model is given as, $y_{Htt} = \left[y^H_{00}U_{11}V_{11} + y^H_{01}U_{11}V_{21} + y^H_{10}U_{12}V_{11} + y^H_{11}U_{12}V_{12}\right]$, where U_{ij}, V_{ij} with $i,j = \{1,2,3\}$, is the (i,j) entry of the rotation matrices U, V. Other Yukawa couplings of the H can be obtained, using different combinations of U, V matrix elements as,

$$\mathcal{L}^{\rm Yuk}_H \supset \frac{H}{\sqrt{2}}\left[y^H_{00}U_{j1}V_{k1} + y^H_{01}U_{j1}V_{k2} + y^H_{10}U_{j2}V_{k1} + y^H_{11}U_{j2}V_{k2}\right]\hat{t}_j\hat{t}^c_k + \text{h.c.}\ . \tag{3.13}$$

The $\hat{t}_j, \hat{t}_k$ are the fermions in the mass basis after full diagonalization.

The A Yukawa couplings to the top sector fermions are written as,

$$\mathcal{L}^{\rm Yuk}_A \supset \frac{A}{\sqrt{2}}\left[\lambda_1\left(\cos\beta\, t - \sin\beta\, t'\right)t^c - \lambda_2\left(\sin\beta\, t\psi^c_1 + \cos\beta\, b\psi^c_2\right)\right] + \text{h.c.}\ . \tag{3.14}$$

After diagonalizing the f terms, in the basis of Eq. (2.11) and using the field redefinitions shown there the CP-odd scalar Yukawa coupling is,

$$\mathcal{L}^{\rm Yuk}_A \supset \frac{i\,A}{\sqrt{2}}\left[y^A_{00}t_0t^c_0 + y^A_{01}t_0t^c_1 + y^A_{10}t_1t^c_0 + y^A_{11}t_1t^c_1\right] + \text{h.c.}\ , \tag{3.15}$$

with

$$\begin{aligned}
y^A_{00} &\equiv \lambda_1 c_\beta c_{14}c_{23} - \lambda_1 s_\beta c_{14}s_{23} - \lambda_2 s_\beta s_{14}c_{23},\\
y^A_{01} &\equiv \lambda_1 c_\beta s_{14}c_{23} - \lambda_1 s_\beta s_{14}s_{23} + \lambda_2 s_\beta c_{14}c_{23},\\
y^A_{10} &\equiv -\lambda_1 c_\beta c_{14}s_{23} - \lambda_1 s_\beta c_{14}c_{23} + \lambda_2 s_\beta s_{14}s_{23},\\
y^A_{11} &\equiv -\lambda_1 c_\beta s_{14}s_{23} + \lambda_1 s_\beta s_{14}c_{23} + \lambda_2 s_\beta c_{14}s_{23}.
\end{aligned} \tag{3.16}$$

Diagonalizing the v proportional mass terms via the bi-orthogonal rotations U and V, Yukawa couplings in the mass basis are obtained as,

$$\mathcal{L}^{\rm Yuk}_A \supset \frac{i\,A}{\sqrt{2}}\left[y^A_{00}U_{j1}V_{k1} + y^A_{01}U_{j1}V_{k2} + y^A_{10}U_{j2}V_{k1} + y^A_{11}U_{j2}V_{k2}\right]\hat{t}_j\hat{t}^c_k + \text{h.c.}\ . \tag{3.17}$$

For notational brevity, 173 GeV quark $\hat{t}_1$ is simply denoted as t, and the heavier EM charge 2/3 fermions $\hat{t}_2, \hat{t}_3$ are denoted as t_2 and t_3 respectively.

The $H^{\pm}tb$ couplings can be obtained as

$$\begin{aligned}\mathcal{L}^{Yuk} = H^+ \left(y^+_{00} b_0 t^c_0 + y^+_{01} b_0 t^c_1 + y^+_{10} b_1 t^c_0 + y^+_{11} b_1 t^c_1\right) + \\ H^- \left(y^-_{00} t_0 b^c + y^-_{10} t_1 b^c + y^-_{02} t_0 \psi^c_2 + y^-_{12} t_1 \psi^c_2\right) + \text{h.c.}\,,\end{aligned} \tag{3.18}$$

where

$$\begin{aligned} y^+_{00} &= \lambda_1 s_\beta s_{23} c_{14} - \lambda_1 c_\beta c_{23} c_{14} + \lambda_2 s_\beta c_{23} s_{14}, \\ y^+_{01} &= \lambda_1 s_\beta s_{23} s_{14} - \lambda_1 c_\beta c_{23} s_{14} - \lambda_2 s_\beta c_{23} c_{14}, \\ y^+_{10} &= -\lambda_1 s_\beta c_{23} c_{14} - \lambda_1 c_\beta s_{23} c_{14} + \lambda_2 s_\beta s_{23} s_{14}, \\ y^+_{11} &= -\lambda_1 s_\beta c_{23} s_{14} - \lambda_1 c_\beta s_{23} s_{14} - \lambda_2 s_\beta s_{23} c_{14}, \\ y^-_{00} &= (-y^b_1 c_\beta + y^b_1 s_\beta) c_{23}, \quad y^-_{10} = (y^b_1 c_\beta - y^b_2 s_\beta) s_{23}, \\ y^-_{02} &= -\lambda_2 c_\beta c_{23}, \qquad\qquad y^-_{12} = \lambda_2 c_\beta s_{23}. \end{aligned} \tag{3.19}$$

The rotations U, V, that diagonalize the $v_{1,2}$ proportional off-diagonal terms are then applied on these to get the charged Higgs Yukawa couplings. The $H^{\pm}cs$ and $H^{\pm}\tau\nu$ couplings can be obtained as

$$\mathcal{L}^{Yuk} \supset \left(y^c_1 c_\beta - y^c_2 s_\beta\right) H^+ s c^c + \left(-y^s_1 c_\beta + y^s_2 s_\beta\right) H^- c s^c + \left(-y^\tau_1 c_\beta + y^\tau_2 s_\beta\right) H^- \nu \tau^c + \text{h.c.}\,. \tag{3.20}$$

The heavy scalar couplings to the b-type quarks can be obtained from Eq. 2.9 as

$$\mathcal{L} \supset \frac{c_{23}}{\sqrt{2}} \left[H \left(y^b_1 s_\alpha + y^b_2 c_\alpha\right) + iA \left(y^b_1 c_\beta - y^b_2 s_\beta\right)\right] b_0 b^c + \text{h.c.}\,.$$

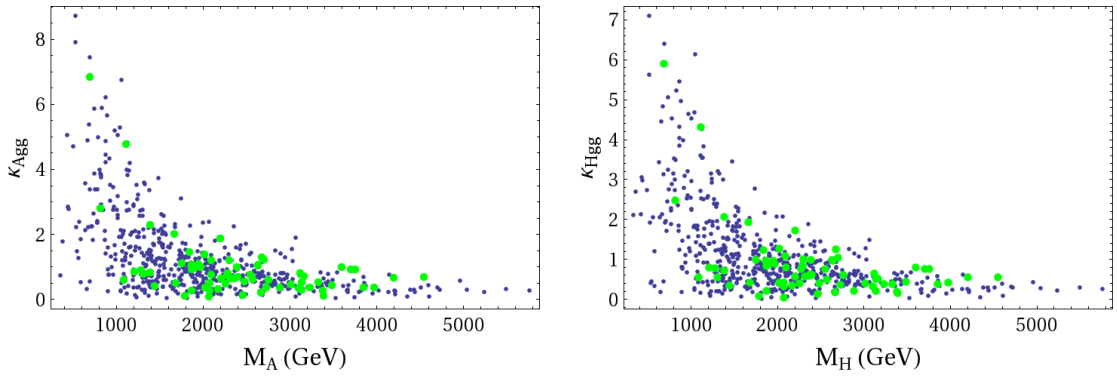

Figure 3.5: κ_{Agg} (left) and κ_{Hgg} (right) for the allowed points of the parameter space.

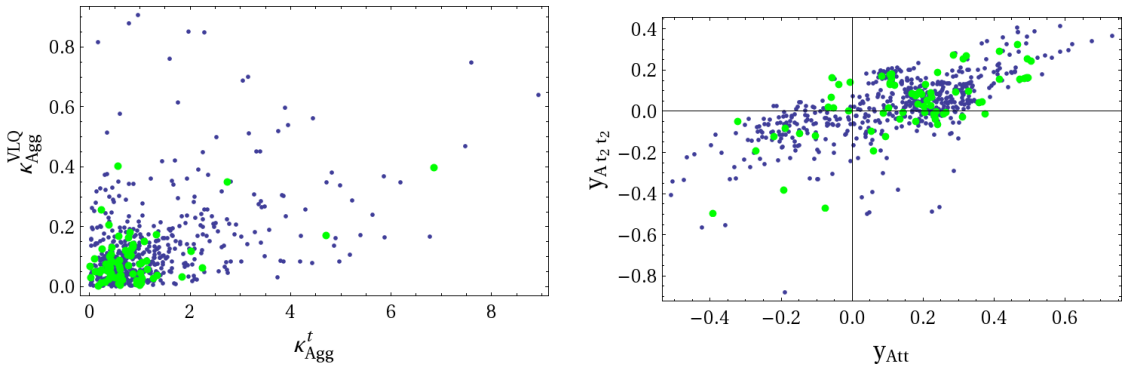

Figure 3.6: κ^t_{Agg} vs. κ^{VLQ}_{Agg} (left), and y_{Att} and $y_{At_2t_2}$ (right) for the allowed points of the parameter space.

3.3.2 Production and Decay of Heavy Scalars

In this section, phenomenology of the new scalars at the LHC is explored in the parameter space allowed after imposing the constraints discussed in Section 3.2. In the constrained parameter space, the production and decay modes of different BSM scalar states are studied with emphasis on the neutral scalars, A and H. To explore the detection prospects, the production cross section of the new scalars is to be studied. As shown in the left side plot of Fig. 3.2, the $\tan\beta$ values that are allowed are typically small. The bottom fusion production, with contributions being directly proportional to $\tan\beta$, is negligible and is not included here. The gluon fusion production mode is explored here as the dominant production mode for the neutral scalars. The ϕgg effective couplings in Fig. 3.5, $\kappa_{\phi gg}$ (with $\phi = \{A, H\}$) along with their one-loop expressions are given in App. A, using the notation defined in Ref. [61]. The effects of the presence of vector-like fermions in the LSS

model can be probed in the gluon fusion production channel of the neutral scalars. To quantify the contributions due to the vector-like quarks compared to their SM counterpart in the production cross section, it is important to present their relative contribution. The SM contributions to the effective coupling $|\kappa_{Agg}|$ that provides a measure of the gluon fusion cross section mainly come from the top-quark (t) and represented by κ^t_{Agg}. The contributions from VLQs (i.e. t_2, t_3 and b_2, b_3), denoted as κ^{VLQ}_{Agg} are separately presented with κ^t_{Agg} in Fig. 3.6 (left). The total gluon fusion amplitude is a coherent sum of these two. For some points in the allowed parameter space the VLQ contributions can be significant either being of the same order as the SM one or sometimes dominating over the top contribution. To probe the reason behind this, the Yukawa couplings y_{Att} and $y_{At_2t_2}$ that quantify the two contributions are separately presented in Fig. 3.6 (right). It is shown there that for some allowed points the VLQ Yukawa couplings can either be of similar magnitude or even larger than the top Yukawa. These indicate that the vector-like fermion contributions play important role in the neutral BSM scalar phenomenology.

Once the production cross section of the scalars are discussed, the focus is next on the decay modes of those BSM scalars. The total width (Γ) and branching ratios (BR) of the new scalars into SM final states are explored. How to obtain the analytical expressions of partial widths in all the relevant channels are outlined for example in Ref. [91]. As all the 125 GeV scalar couplings are fixed close to the SM values, the $BR(h \to XX)$ does not deviate much in the alignment limit. Therefore all the the LHC constraints are easily satisfied. The hbb coupling is not fixed here, so BR to bb could in principle be shifted. If one of y^b_i is zero, the ratio of hbb coupling with respect to the SM is $\approx \pm 1$ in the alignment limit, reducing the coupling to SM values. Similar conclusions can be drawn for the other lighter fermions, τ, c. In this work, the case is taken where $y^{b,\tau,c}_1 = 0$ and $y^{b,\tau,c}_2$ are nonzero.

All the total decay widths and the branching ratios of the heavy scalars, $A, H, H^\pm$ are shown in Figs. 3.7, 3.8, 3.10. Although from the CP symmetry arguments, AVV is generically zero with HVV non-zero at the tree-level, Γ_A and Γ_H gives almost identical numbers. This happens because tree level HVV couplings get suppressed for most of the

allowed points, as they satisfy the alignment limit to a very good degree. Also, at the alignment limit the H and A couplings to the SM fermions become identical. Therefore, the partial widths of H and A to the fermionic decay channels are almost same.

The total width of the CP-odd scalar, Γ_A is a sum over the partial-widths to $tt, bb, cc, \tau\tau$ decay modes. The branching ratios of the CP-odd scalar (A) in the $\gamma\gamma$, $\tau\tau$, bb, tt, Zh channels are presented in Fig. 3.7. for the allowed points of the parameter space. As the alignment limit is satisfied for most part of the parameter space, allowed $c_{\beta-\alpha}$ values are mostly closer to zero. Therefore the AZh coupling being proportional to $c_{\beta-\alpha}$ reduces the BR ($A \to Zh$) to very small values for large part of the parameter space. For the few points where there are deviations from the alignment limit along with small y_{Att} couplings due to accidental cancellations, BR($A \to Zh$) can become significant.

In the total decay width (Γ_H) of the CP-even scalar (H), major contributions come from the $tt, bb, cc, \tau\tau, WW, ZZ$ decay modes. The branching ratios of the H in the fermionic decay modes are quite similar to the corresponding $BR(A \to XX)$ and so they are not separately presented here. The changes in the $H \to \gamma\gamma$ channel compared to the CP-even case are minimal with the largest BR for the H is about 4.2×10^{-6} which is larger than highest $BR(A \to \gamma\gamma)$. Unlike the CP-odd scalar A, the $H \to Zh$ mode is not possible here from the requirement of CP-invariance. The CP-even H can additionally decay to WW, ZZ, hh at tree-level which was not possible for A. As the alignment is satisfied almost perfectly for most of the allowed points, the decays to WW, ZZ are in general suppressed in the LSS model. In Fig. 3.8 branching ratios in ($H \to ZZ, WW, hh$) channels are presented, and it is observed that these BRs can become sizable only for few allowed points. These modes can become dominant either because of the deviation from the alignment limit making the HZZ and HWW modes significant or due to the accidental cancellation between different contributions to the Htt coupling of Eq. (3.8) reducing it to small values making BR($H \to tt$) small. To illustrate the first effect, the correlation of BR($H \to ZZ$) with $|c_{\beta-\alpha}|$ is presented in Fig. 3.9 where $c_{\beta-\alpha}$ quantifies the deviation from the alignment limit. To illustrate the second effect, the correlation of BR($H \to ZZ$)

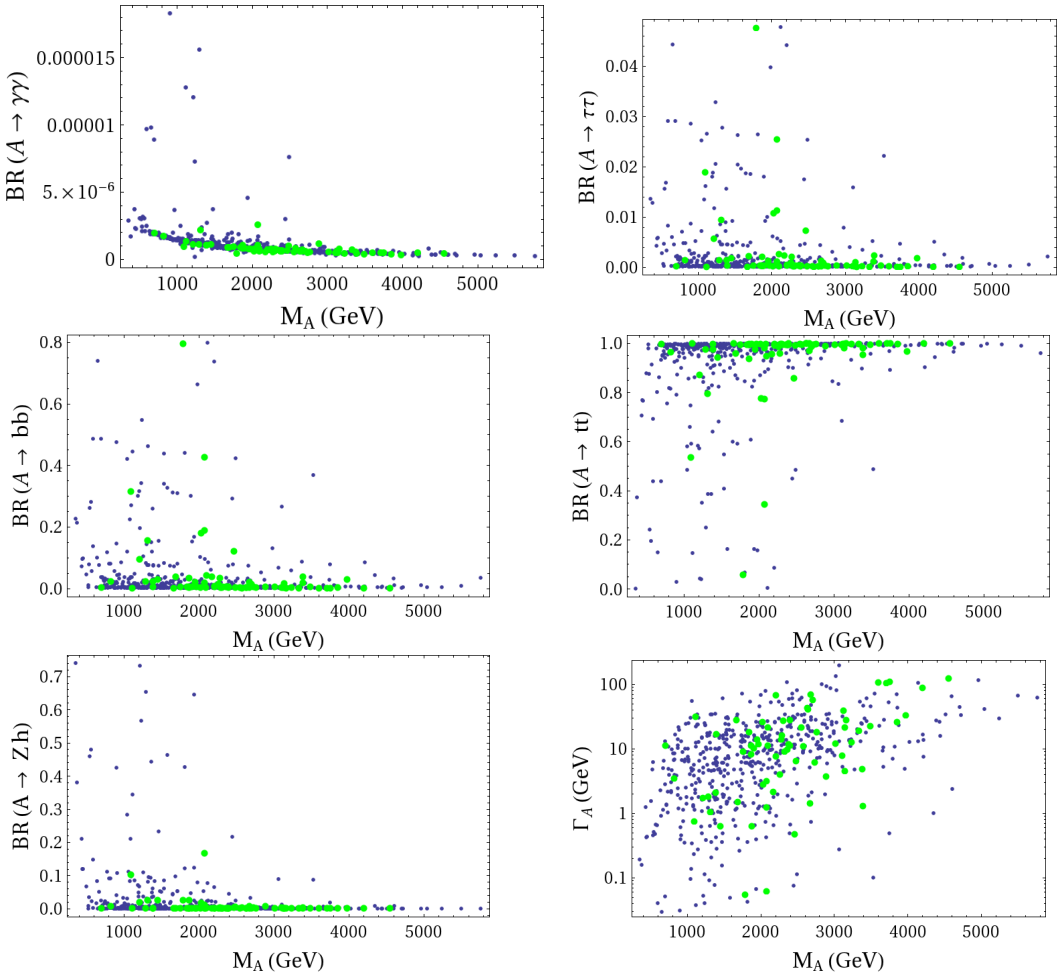

Figure 3.7: BR $(A \to \gamma\gamma)$ (top left), BR $(A \to \tau\tau)$ (top right), BR $(A \to bb)$ (middle left), BR $(A \to tt)$ (middle right), BR $(A \to Zh)$ (bottom left) and total A width (bottom right) for the allowed points of the parameter space.

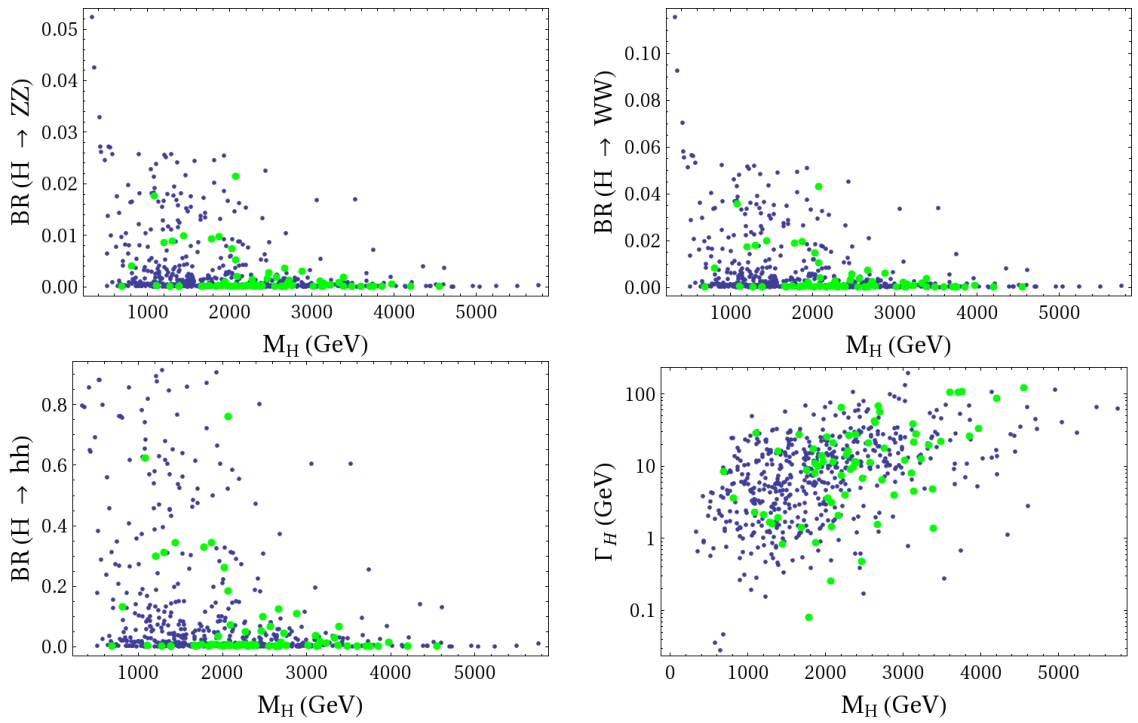

Figure 3.8: BR($H \to ZZ$) (top left), BR($H \to WW$) (top right), BR($H \to hh$) (bottom left) and H total width (bottom right) for the allowed points of the parameter space.

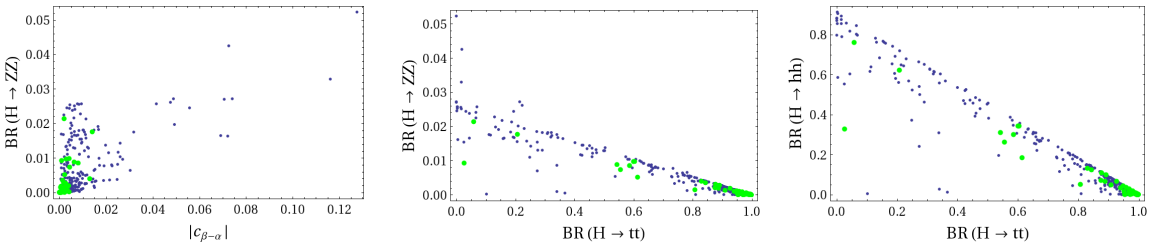

Figure 3.9: Correlation between BR($H \to ZZ$) with $|c_{\beta-\alpha}|$ (left), BR($H \to tt$) with BR($H \to ZZ$) (middle) and BR($H \to hh$) with BR($H \to tt$) (right) for the allowed points of the parameter space.

and BR($H \to hh$) with $BR(H \to tt)$ is shown in Fig. 3.9. Those depict that the allowed points with sizable BR($H \to ZZ, hh$) correspond to the small BR($H \to tt$) numbers. Similar conclusions can be drawn for the $H \to WW$ channel.

The charged Higgs total width $\Gamma_{H^\pm}$ is the sum of partial widths in $tb, cs, \tau\nu$ decay channels. In Fig 3.10, the branching ratios in ($H^+ \to t\bar{b}$, $\tau^+\nu_\tau$, $c\bar{s}$, W^+h) channels are presented, with the assumption of nonzero y_2's. BR($H^+ \to t\bar{b}$) is the largest for most part of the parameter space since the H^+tb coupling is generically large. The H^+tb coupling can become small due to partial cancellations between different terms in y^+_{00} of Eq. (3.19)

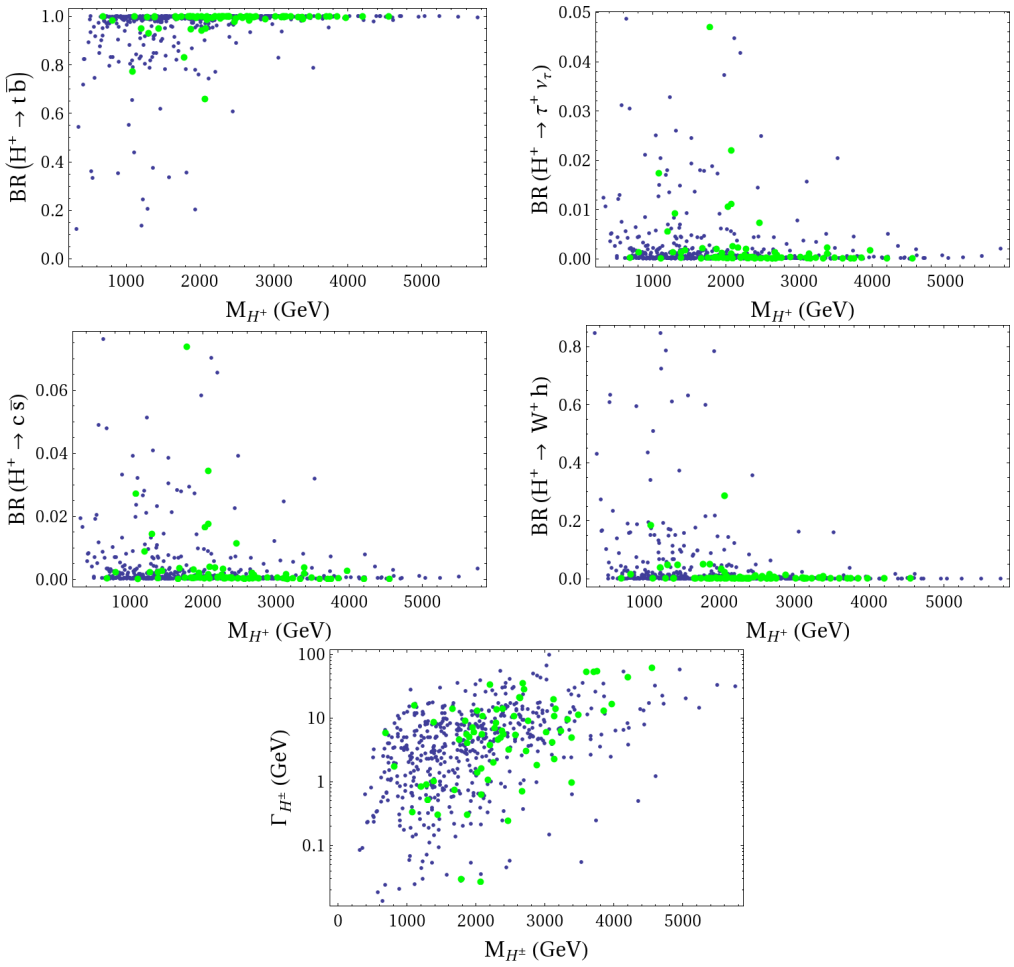

Figure 3.10: BR($H^+ \to t\bar{b}$) (top left), BR($H^+ \to \tau^+\nu_\tau$) (top right), BR($H^+ \to c\bar{s}$) (middle left), BR($H^+ \to W^+h$) (middle right) and H^+ total width (bottom) for the allowed points of the parameter space.

for few allowed points where sizable values of BR($H^+ \to \tau^+\nu_\tau, c\bar{s}, W^+h$) are possible.

The LHC signatures and the discovery potential in different channels for the LSS model BSM scalars are briefly discussed here. With the $BR(H, A \to XX)$ and $\kappa_{\phi gg}$ determined above for the LSS model, our effective analysis in Ref. [61] can be used to know whether one point in the parameter space is allowed by the 8 TeV LHC exclusion limits. The 14 TeV signal cross section ($\sigma \times BR$) of H, A in the $\gamma\gamma, \tau\tau, t\bar{t}$ channels at the LHC can also be found from those. In the constrained LSS model, the allowed BR($\phi \to \gamma\gamma$) is so small ($\sim 10^{-6}$) that even the lightest A ($\sim 600\ GeV$) is difficult to be searched at the LHC in this channel. Due to the lack of efficient LHC probe in the $\tau\tau$ channel, $BR_{\tau\tau} \sim 10^{-2}$ makes this mode very challenging to search for A, H. Although the $BR_{b\bar{b}}$ is reasonable, a

large QCD background makes it difficult to use as a search channel. This leaves the $t\bar{t}$ mode as a good possibility which is described with an example point of the LSS model. The $\kappa_{Agg,\,Hgg} \approx 2.5$ for the $m_{A,H} \approx 900$ GeV green point in Fig. 3.5, and from Ref. [61], this point is allowed after the LHC 8 TeV constraints with $\sigma(gg \to \phi) \approx 20$ fb at the 14 TeV LHC. Since $BR_{t\bar{t}}$ is large (~ 1), it can make the $t\bar{t}$ mode the most promising discovery channel. Expected BR($H^+ \to c\bar{s}$) values are of same order as BR($H^+ \to \tau^+\nu_\tau$). Since both of their coupling involving $H^\pm$ is $(m_{c,\tau} \tan\beta/v)$, the former rate enhanced by a color factor 3 and $m_c/m_\tau \approx 0.7$ lead to BR($H^+ \to c\bar{s}$) $\approx 3 * (0.7)^2 * BR(H^+ \to \tau^+\nu_\tau)$. The exclusion limit on $\sigma(H^+) \times$ BR($H^+ \to \tau\nu_\tau$) from Ref. [92] does not constrain the LSS model any further. The $H^\pm \to tb$ decay channel at CMS and ATLAS is discussed in Refs. [93] only for $m_{H^\pm} < 600$ GeV and it can be a very promising $H^\pm$ discovery channel in future. Detailed analysis of the LHC signatures of the $H^\pm$ in the context of a CP-violating Type-II 2HDM, is done in Refs. [94, 95], including the $B \to X_s\gamma$ and perturbativity constraints. A detailed analysis of the LHC signatures, including signal and background study of the BSM scalars for some LSS benchmark points, can be the subject of future studies.

To satisfy the experimental constraints, the amount of fine-tuning required in this model can be quantified by a measurement of sensitiveness of $\hat{v} \equiv v/f$ to the variation of all free parameters. Various measures of fine-tuning f_T are possible, One measure of fine tuning which is adopted in this work is along the way outlined in Ref. [96] and fine-tuning f_T is defined as:

$$f_T^{-1} \equiv \text{Max}_i \left| \frac{\partial(\log \hat{v}^2)}{\partial(\log \alpha_i)} \right| , \tag{3.21}$$

where α_i are the 9 input parameters discussed above. The $\hat{v}$ dependence on the input parameters can be obtained via Eq. (2.18) using Eqs. (3.2). The measure of fine-tuning, f_T is presented in Fig. 3.11 as a function of f. Minimum amount of fine-tuning required for all points that satisfy the constraints of Table B.1 is at a level of about 2 %. This implies that v cannot remain stable if a free parameter of the LSS model is varied more than 2 %.

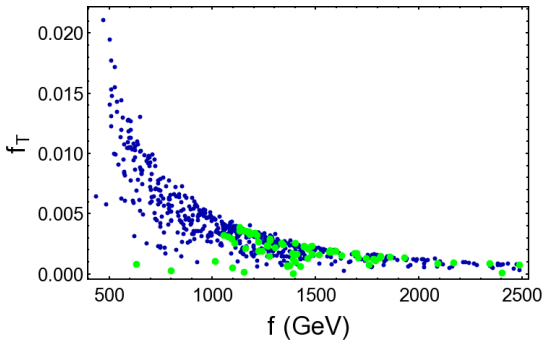

Figure 3.11: The fine-tuning f_T as a function of f in the LSS model.

When the precision constraints are also taken into account, the fine-tuning becomes worse than 0.3 %. The expressions in Eq. (3.2) imply $v^2/f^2 \propto (b^2/f^2 - m_1^2 \tan\beta/f^2)$, with the one-loop generated terms in the right-hand side given explicitly in Eq. (2.18). This model appears to be so severely fine-tuned because, for the allowed points in the parameter space, the Yukawa and gauge couplings are large, and that makes $b^2/f^2, m_{1,2}^2/f^2 \sim \mathcal{O}(1)$, overcoming the loop suppression. A cancellation between two $\mathcal{O}(1)$ quantities becomes necessary to ensure a small v^2/f^2, which in turn heavily fine-tunes the model. As f increases, the requirement of a more precise cancellation makes the fine-tuning worse as seen from Fig. 3.11.

Chapter 4

B-L Model

The ATLAS and CMS collaborations had earlier observed an excess of events at the LHC in the $\gamma\gamma$ channel around a mass of 750 GeV [8, 9]. This hint of a new resonance had enthused the studies of various possible new physics models where potentially a new heavy BSM scalar can be present. A work [13] was also pursued by us, explaining the excess from the decay of BSM scalar in a gauged $U(1)_{B-L}$ model [50]. The latest data which was analyzed few months after our work is published, does not confirm the excess [10, 11]. Many BSM scenario incorporate extended Higgs sector which is expected to have heavy scalars. Moreover, the $\gamma\gamma$ channel is an important new physics discovery channel. Here, a kind of BSM physics with a heavy scalar is explored, that leads to decays to the diphoton channel. The presence of such a heavy scalar is connected to the generation of neutrino masses (and their relative smallness) and (or) the presence of dark matter, in the context of the gauged $B - L$ model [50]. There are three extra scalars apart from the SM Higgs in this model. This model can also naturally explain the smallness of the Dirac neutrino mass term along with the presence of a scalar dark matter candidate with the correct relic abundance.

In this chapter, different gauged $B-L$ models are described, outlining their construction where tiny Dirac and Majorana neutrino mass terms are possible. Then, a particular gauged $B - L$ model [50, 97] is chosen, which can naturally explain a tiny Dirac neutrino

mass. How a scalar particle of that model can be a dark matter candidate with the required relic density is also demonstrated. The particle content of this model along with their gauge quantum numbers is provided, keeping in mind the neutrino mass generation, dark matter and the gauge anomaly cancellation. The structure of the scalar and the gauge sector of this model is presented, exploring the possibility of a simplified description of the scalar mass matrix.

4.1 Gauged $B - L$ Model: Neutrino Mass and Dark Matter

The gauged $B - L$ model [98, 99] is a well studied extension of the SM, where the SM gauge group is extended by an $U(1)_{B-L}$ symmetry. Historically, Baryon number (B) and Lepton flavor numbers ($L_i, i \equiv e, \mu, \tau$) were introduced to explain the stability of the proton and the absence of lepton flavor changing processes respectively. In the SM, the Baryon number B and the Lepton number L are accidentally conserved classical symmetries. Though both the B and L currents are anomalous, the combination $B - L$ is anomaly free. A detailed analysis of this model is provided in Ref. [50].

4.1.1 Neutrino Mass

One of the most important issues in neutrino physics is to understand the nature of neutrinos i.e. whether they are Majorana or Dirac particles. Answering this question is essential in understanding the basic physics of neutrino mass generation and mixing. Neutrinoless double beta decay experiments ($0\nu\beta\beta$) can potentially address this issue. Currently several ongoing experiments are looking for signals of $0\nu\beta\beta$, but none has observed any such signal so far [100–102]. At present, there are no concrete experimental or cosmological evidences to favor either Dirac or Majorana nature of neutrinos. In this thesis, one simple model based on a gauged $B-L$ symmetry is chosen, explaining naturally

tiny mass for Dirac neutrinos.

There are variants of the gauged $B-L$ model that explain either Dirac or Majorana neutrino mass, depending on the different $B-L$ quantum numbers assigned to the additional fermions. While $B-L$ is a symmetry of the SM, it is an accidental symmetry which need not be conserved by BSM physics. The introduction of a new $U(1)_{B-L}$ gauge symmetry results in new gauge triangle anomalies that need to be cancelled. The relevant anomalies in the gauged $U(1)_{B-L}$ are, Tr $\left(U(1)_{B-L}\left[SU(2)_L\right]^2\right)$, Tr $\left(U(1)_{B-L}\left[U(1)_Y\right]^2\right)$ and Tr $\left(U(1)_{B-L}\right)^3$. With the particle content of the SM, the first two anomalies are automatically canceled. The new particle content of the gauged $B-L$ model has to cancel the third anomaly to be consistent. The gauged $B-L$ symmetry can be embedded in other BSM scenarios, for example the Left-Right symmetric model and in GUT groups e.g. $SO(10)$.

In the conventional gauged $B-L$ model, the $B-L$ symmetry is established to be an anomaly free gauge symmetry with the addition of three right handed neutrinos ν_R^i, where each of them transform as -1 under the $U(1)_{B-L}$ [98, 99] satisfying $\sum U(1)_{B-L}^3 = 0$ and the gauge-gravitational anomalies. In addition to the right handed neutrinos, an $SU(2)_L$ singlet scalar χ_2 having two units of $B-L$ charge is also introduced. The $\chi_2 \sim 2$ under $B-L$ is chosen to break the gauge symmetry, so that ν_R can get a Majorana mass. In this case, the $SU(3)_C \otimes SU(2)_L \otimes U(1)_Y \otimes U(1)_{B-L}$ invariant Yukawa coupling for neutrinos is given by

$$-\mathcal{L}_Y^{\nu} = \sum_{i,j} y_{ij} \bar{L}_{iL} \hat{\Phi}^* \nu_{jR} + \frac{1}{2} \sum_{i,j} f_{ij} \bar{\nu}_{iR}^c \chi_2 \nu_{jR} + \text{h.c.}. \tag{4.1}$$

Here the VEV of the scalar χ_2 breaks this $B-L$ symmetry spontaneously, enabling the right handed neutrinos to acquire a Majorana mass term M_R proportional to the vacuum expectation value (VEV) u_2 of the singlet scalar. Therefore, if the $B-L$ symmetry breaking scale is far greater than the electroweak scale then the right handed neutrinos get a large mass, leading to a natural implementation of Type-I seesaw mechanism providing

a Majorana neutrino mass. But a very high $B-L$ breaking scale with a mass of the order of seesaw scale ($\sim 10^{14}$ GeV for Yukawa coupling ~ 1), makes it very difficult to probe the model at the LHC.

Apart from Majorana neutrinos, a $B-L$ model for Dirac neutrinos can also be constructed. To explore the possibility of Dirac neutrinos in this scenario, right handed neutrinos are added with -1 charge under $U(1)_{B-L}$ which allows one to have a gauge invariant Yukawa coupling for neutrinos. The $SU(3)_C \otimes SU(2)_L \otimes U(1)_Y \otimes U(1)_{B-L}$ invariant Yukawa coupling for neutrinos is then given by

$$-\mathcal{L}_Y^{\nu} = \sum_{i,j} y_{ij} \bar{L}_{iL} \hat{\Phi}^* \nu_{jR} + \text{h.c.} \tag{4.2}$$

where $\hat{\Phi}^* = i\tau_2 \Phi^*$ and $\Phi = (\phi^+, \phi^0)^T$ is the SM Higgs doublet. Since the right as well as left handed neutrinos transform non-trivially under the gauged $U(1)_{B-L}$ symmetry, this implies that the Majorana mass term for ν_{iR} is forbidden and neutrinos are Dirac particles. In this case, the $U(1)_{B-L}$ symmetry remains unbroken. However, in such a scenario the smallness of neutrino masses requires unappealingly small Yukawa couplings and the model does not provide any explanation for their smallness.

Recently, another simple choice of $B-L$ charges for right handed neutrinos, leading to an anomaly free $U(1)_{B-L}$ gauge symmetry has been proposed [50]. It is shown that such a charge assignment can lead to Dirac neutrinos with naturally small masses if the $B-L$ symmetry is spontaneously broken by $SU(2)_L$ singlet scalars χ_3, χ_6 transforming as 3 and -6 under the $U(1)_{B-L}$ symmetry respectively. Unlike the previous case, here the three right handed neutrinos transform as ν_{iR} with charges $(+5, -4, -4)$ under the $B-L$ symmetry [50, 97, 103, 104]. Since ν_{iR} charges are $(+5, -4, -4)$ under the $U(1)_{B-L}$, one can have

$$-(+5)^3 - (-4)^3 - (-4)^3 = +3, \tag{4.3}$$

$$-(5) - (-4) - (-4) = +3. \tag{4.4}$$

Thus, in this case also the model is free from gauge as well as gauge-gravitational anomalies. Now, the SM Higgs doublet $(\phi^+, \phi^0)^T$ does not connect ν_L with ν_R. Therefore, the neutrinos do not get mass from the standard electroweak symmetry breaking. To generate the neutrino masses three heavy Dirac singlet pair of fermions $N^i_{L,R}$ are added, transforming as -1 under the $B-L$ symmetry. These are required to arrange a seesaw mechanism for Dirac neutrinos, in a way analogous to that for Majorana neutrinos. The fermions $N^i_{L,R}$ will not change the anomaly cancellation conditions and the model will remain anomaly free. Now, for ν_{R2} and ν_{R3}, $(\bar{\nu}_L, \bar{N}_L)$ is linked to (ν_R, N_R) through the 2×2 mass matrix as follows

$$M_{\nu,N} = \begin{pmatrix} 0 & m_0 \\ m_3 & M \end{pmatrix}, \tag{4.5}$$

where m_0 comes from $\langle\phi^0\rangle$. Moreover, m_3 comes from $\langle\chi_3\rangle$, due to the Yukawa coupling $\bar{N}_L\nu_R\chi_3$. The N fermion mass, M is naturally large, so the Dirac seesaw [105] yields a small neutrino mass $m_3 m_0/M$.

Here, the presence of χ_3 with charge 3 under the $B-L$ symmetry means that it is impossible to construct an operator of any dimension for a Majorana mass term and L remains a conserved global symmetry, with $\nu_{L,R}$ and $N_{L,R}$ all having $L=1$. Any pair of left handed or right handed fermions cannot have $B-L$ charge $3, -3$ together. Therefore, they cannot form a $B-L$ invariant Lagrangian term with χ_3. Since ν_{R1} has charge $+5$ under the $U(1)_{B-L}$, it does not connect with ν_L or N_L directly, there is one massless neutrino in this case. The dimension-five operator $\bar{N}_L\nu_{R3}\chi_3^*\chi_3^*/\Lambda$ is allowed by $U(1)_{B-L}$ and would give it a small Dirac mass. Alternatively, one can add a second scalar χ_6 with charge -6 under the $U(1)_{B-L}$ to the model to account for mass of ν_{R1}. The spontaneous $B-L$ symmetry breaking (SSB) through $\langle\chi\rangle = u$ gives the right handed neutrinos a Majorana mass $M_{ij} = \sqrt{2}f_{ij}u$. If $u \;\; v$, the right handed neutrino mass scale is far greater than the electroweak scale, leading to a natural implementation of Type I seesaw mechanism.

4.1.2 Dark Matter

The new $B-L$ model discussed above [50], can also have a dark matter candidate when one new singlet scalar χ_2, with charge 2 under $U(1)_{B-L}$ symmetry, is included in the model. The possibility of having a long-lived self-interacting dark matter in this model is discussed in Ref. [106].

All right handed neutrinos ν_R's, vector-like fermions N's and the singlet scalars χ_3 and χ_6 are introduced already with $B-L$ charges required for neutrino mass generation. One more scalar singlet, χ_2 is introduced with $B-L$ charges 2. This singlet scalar with zero vev is taken as a dark matter candidate in this model. The $B-L$ symmetry is broken by the vevs of χ_3 and χ_6. Then the relevant terms like $\bar{N}_L\nu_{R1}\chi_6$, $\chi_2 N_L N_L$, $\chi_2 N_R N_R$, $\chi_2^3\chi_6$, $\chi_3^2\chi_6$ will appear in the Lagrangian. There is no symmetry in this model that can stabilize the dark matter i.e. χ_2 decay modes are possible here. To be a dark matter candidate which is stable, the decay lifetime of χ_2 must be bigger than the age of the Universe, which can be achieved in this model. The χ_2 Yukawa coupling with one N is taken as

$$L_{\chi_2} = f_1\chi_2 N_L N_L + f_2\chi_2 N_R N_R + h.c., \tag{4.6}$$

with the Yukawa coupling constants f_1, f_2. The $\nu_L - N_L$ and $\nu_R - N_R$ mixing can happen in this model with mixing parameters ξ_1, ξ_2 respectively, both of which are suppressed as $\sim 1/m_N$. The $\chi_2 \to \nu\nu$ decay is possible due to these mixing and the decay mode is function of f_i, ξ_i. With the parameter choice as used in Ref. [106], the limit from the age of the Universe can put the constraint as

$$\sqrt{f}\xi < 3\times 10^{-11}. \tag{4.7}$$

This will guarantee χ_2 to be stable up to present day, and allow it to be a dark matter candidate. The mass of the singlet Majorana neutrino is taken as $\sim 10^{13}$ GeV, which is also the usual mass scale for canonical seesaw mechanism.

The $U(1)_{B-L}$ gauge boson of the model, Z' couples to the nuclei through its couplings to u, d quarks. At the same time Z' also can decay to pair of χ_2, the dark matter candidate. From the interaction of χ_2 with nuclei through Z', the scattering of dark matter off the nuclei takes place, imposing a significant constraint from dark matter direct search experiments. Using the scattering cross section upper limit from the recent LUX data the lower limit on the Z' mass is around ~ 10 TeV [106].

The process of dark matter annihilation into the SM particles pairs determine the relic abundance of the dark matter. In this model, as discussed in Ref. [106], neither the SM Higgs nor Z' exchange is important for $\chi_2\chi_2$ annihilation. The important contributions come from the diagrams which emerge from the χ_2 interaction with other singlet scalars $\chi_{3,6}$. The thermal equilibrium with other SM particles are maintained in these diagrams through the SM Higgs coupling with $\chi_{3,6}$. This scenario can explain the relic abundance with the assumption that dark matter mass has to be greater than one of the physical scalars in the $\chi_{3,6}$ sector.

4.2 Particle Content of the Gauged $B - L$ Model

Gauged $B - L$ models require unconventional $B - L$ charges for the newly added particles to introduce naturally small mass terms for both Majorana [97] and Dirac [49,50] neutrinos. Here, the particles are added in a way to ensure that only tiny Dirac neutrino mass terms can be generated. The new particles introduced in any model can potentially lead to triangle anomalies. Thus, it is important to assign proper $B - L$ charges that ensure the

model to be anomaly free. The new particles can induce following triangular anomalies:

$$
\begin{aligned}
[SU(3)_c]^2\, U(1)_{B-L} \quad &\rightarrow \quad \sum_q (B-L)_{q_L} - \sum_q (B-L)_{q_R}, \\
[SU(2)_L]^2\; U(1)_{B-L} \quad &\rightarrow \quad \sum_l (B-L)_{l_L} + 3\sum_q (B-L)_{q_L}, \\
[U(1)_Y]^2\; U(1)_{B-L} \quad &\rightarrow \quad \sum_{l,q} \left[Y_{l_L}^2\,(B-L)_{l_L} + 3\,Y_{q_L}^2\,(B-L)_{q_L},\right] \\
&\qquad\qquad - \sum_{l,q} \left[Y_{l_R}^2\,(B-L)_{l_R} + 3\,Y_{q_R}^2\,(B-L)_{q_R}\right], \\
U(1)_Y\; [U(1)_{B-L}]^2 \quad &\rightarrow \quad \sum_{l,q} \left[Y_{l_L}\,(B-L)_{l_L}^2 + 3\,Y_{q_L}\,(B-L)_{q_L}^2\right] \\
&\qquad\qquad - \sum_{l,q} \left[Y_{l_R}\,(B-L)_{l_R}^2 + 3\,Y_{q_R}\,(B-L)_{q_R}^2\right], \\
[U(1)_{B-L}]^3 \quad &\rightarrow \quad \sum_{l,q} \left[(B-L)_{l_L}^3 + 3\,(B-L)_{q_L}^3\right] - \left[(B-L)_{l_R}^3 + 3\,(B-L)_{q_R}^3\right], \\
[\text{Gravity}]^2\; [U(1)_{B-L}] \quad &\rightarrow \quad \sum_{l,q} \left[(B-L)_{l_L} + 3\,(B-L)_{q_L}\right] - \left[(B-L)_{l_R} + 3\,(B-L)_{q_R}\right].
\end{aligned}
$$

The $B-L$ quantum number of the fermions should be allotted in a way such that all these anomalies vanish for the usual $B-L$ charge of the SM fermions.

The $SU(2)_L$ singlet scalars are introduced in the model to break the gauge $B-L$ symmetry and construct proper Dirac mass terms. Also, one of them can potentially be a dark matter candidate. Proper $B-L$ quantum number allocation of these scalars is also necessary to accommodate a long lived dark matter particle in the model for Dirac neutrinos, further extended in Ref. [106]. For this thesis, an extended version of the model discussed in [106] is studied, where two pairs of $SU(2)_L$ singlet exotic "quarks", $X_{L,R}$ and $Y_{L,R}$ are introduced. Although they are $SU(2)_L$ singlets, these exotic quarks do carry $SU(3)_c$ colour charges as well as $U(1)_Y$, $U(1)_{B-L}$ charges. It has already been shown in [50], that for the case when the exotic quarks X, Y are not present, the model is completely anomaly free. It can also be easily seen that the addition of the X, Y quarks does not spoil the anomaly cancellation and hence the model remains anomaly free.

In Table 4.1, apart from the SM particles three right handed neutrinos ν_R^i, three

$SU(2)_L$ singlet heavy fermions $N^i_{L,R}$ (as in the previous model [106]) and two pair of exotic "quarks" $X_{L,R}$, $Y_{L,R}$ which carry color and electromagnetic charges but are singlet under $SU(2)_L$. The $SU(3)_c \times SU(2)_L \times U(1)_Y$ and $U(1)_{B-L}$ charge assignment for the fermions and scalars of the model are as shown in Table 4.1 and Table 4.2 respectively:

Fields	$SU(3)_c \times SU(2)_L \times U(1)_Y$	$U(1)_{B-L}$	Fields	$SU(3)_c \times SU(2)_L \times U(1)_Y$	$U(1)_{B-L}$
Q^i_L	$(3, 2, \frac{1}{3})$	$\frac{1}{3}$	L^i_L	$(1, 2, -1)$	-1
u^i_R	$(3, 1, \frac{4}{3})$	$\frac{1}{3}$	l^i_R	$(1, 1, -2)$	-1
d^i_R	$(3, 1, -\frac{2}{3})$	$\frac{1}{3}$	ν^1_R	$(1, 1, 0)$	5
ν^2_R	$(1, 1, 0)$	-4	ν^3_R	$(1, 1, 0)$	-4
N^i_L	$(1, 1, 0)$	-1	N^i_R	$(1, 1, 0)$	-1
X_L	$(3, 1, \frac{4}{3})$	3	X_R	$(3, 1, \frac{4}{3})$	0
Y_L	$(3, 1, -\frac{4}{3})$	-3	Y_R	$(3, 1, -\frac{4}{3})$	0

Table 4.1: The $SU(3)_c \times SU(2)_L \times U(1)_Y$ and $U(1)_{B-L}$ charge assignment for the fermions. Here $i = 1, 2, 3$ represents the three generations.

In Table 4.2, $\Phi = (\phi^+, \phi^0)^T$ is the usual $SU(2)_L$ doublet scalar and χ_i are $SU(2)_L$ singlet scalars. The charge assignment for the scalars in this model (which are same as in [106]) are as follows:

Fields	$SU(3)_c \times SU(2)_L \times U(1)_Y$	$U(1)_{B-L}$	Fields	$SU(3)_c \times SU(2)_L \times U(1)_Y$	$U(1)_{B-L}$
Φ	$(1, 2, 1)$	0	χ_2	$(1, 1, 0)$	2
χ_3	$(1, 1, 0)$	3	χ_6	$(1, 1, 0)$	-6

Table 4.2: The $SU(3)_c \times SU(2)_L \times U(1)_Y$ and $U(1)_{B-L}$ charge assignment for the scalars.

4.3 Scalar and Gauge Sector of $B - L$ Model

In this section, the details of the scalar and Yukawa sector of the gauged B-L model are discussed and probable heavy resonance candidates are identified. With the scalar sector of the gauged $B - L$ model, given in the Table 4.2, the $B - L$ gauge invariant scalar

potential of this model is given by

$$\begin{aligned} V &= -\mu_0^2(\Phi^\dagger\Phi) + m_2^2(\chi_2^*\chi_2) - \mu_3^2(\chi_3^*\chi_3) - \mu_6^2(\chi_6^*\chi_6) + \frac{1}{2}\lambda_0(\Phi^\dagger\Phi)^2 + \frac{1}{2}\lambda_2(\chi_2^*\chi_2)^2 \\ &+ \frac{1}{2}\lambda_3(\chi_3^*\chi_3)^2 + \frac{1}{2}\lambda_6(\chi_6^*\chi_6)^2 + \lambda_{02}(\chi_2^*\chi_2)(\Phi^\dagger\Phi) + \lambda_{03}(\chi_3^*\chi_3)(\Phi^\dagger\Phi) + \lambda_{06}(\chi_6^*\chi_6)(\Phi^\dagger\Phi) \\ &+ \lambda_{23}(\chi_2^*\chi_2)(\chi_3^*\chi_3) + \lambda_{26}(\chi_2^*\chi_2)(\chi_6^*\chi_6) + \lambda_{36}(\chi_3^*\chi_3)(\chi_6^*\chi_6) + [\frac{1}{2}f_{36}(\chi_3^2\chi_6) + h.c.] \\ &+ [\frac{1}{6}\lambda'_{26}(\chi_2^3\chi_6) + h.c.]. \end{aligned} \tag{4.8}$$

The scalar fields have vacuum expectation values as $\langle\phi^0\rangle = v, \langle\chi_3\rangle = u_3, \langle\chi_6\rangle = u_6$ and the fields are expanded around those minima. Moreover, the singlet scalar χ_2, being a dark matter candidate here, does not acquire any vev i.e. $\langle\chi_2\rangle = 0$. The minimum of the V is given as

$$V_0 = -\mu_0^2v^2 - \mu_3^2u_3^2 - \mu_6^2u_6^2 + \lambda_0\frac{v^4}{2} + \lambda_3\frac{u_3^4}{2} + \lambda_6\frac{u_6^4}{2} + \lambda_{03}u_3^2v^2 + \lambda_{06}u_6^2v^2 + \lambda_{36}u_3^2u_6^2 + f_{36}\frac{u_3^2u_6}{2}, \tag{4.9}$$

with the potential minimization conditions,

$$\begin{aligned} \mu_0^2 &= \lambda_0v^2 + \lambda_{03}u_3^2 + \lambda_{06}u_6^2, \\ \mu_3^2 &= \lambda_3u_3^2 + \lambda_{03}v^2 + \lambda_{36}u_6^2 + f_{36}u_6, \\ \mu_6^2 &= \lambda_6u_6^2 + \lambda_{06}v^2 + \lambda_{36}u_3^2 + \frac{f_{36}u_3^2}{2u_6}. \end{aligned} \tag{4.10}$$

There are (no of scalars) physical scalars in the gauged $B-L$ model and those are listed below. Since $\langle\chi_2\rangle = 0$, there is one dark matter scalar boson χ_2 with mass given by

$$m_{\chi_2}^2 = m_2^2 + \lambda_{02}v^2 + \lambda_{23}u_3^2 + \lambda_{26}u_6^2. \tag{4.11}$$

This model has three CP-odd scalar degrees of freedom, spanning the basis $G, \sqrt{2}Im(\chi_3), \sqrt{2}Im(\chi_6)$. Two linear combinations amongst these are eaten as Goldstone bosons by the SM Z and

the neutral Z' bosons, leaving one physical CP-odd scalar state as

$$A = \sqrt{2} Im(2u_6\chi_3 + u_3\chi_6)/\sqrt{u_3^2 + 4u_6^2}, \tag{4.12}$$

with its mass given by

$$m_A^2 = -f_{36}(u_3^2 + 4u_6^2)/2u_6. \tag{4.13}$$

There are three physical CP-even scalar bosons spanning the basis $[h, \sqrt{2}Re(\chi_3), \sqrt{2}Re(\chi_6)]$, with the 3×3 mass-squared matrix given by

$$M^2 = \begin{pmatrix} 2\lambda_0 v^2 & 2\lambda_{03}u_3 v & 2\lambda_{06}u_6 v \\ 2\lambda_{03}u_3 v & 2\lambda_3 u_3^2 & 2\lambda_{36}u_3 u_6 + f_{36}u_3 \\ 2\lambda_{06}u_6 v & 2\lambda_{36}u_3 u_6 + f_{36}u_3 & 2\lambda_6 u_6^2 - f_{36}u_3^2/2u_6 \end{pmatrix}. \tag{4.14}$$

The mass matrix in Eq. 4.14 can be diagonalized to give three CP-even scalars which will be linear combinations of Φ, χ_3, χ_6 scalars. However for sake of illustration, a special case of the generic mass matrix is chosen, and that takes a simple form with the assumption

$$\begin{aligned}
2\lambda_0 v^2 &= a^2 && \Rightarrow \lambda_0 = \frac{a^2}{2v^2}, \\
4\lambda_{03}u_3 v &= ab && \Rightarrow \lambda_{03} = \frac{ab}{4u_3 v}, \\
4\lambda_{06}u_6 v &= ab && \Rightarrow \lambda_{06} = \frac{ab}{4u_6 v}, \\
2\lambda_3 u_3^2 &= b^2 && \Rightarrow \lambda_3 = \frac{b^2}{2u_3^2}, \\
4\lambda_{36}u_3 u_6 + 2f_{36}u_3 &= b^2 && \Rightarrow f_{36} = \frac{1}{2\,u_3}\left(b^2 - 4\lambda_{36}u_3 u_6\right), \\
2\lambda_6 u_6^2 - \frac{f_{36}u_3^2}{2u_6} &= b^2 && \Rightarrow \lambda_6 = \frac{1}{2u_6^2}\left(b^2 + \frac{f_{36}u_3^2}{2u_6}\right),
\end{aligned} \tag{4.15}$$

where a and b are two independent parameters. With these simplifying assumptions, the

mass matrix of Eq. 4.14 becomes

$$\begin{pmatrix} a^2 & ab/2 & ab/2 \\ ab/2 & b^2 & b^2/2 \\ ab/2 & b^2/2 & b^2 \end{pmatrix}. \tag{4.16}$$

The eigenvalues of the mass matrix in Eq. 4.16 are given by

$$\begin{aligned} \Sigma_1 &= \frac{1}{4}\left(2a^2 + 3b^2 - \sqrt{4a^4 - 4a^2b^2 + 9b^4}\right), \\ \Sigma_2 &= \frac{b^2}{2}, \\ \Sigma_3 &= \frac{1}{4}\left(2a^2 + 3b^2 + \sqrt{4a^4 - 4a^2b^2 + 9b^4}\right). \end{aligned} \tag{4.17}$$

The masses of the scalars are then given by

$$m_1 = \sqrt{2\Sigma_1}, \quad m_2 = \sqrt{2\Sigma_2}, \quad m_3 = \sqrt{2\Sigma_3}. \tag{4.18}$$

One scalar combination mass can be fixed as the 125 GeV and another having a larger mass (which is taken as 750 GeV in this thesis). For sake of definiteness, the first eigenstate is identified with the 125 GeV scalar (henceforth called "Higgs") and the second eigenstate as the heavy scalar i.e. $m_1 = 125$ GeV and $m_2 = 750$ GeV. The mass of the third scalar then depends on the value of a and b. Solving for a and b, it is found that $a = 108.5$ GeV and $b = 750$ GeV lead to the desired masses for the scalars, m_1 and m_2. For this parameter choice, the mass of the third scalar m_3 then becomes $m_3 = 1.30$ TeV.

The masses of the CP-odd scalar, dark matter and Z' are dependent on the values of other free parameters e.g. the value of vevs u_3, u_6, the $U(1)_{B-L}$ coupling g_X as well as on the quartic coupling of scalars λ_{ij}. It should be noted that in this limit, other scalars as well as the Z' boson can be made heavy (assuming all couplings to be $\sim O(1)$) in congruence with the experimental bounds for these particles [106]. Also, the mass of the Z' boson is kept at $m_{Z'} > 12$ TeV which is well above the dark matter direct detection

bound from the LUX experiment [106, 107].

It should be noted that in the simplified mass matrix of Eq. 4.16, not all of the λ_{ij} are independent parameters, as evident from Eq. 4.15. The mass of dark matter χ_2 is also dependent on the additional parameter m_2^2 and the quartic couplings λ_{i2}; $i = 0, 3, 6$. As required by the constraints from the LUX dark matter direct detection experiment [106, 107], the presence of a heavy Z' is secured for a large range of parameter space. Since the mass of the dark matter m_{χ_2} depends on additional free parameters, it can be chosen to be lighter than any other scalar. This leads to two distinct cases; when the dark matter mass is less than half of the heavy scalar mass, then the heavy resonance can decay into dark matter and it can lead to a significant invisible decay width. In the case where the dark matter mass is greater than half of the heavy scalar mass, this decay is kinematically forbidden. In the next chapter, both these cases are studied in detail, with a discussion on heavy scalar phenomenology.

Chapter 5

Heavy Scalar in the Gauged $B - L$ Model

The gauged $B - L$ model discussed in Chapter 4 has a rich structure in the scalar sector at TeV scale. All the new scalars are introduced in the model either from the requirement of neutrino mass generation or to have a dark matter candidate. To probe the gauged $B - L$ model at the LHC, it is important to explore BSM scalar production and decay modes. All the BSM scalars of the gauged $B - L$ model are $SU(2)$ singlets and EM neutral. Therefore, their decay to the SM fermions and gauge bosons are highly suppressed. Among other decay modes, the $\gamma\gamma$ channel is a clean one i.e. relatively less affected by the background. So, BSM scalar phenomenology can be studied with an emphasis on the $\gamma\gamma$ channel.

In this chapter, main focus is on the phenomenology of a heavy BSM scalar. The LHC phenomenology of BSM scalars of the gauged $B - L$ model described in Chapter 4, is presented in this chapter. In the models described in Refs. [50, 106], it is hard to directly probe these models in the diphoton channel at the LHC due to a small cross section. Compared to the model described in Ref. [106] the fermion sector is modified here, with the addition of two exotic colored fermion pair, $X_{L,R}, Y_{L,R}$. These newly added fermions can modify heavy BSM scalar phenomenology at the LHC, contributing through the triangle loops. These new quarks can boost BSM scalar gluon fusion production and the

loop dominated $\gamma\gamma, Z\gamma, ZZ$ decays, and those effects are quantified in this chapter. For the purpose of following our work [13], the heavy scalar mass is taken to be 750 GeV. How the previously observed 750 GeV excess was explained in our work is also outlined.

5.1 Higgs Boson and BSM Scalars

Apart from the 125 GeV Higgs boson, other heavy scalar particles are also present in the gauged $B-L$ model discussed in Chapter 4. Three extra physical scalars apart from the SM-like Higgs are present in this model. Two of these scalars are CP-even, while one is CP-odd. In this work, one CP-even spin-0 particle of the gauged $U(1)_{B-L}$ model is taken to have mass of 750 GeV. Other BSM scalars are also chosen to be heavier than the SM Higgs.

In Chapter 4, the scalar sector of the gauged B-L model is analyzed in a simplified set-up which provides three physical scalar combinations. For the sake of presentation, the simplified mass matrix of Eq. 4.16 is taken. This matrix mixes real part of the ϕ^0, χ^3, χ^6 fields i.e. $\phi_0^R, \chi_3^R, \chi_6^R$ states with each other. Diagonalizing the simplified mass matrix, physical scalar eigenstates are found as

$$\begin{aligned} h &= \cos\theta\,\phi_0^R - \sin\theta(\chi_6^R + \chi_3^R), \\ H_1 &= (\chi_6^R - \chi_3^R), \\ H_2 &= \sin\theta\,\phi_0^R + \cos\theta(\chi_6^R + \chi_3^R), \end{aligned} \tag{5.1}$$

with the mass eigenvalues m_1, m_2, m_3 of Eq. 4.18 being assigned with scalar states h, H_1, H_2 respectively. The mixing angle θ is expressed as

$$\tan 2\theta = \frac{2\sqrt{2}ab}{3b^2 - 2a^2}. \tag{5.2}$$

One of the scalar combinations, $h = \cos\theta\,\phi_0^R - \sin\theta(\chi_6^R + \chi_3^R)$ can be identified as the 125 GeV Higgs which is discovered at the LHC. The recent results from both the

ATLAS and CMS experiments suggest that the 125 GeV scalar couples to the SM gauge bosons and fermions in a way very similar to the SM Higgs. From Eq. 5.1, it is observed that in the $B-L$ model, there exists a decoupling limit where h will have almost SM Higgs-like couplings with other SM particles. As is evident from Eq. 5.1, with $\sin\theta \to 0$, the 125 GeV physical scalar state has minimal contribution from the scalar singlets χ_3, χ_6. This fixes the h couplings to the SM gauge bosons to be almost SM like.

Another scalar H_1 with mass m_2, is chosen to have a mass of 750 GeV i.e. $b = 750$ GeV. For the case of $a = 108.5$ GeV and $b = 750$ GeV which keeps the mass of h state at 125 GeV, the mixing parameters are $\cos\theta = 0.997$, $\sin\theta = 0.069$. For other a, b values which can keep h at 125 GeV and H_1 with heavier mass, the mixing angle remains small, within the experimental limit. This implies that in this model the couplings of the scalar h of mass 125 GeV with W, Z gauge bosons are almost SM like. The deviations from the SM couplings are small and are well within the experimental limits (see Ref. [108]).

The heavy scalar H_1 in this model is chosen to be the BSM scalar whose phenomenology is going to be explored here. The Yukawa couplings of this scalar with fermions are discussed in detail in Ref. [106]. Due to inclusion of two new quarks, apart from its coupling to the scalars, χ_3 has following Yukawa couplings:

$$\mathcal{L}_{\chi_3} \;=\; f_X\,\bar{X}_L X_R \chi_3 \;+\; f_Y\,\bar{Y}_L Y_R \chi_3^* + h.c.. \tag{5.3}$$

As evident from Eq. 5.3 both quarks X, Y acquire mass after χ_3 spontaneously breaks the $B-L$ symmetry. The fermionic masses are proportional to the VEV u_3 of χ_3. In a $B-L$ symmetric Lagrangian of the model, a Yukawa term of the singlet scalar χ_6 ($\chi_6 \sim -6$ under $U(1)_{B-L}$) with these new quarks, cannot be included. Therefore, the χ_3 Yukawa coupling of Eq. 5.3 generates the Yukawa coupling of the scalar $H_1 \equiv \chi_3 - \chi_6$. Owing to the coupling of χ_3 with quarks X, Y; the heavy scalar H_1 (with a mass of 750 GeV) can be efficiently produced through the gluon-gluon fusion at the LHC. The production and decay of this scalar are discussed in detail in the next section.

5.2 Phenomenology of the Heavy Scalar H_1

In this section, the details of the LHC production and decay channels of H_1 are discussed, identifying it as a heavy scalar with mass of 750 GeV. It is explained how, in the gauged $B-L$ model, the enhanced diphoton decay of this scalar can lead to better search prospects in this channel. Moreover, as the decay rates of H_1 to the SM fermion, Higgs and other gauge boson channels are suppressed, that can explain the non-observation of this scalar in other channels.

The heavy scalar $H_1 \equiv \chi_6^R - \chi_3^R$ does not couple to the SM fermions at the tree level. So, the H_1 production rate through the SM quark dominated triangle loops is negligibly small. From the χ_3 Yukawa coupling to X, Y given in Eq. 5.3, the linear combination $H_1 = (\chi_6^R - \chi_3^R)$ also can couple to the new quarks. Therefore, H_1 can dominantly be produced by gluon-gluon fusion through the triangle loops involving X, Y.

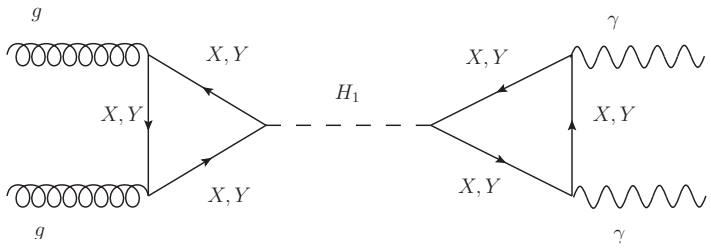

Figure 5.1: Gluon fusion production and diphoton channel decay of heavy scalar.

If both X, Y are heavier than $m_{H_1}/2$, then the tree level H_1 decay to the pair of X, Y is kinematically forbidden. In such a case, its decay to two photons through triangular loop involving X, Y as shown in Fig 5.1, can be significant, leading to an excess in the diphoton channel. Apart from its decay to two photons, H_1 can also decay to a pair of gluons or Higgs (h) bosons, as shown in Fig. 5.2 and Fig 5.3 respectively. Moreover, if the mass of the dark matter $m_{\chi_2} \leq m_{H_1}/2$, then it can also decay into a pair of dark matter particles as shown in Fig. 5.4. This can lead to an appreciable invisible decay width of H_1. From the terms of the scalar potential with coefficients λ_{03} and λ_{06} in Eq. 4.8, using the simplified definitions of Eq. 4.15, it is shown that the pair of SM like Higgs (h) couple to both χ_3 and χ_6 with the same coupling strength. This will result in

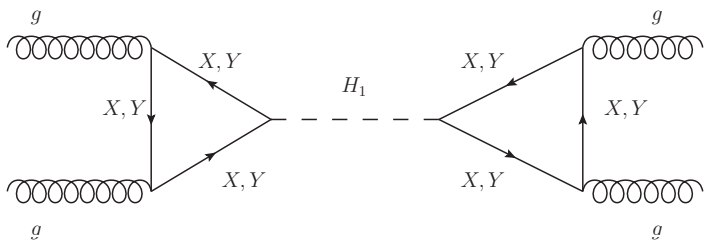

Figure 5.2: Gluon fusion production and decay of heavy scalar to two gluons.

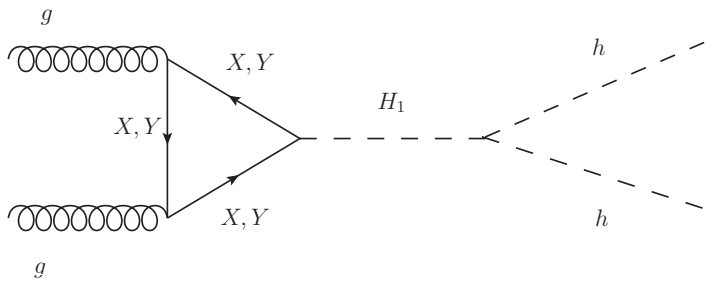

Figure 5.3: Gluon fusion production and decay of heavy scalar to two Higgs. Owing to negligible H_1hh coupling, this decay mode is highly suppressed.

a cancellation of their interaction strength with $H_1 \equiv \chi_3 - \chi_6$, resulting in a very small H_1hh coupling. Hence the $H_1 \to hh$ decay will be negligibly small. The heavy scalar H_1 is primarily a mixed state of $SU(2)_L$ singlets χ_3 and χ_6, as shown in Eq. 5.1. Therefore, it does not have a tree level coupling to the SM fermions as these $SU(2)_L$ singlet scalars cannot form gauge invariant Yukawa term with the SM fermions. As the χ_3 and χ_6 scalars are electromagnetically neutral and singlet under $SU(2)$, H_1 does not couple to W and Z boson pair. Therefore, its decays to the dilepton, dijet and diboson channels are extremely suppressed. This observation is also in line with the experimental results which show lack

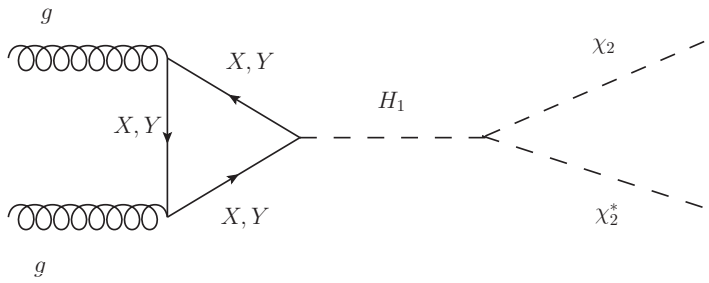

Figure 5.4: Production and decay of heavy scalar to dark matter. This decay mode is only allowed if $m_{\chi_2} \leq m_{H_1}/2$.

of any statistically significant excess in these channels.

Apart from the earlier hint of the 750 GeV excess, ATLAS and CMS have not seen any hint or excess in any channel at other masses. Unless they are hidden due to very small decay rate in all decay channels, all the new particles (except the dark matter) should be sufficiently massive. So, the mass of the CP-odd scalar of this model can be safely fixed at $m_A > 1$ TeV. As obtained in Section 5.1, the mass of the other CP-even scalar (H_2) is also greater than 1 TeV. The mass of the dark matter m_{χ_2} is left as a free parameter and depending on its mass, the $H_1 \to \chi_2 \chi_2^*$ decay may or may not be kinematically forbidden (Here χ_2^* denotes the anti-particle). Both the cases will be considered in the next section.

Thus, the only prominent decay modes of interest are $H_1 \to \gamma\gamma$, $H_1 \to gg$ and if $m_{\chi_2} \leq m_{H_1}/2$ then $H_1 \to \chi_2\chi_2$ also. The partial decay widths of H_1 in these modes are given as,

$$\begin{aligned}
\Gamma(H_1 \to \gamma\gamma) &= \frac{\alpha^2 m_{H_1}}{64\pi^3} \left| 2N_c \sum_{i=X,Y} f_i Q_i^2 \sqrt{\tau_i}(1 + (1-\tau_i) f(\tau_i) \right|^2 , \\
\Gamma(H_1 \to gg) &= \frac{\alpha_s^2 m_{H_1}}{32\pi^3} \left| 2 \sum_{i=X,Y} f_i \sqrt{\tau_i}(1 + (1-\tau_i) f(\tau_i) \right|^2 , \\
\Gamma(H_1 \to \chi_2\chi_2) &= \frac{(\kappa_{\chi_2} u_3)^2}{32\pi m_{H_1}} \left(1 - \frac{4m_{\chi_2}^2}{m_{H_1}^2}\right)^{\frac{1}{2}}
\end{aligned} \tag{5.4}$$

where $\tau_i = 4m_i^2/m_{H_1}^2$ with m_i, Q_i being corresponding fermion (X, Y) masses and electromagnetic (EM) charges respectively. The f_i s here denote the Yukawa couplings with the scalar H_1 whereas α_s, α denote strong and EM interaction coupling strengths respectively. N_c is the color factor which is 3 for the quarks and 1 for the leptons. Also, without loss of generality, the dimensionful coupling between χ_2 and H_1 has been normalized by the vev u_3, with κ_{χ_2} being a dimensionless parameter. As given in Eq. 4.8, the κ_{χ_2} parameter is a function of the vevs u_3, u_6 as well as the quartic couplings between χ_2 and χ_3, χ_6 fields.

The $f(\tau_i)$ for this case, with $m_{X,Y} > m_{H_1}/2$ is given as

$$f(\tau_i) = (\sin^{-1}[\frac{1}{\sqrt{\tau_i}}])^2. \tag{5.5}$$

In addition to these decay modes, H_1 can also decay to $Z\gamma$ and ZZ through the triangular loops involving the X, Y quarks. For $m_Z^2 << m_{H_1}^2$, which is valid here, the decay width to the $Z\gamma$ and ZZ channels are given as

$$\begin{aligned}
\Gamma(H_1 \to Z\gamma) &= \frac{\alpha^2 m_{H_1}}{32\pi^3 s_W^2 c_W^2} \left| 2N_c \sum_{i=X,Y} f_i Q_i (-Q_i s_W^2) \sqrt{\tau_i}(1 + (1-\tau_i) f(\tau_i) \right|^2, \\
\Gamma(H_1 \to ZZ) &= \frac{\alpha^2 m_{H_1}}{64\pi^3 s_W^4 c_W^4} \left| 2N_c \sum_{i=X,Y} f_i (-Q_i s_W^2)^2 \sqrt{\tau_i}(1 + (1-\tau_i) f(\tau_i) \right|^2,
\end{aligned} \tag{5.6}$$

where $s_W = \sin\theta_W$, $c_W = \cos\theta_W$ and θ_W is the electroweak angle. Since the new quarks X, Y are both $SU(2)_L$ singlets and all the three decays namely $H_1 \to \gamma\gamma, Z\gamma, ZZ$ proceed through the same triangle loops, the ratio of the partial decay widths in these three channels are given by

$$\frac{\Gamma(H_1 \to Z\gamma)}{\Gamma(H_1 \to \gamma\gamma)} \approx 2\tan^2\theta_W, \qquad \frac{\Gamma(H_1 \to ZZ)}{\Gamma(H_1 \to \gamma\gamma)} \approx \tan^4\theta_W. \tag{5.7}$$

As clear from Eq. 5.7, the loop decays of H_1 to $Z\gamma$ and ZZ are suppressed compared to the $\gamma\gamma$ decays by a factor proportional to the electroweak mixing angle. Thus, H_1 is an ideal candidate for search in the diphoton channel at the future LHC run along with lack of significant excess in other decay channels.

For H_1 to be a viable candidate to be observed in the diphoton channel, it not only requires to have an enhanced cross section in the 13 TeV run of the LHC but should also explain the non-observation of any statistically significant excess in different channels in the previous 8 TeV LHC run. In this model, some significant decay channels for H_1 are the loop induced gg, $\gamma\gamma$, $Z\gamma$ and ZZ decays. Moreover, if $m_{\chi_2} \leq m_{H_1}/2$ then it can also decay to two dark matter particles through the $H_1\chi_2\chi_2^*$ tree level coupling. The 8 TeV

LHC constraints on $\sigma \times BR(H_1 \to f_i f_j)$; $f_{i,j} \equiv g, \gamma, Z, \chi_2$, of these channels are [109,110]:

$$\begin{aligned}
\sigma \times \mathrm{Br}(\mathrm{H}_1 \to \gamma\gamma) &< 1.5\,\mathrm{fb}, \\
\sigma \times \mathrm{Br}(\mathrm{H}_1 \to \mathrm{gg}) &< 2500\,\mathrm{fb}, \\
\sigma \times \mathrm{Br}(\mathrm{H}_1 \to \mathrm{inv}) &< 800\,\mathrm{fb} \\
\sigma \times \mathrm{Br}(\mathrm{H}_1 \to \mathrm{Z}\gamma) &< 11\,\mathrm{fb}, \\
\sigma \times \mathrm{Br}(\mathrm{H}_1 \to \mathrm{ZZ}) &< 12\,\mathrm{fb}.
\end{aligned} \tag{5.8}$$

Compared to the $H_1 \to \gamma\gamma$, the ZZ, $Z\gamma$ decays are suppressed. Furthermore, as shown in Eq. 5.8, the exclusion limits on these decay channels are also relatively weaker. Thus, the constraints from these decay channels are quite weak and do not impose any additional constraints on the allowed parameter range. Finally the H_1 decay to gluons is also well below the experimental limit and does not impose any additional constraints on the allowed parameter range. The only significant constraint from the 8 TeV run comes from the $\gamma\gamma$ decay channel which is also plotted in the Fig. 5.5 and Fig. 5.6 later. The constraints from the other channels, including the invisible decay to dark matter are rather weak and do not give any additional constraint.

Numerical values of $\sigma \times BR$ for both the cases, $m_{\chi_2} > m_{H_1}/2$ and $m_{\chi_2} \leq m_{H_1}/2$ in all the decay channels are presented. For the numerical analysis, the heavy scalar mass is taken as 750 GeV. For the first case, a benchmark point ($m_X = 1$ TeV and $u_3 = 205$ GeV) is chosen on the $\gamma\gamma$ exclusion line and the values for these decay channels are given as:

$$\begin{aligned}
\sigma \times \mathrm{Br}(\mathrm{H}_1 \to \gamma\gamma) &= 1.5\,\mathrm{fb}, \\
\sigma \times \mathrm{Br}(\mathrm{H}_1 \to \mathrm{gg}) &= 490\,\mathrm{fb}, \\
\sigma \times \mathrm{Br}(\mathrm{H}_1 \to \mathrm{Z}\gamma) &= 0.89\,\mathrm{fb}, \\
\sigma \times \mathrm{Br}(\mathrm{H}_1 \to \mathrm{ZZ}) &= 0.14\,\mathrm{fb}.
\end{aligned} \tag{5.9}$$

For the second case, the $\sigma \times BR$ values for these decay channels for a benchmark point

($m_X = 1$ TeV and $u_3 = 180$ GeV) on the $\gamma\gamma$ exclusion line are given as:

$$\begin{aligned}
\sigma \times \mathrm{Br}(\mathrm{H}_1 \to \gamma\gamma) &= 1.5\,\mathrm{fb}, \\
\sigma \times \mathrm{Br}(\mathrm{H}_1 \to \mathrm{gg}) &= 409\,\mathrm{fb}, \\
\sigma \times \mathrm{Br}(\mathrm{H}_1 \to \mathrm{Z}\gamma) &= 0.89\,\mathrm{fb}, \\
\sigma \times \mathrm{Br}(\mathrm{H}_1 \to \mathrm{ZZ}) &= 0.14\,\mathrm{fb}, \\
\sigma \times \mathrm{Br}(\mathrm{H}_1 \to \chi_2\chi_2^*) &= 244\,\mathrm{fb}.
\end{aligned} \tag{5.10}$$

The constraints on the model parameter space coming from 8 TeV $\gamma\gamma$ channel exclusion limits are shown in Fig. 5.5 and Fig. 5.6.

Finally, before ending this section a brief discussion is done about the total decay width of H_1 for the two cases. In this model, if the H_1 decay to dark matter is kinematically forbidden, then the dominant decay channels will all be loop induced, with $H_1 \to gg$ being the most significant. In such a scenario, H_1 will be a narrow resonance with a total decay width only up to a GeV. However, if H_1 decay to dark matter is kinematically allowed then it can have significant invisible decay width owing to the fact that such a decay is not loop suppressed. In this case, the heavy scalar H_1 can be a broad resonance. If the LHC in the future run demands the heavy scalar to be a broad resonance, then for this model it will imply a significant invisible decay width. Depending on the value of κ_{χ_2}, H_1 can have decay width up to around 50 GeV. That happens for a small parameter range, because the $BR(H_1 \to \gamma\gamma)$ becomes insignificant at rest of the parameter points due to a large width of the scalar resonance. In such a case, a larger $\sigma \times BR$ can be obtained by adding a pair of $SU(2)_L$ singlet charged leptons to this model, which will improve the diphoton signal cross section. However, at this stage such an extension of this model is not necessary.

5.3 750 GeV Diphoton Excess

Previously observed 750 GeV diphoton excess had drawn significant attention, as it was explored as a hint of new physics at the LHC. The reports from the ICHEP conference [10, 11], after the analysis with more LHC data, indicate the diphoton excess to be a statistical fluctuation. Here, it is discussed how a BSM scalar in our work [13] can explain the previously seen excess.

The ATLAS and CMS collaborations at the LHC had reported an excess of events in the invariant mass distribution of two photons at $\sqrt{s} = 13$ TeV [111–113]. The ATLAS Collaboration [112], with 3.2 fb^{-1} data, had reported an excess of 3.9σ at diphoton invariant mass around 750 GeV. The significance was 2.3 σ once the Look Elsewhere Effect is included. That was translated to an excess in signal $\sigma(pp \to \gamma\gamma)$ of about 10 ± 3 fb, with a best fit width $\sim$ 45 GeV. The CMS collaboration had also found an excess in diphoton events with local significance 2.6σ [113] at $\sqrt{s} = 13$ TeV with 2.6 fb^{-1} data at a mass around 750 GeV. With the assumption of large width ($\sim$ 45 GeV), this significance reduced to 2.0σ. Corresponding excess in the signal cross section $\sigma(pp \to \gamma\gamma)$ was of about 6 ± 3 fb. These excess events did not have any significant missing energy, leptons or jets associated with them. No excess of events had been found in ZZ, WW, dilepton, dijet channels in the same invariant mass region. These were all the experimental details that one had to satisfy to explain the observed diphoton excess from a BSM particle decay. Although this excess has turned out to be a statistical fluctuation later, it had drawn significant attention as it was expected to be a possible new physics particle decay, with invariant diphoton mass around 750 GeV [114].

From the Landau-Yang theorem, a massive vector boson can not decay to two photons (see Refs. [115, 116]). So the excess which was previously observed at the LHC, cannot be attributed to the decay a spin-1 particle. If a resonance has to explain the excess, there remains the possibility of the particle being either a spin-0 or spin-2 particle. The BSM model scalar spectrum should have a 125 GeV Higgs boson with properties similar to

the resonance discovered earlier at the LHC. In this section, it is discussed how a heavy scalar in the gauged $B-L$ model [50] can generate a diphoton excess at 750 GeV similar to that observed before. Production channels and decay modes of the 750 GeV BSM scalar mimic the heavy scalar discussed above, with an important role of exotic fermions. The numerical results showing the allowed parameter space for both the cases where the resonance is either wide or narrow are presented. It is also discussed why there are no excesses observed in various other channels.

In this section, the numerical results are presented, showing the allowed parameter range that can explain the diphoton excess previously observed at the LHC. Allowed points are presented by the parameter region of mass and Yukawa couplings of the new quarks, X, Y. For this part, MadGraph5aMC@NLO [117] with NN23LO1 PDF set [118] is used to obtain the numerical estimates taking K factor of 1.5 into account for the NLO correction [119].

As mentioned before, since in this model the dark matter mass m_{χ_2} is not fixed, there arise two distinct possibilities; either $m_{\chi_2} > m_{H_1}/2$ or $m_{\chi_2} \leq m_{H_1}/2$. For the first case, H_1 decay to two dark matter particles is kinematically forbidden and the only prominent channels are its loop decays to $gg, \gamma\gamma$ as well as $\tan\theta_W$ suppressed loop decays to $Z\gamma$ and ZZ. In the second case, H_1 can also additionally decay to two dark matter particles. Both of these possibilities are analyzed below.

In the first case the only important decay modes for H_1 are $H_1 \to \gamma\gamma$ and $H_1 \to gg$ along with $H_1 \to Z\gamma$ and $H_1 \to ZZ$ both of which are θ_W suppressed. All of these decay modes are at loop level, going through triangle loops involving X, Y quarks. As g, γ and Z all couple to the quarks through gauge interactions, their interaction strengths are fixed, and are proportional to α_s, α, the strong and electromagnetic coupling constants respectively. Hence, for this case of our model the production and decay rate of H_1 depends on only two free parameters, the masses of X, Y quarks and the Yukawa coupling between H_1 and quarks. Moreover, since the quarks X, Y acquire mass through the vev of χ_3 so the Yukawa coupling can be equivalently replaced by the vev u_3 as a free

parameter. Fig. 5.5 shows the allowed ranges of the exotic quark masses and the value of the vev, $\langle \chi_3 \rangle = u_3$, that can explain the previously observed 750 GeV diphoton excess for both the CMS and ATLAS experiments within 95% confidence level. In obtaining

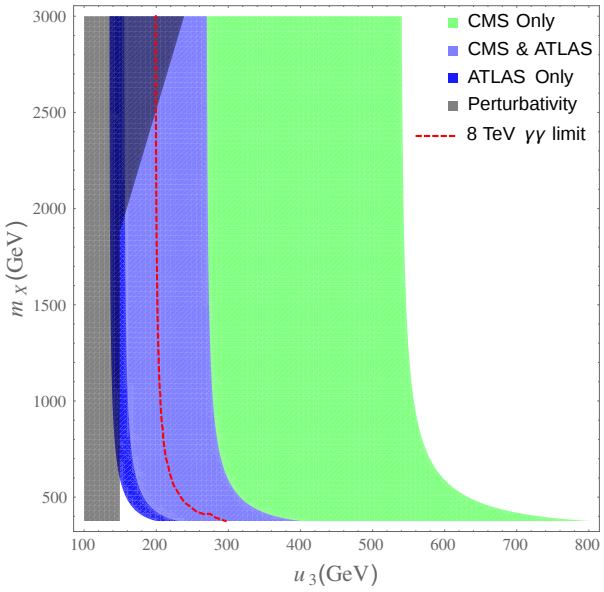

Figure 5.5: The allowed m_X - u_3 range corresponding to CMS (green), ATLAS (deep blue) and the overlap (light blue) ranges with 95% confidence level. Also, shown is the 95% confidence level $H_1 \to \gamma\gamma$ exclusion line (red dashed) from 8 TeV run with the regions on the left of the line being incompatible with it. The black shaded region is also excluded by the perturbativity constraints.

the numerical results, for simplicity it is assumed that the masses of the exotic quarks X, Y are degenerate i.e. $m_X = m_Y$ and they are treated as a single parameter m_X. In addition the perturbativity of all the couplings in our model is ensured. The region of the parameter space excluded due to non-perturbativity of the couplings is explicitly shown in Fig. 5.5.

Furthermore, in plotting Fig. 5.5 the 8 TeV exclusion limits are imposed for the 750 GeV scalar in all other channels. The strongest constraint from 8 TeV exclusion limits actually comes from non-observance of any statistically significant excess in the $\gamma\gamma$ decay channel. In Fig. 5.5 the dotted red line corresponds to the $\gamma\gamma$ exclusion limit of Eq. 5.8. The parameter space on the left of the red line is incompatible with the 8 TeV data.

As mentioned before, the scalar H_1 that is considered here, does not couple significantly to the SM fermions at tree level. Therefore the limits given in [120] can be easily satisfied.

The coupling H_1hh is also negligibly small and $\sigma(pp \to H_1 \to hh)$ is well under the experimental limit [121]. Moreover, the scalar is a EM charge neutral SU(2) singlet. Therefore, it does not have any tree level coupling to either W or Z bosons. As the newly added fermions are SU(2) singlets even the $H_1 \to WW$ decay through the triangle loop is not possible. However, it can couple to ZZ, $Z\gamma$ at loop level through triangle loop of the exotic fermions and it has to be taken into account. As clear from Eq. 5.9, for this case of our model, apart from the $\gamma\gamma$ decay channel, the constraints from all other decay channels are easily satisfied. Even for the $\gamma\gamma$ channel, our model has enough parameter space compatible with both the previously observed 13 TeV excess and the current 8 TeV constraints.

In the second case, in addition to the decay channels discussed in previous case, H_1 decay to dark matter is also kinematically allowed and it can have appreciable invisible decay width. Fig. 5.6 presents the allowed parameter range for the exotic quark masses and u_3, that can explain the observed diphoton excess within 95% confidence level. In plotting Fig. 5.6 the dark matter coupling with the scalar is taken as $\kappa_{\chi_2} = 0.5$ and have all the constraints from 8 TeV run listed in Eq. 5.8 are also imposed.

As evident from Eq. 5.10, like the previous case here also only the constraints from $\gamma\gamma$ channel for 8 TeV run are important. The constraints from all other channels are comfortably satisfied. Furthermore, just like the previous case, in this case also our model has enough parameter space compatible with both the previously observed 13 TeV excess and the current 8 TeV constraints. Thus, the 750 GeV diphoton excess seen earlier at the LHC can be understood in our model as the decay of H_1 to a pair of photons.

The first thing to note is that given the current low statistics, the estimates of decay width are very poor. This aspect is highlighted by the fact that while CMS data prefers narrow decay width of around a few GeV for the resonance, the ATLAS prefers a relatively broader resonance with decay width $\sim$ 45 GeV. Thus, the current estimates of decay width are highly uncertain and are likely to change significantly in the future runs.

The model was originally constructed to obtain Dirac neutrinos with naturally small

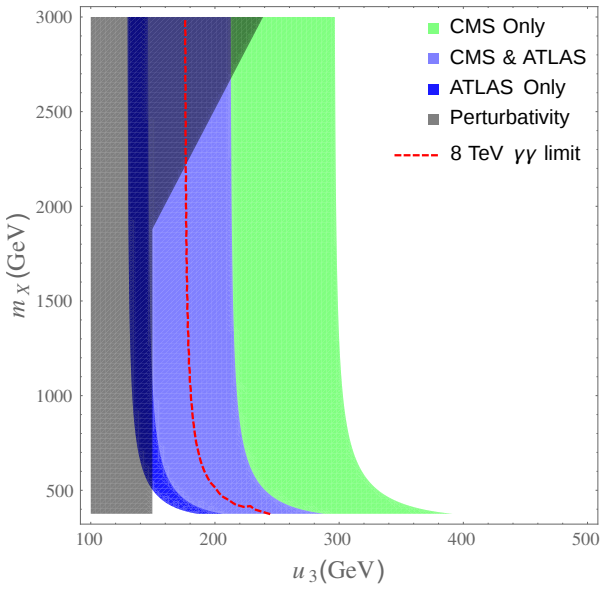

Figure 5.6: The allowed m_X - u_3 range (for $\kappa_{\chi_2} = 0.5$) corresponding to CMS (green), ATLAS (deep blue) and the overlap (light blue) ranges with 95% confidence level. Also, shown is the 95% confidence level $H_1 \to \gamma\gamma$ exclusion line (red dashed) from 8 TeV run with the regions on the left of the line being incompatible with it. The black shaded region is also excluded by the perturbativity constraints.

masses and also has a long lived dark matter particle. Unlike the conventional gauged $B - L$ symmetry model where the $B - L$ scale is expected to be quite high, being related with the seesaw scale, the $B - L$ scale can well be within the LHC range in our model , opening up the possibility of testing its various aspects at LHC. Thus to conclude, the gauged $B - L$ model considered here appears to be a promising candidate for new physics. It has all the right ingredients to explain not only the previously seen 750 GeV diphoton excess but all the other experimental results both for a proposed 750 GeV resonance as well as the 125 GeV Higgs. Moreover, the model also connects the observed new physics with the already well known and long standing problems of neutrino masses and dark matter and attempts to provide a unifying solution to all of them.

Chapter 6

Conclusion and Summary

This thesis deals with the effects of new fermions on the LHC phenomenology of some BSM scalars that arise in two models with symmetries extended beyond the SM: the $SU(6)/Sp(6)$ little Higgs (LSS) model and the gauged $U(1)_{B-L}$ model.

Chapter 1 is an introductory chapter where some theoretical shortcomings of the SM are briefly discussed to motivate the need for BSM physics that can explain some of the unanswered questions of the SM. Due to extension of symmetries beyond the SM, many BSM theories predict the existence of new heavy scalars along with heavy fermions near the TeV scale. In this thesis, the LHC phenomenology of two types of such new heavy scalars in presence of heavy fermions, namely the vector-like quarks (VLQ) are discussed.

In Chapter 2, various little Higgs models are reviewed briefly to show that they can provide a 2HDM structure with the VLFs. It is also discussed, how these models can address the gauge hierarchy problem of the SM, cancelling the quadratic divergent contributions at the one-loop level. To provide good understanding of these little Higgs models, 2HDM and VLF are briefly reviewed. The LSS model is described with a detailed discussion on the collective symmetry breaking in this model, to ensure the cancellation of one-loop quadratic divergent contribution to the Higgs mass. The gauge and Yukawa sector of the LSS model is also studied, showing in detail how the fermion mass matrices are diagonalized.

In Chapter 3, the phenomenological analysis of the LSS model described in Chapter 2 is carried out with an emphasis on studying BSM scalars at the LHC. Here, The 2HDM structure emerging at the LSS model is presented, pointing out the correlation of $m_A, m_{H^\pm}, s_{\beta-\alpha}$ etc.. All the free parameters are chosen and a scan is done over the nine dimesional parameter space. Both theoretical and experimental constraints are then applied to present the allowed parameter space. The constrained parameter space bears out the degeneracy of the BSM scalar masses, shows preference for low $\tan\beta$ region and satisfies the alignment limit almost fully. The gluon fusion production cross section of the neutral scalars are presented, pointing out the dominant contribution of the vector-like quarks in this mode. For the allowed points, different decay modes of neutral scalars and their branching ratios in those channels are presented. Various charged Higgs decays are also studied. Thus, in the LSS model discussed here, the presence of heavy BSM scalars can be probed in the current 13 TeV run of the LHC. The effects of vector-like fermions on the flavor sector of this model can be studied in the future.

Chapter 4 describes a BSM theory with its symmetry extended by a $U(1)_{B-L}$. Three right handed neutrinos with $B-L$ charges $4, 4, -5$ are introduced to construct Dirac mass terms for neutrinos. Two singlet scalars, χ_3 and χ_6 are required in order to spontaneously break the gauged $B-L$ symmetry as well as to obtain Dirac neutrinos with small masses. Another singlet scalar χ_2 is introduced to be the dark matter candidate. The $B-L$ charges of the new fermions are chosen to construct a model free from triangle anomalies. The scalar potential of the model is analyzed, forming a simplified mass matrix which is diagonalized to present CP-even scalar mass eigenstates.

Chapter 5 deals with the possibility that a the scalar particle H_1 can have enhanced decay into two photons. It also has a 125 GeV particle h which has almost the SM Higgs-like couplings to the other SM particles and satisfies all the other experimental constraints for the 125 GeV scalar. A heavy scalar of mass 750 GeV is chosen, exploring its production and decay channels. The effects of the exotic fermions in the gluon fusion production is studied, pointing out the enhanced diphoton decay due to these fermions. It is shown

how the model satisfies all the current experimental constraints like non-observation of any excess in dilepton, dijet, diboson and invisible channels. The total width of the heavy scalar in this model can vary from small (~ 1 GeV) to large (~ 50 GeV) values.

Moreover, the model also connects the observed new physics with the already well known and long standing issues related to neutrino masses and dark matter and attempts to provide a unifying solution to all of them. Thus, the gauged $B - L$ model considered here appears to be a viable candidate for new physics. Also, it has several testable predictions like existence of heavier particles in ~ 1 TeV range which can be probed in current and future run of the LHC. The presence of a dark matter candidate in this model can also be probed in dark matter direct detection experiments.

Appendix A

BSM Scalar in Model Independent Framework

An effective Lagrangian with couplings of the neutral scalars, CP-odd A and CP-even h, H to SM gauge bosons and fermions is described here. The neutral scalars are collectively written as ϕ. In models like 2HDM that contain two CP-even scalars, the lighter one (h) is taken as the 125 GeV scalar observed at the LHC. For any given new physics model, effective Lagrangian can be obtained by integrating out heavier fields, following which the observables of that model can be expressed using the effective couplings defined in this part.

CP invariance requires the CP-odd scalar A coupling to SM gauge bosons to be only via higher dimensional operators. The CP-even scalars can couple to the massive gauge bosons at tree level. Showing only the new physics terms, the effective Lagrangian for any neutral scalar ϕ is

$$\begin{aligned}\mathcal{L}_{eff} = &\frac{1}{2}\partial_\mu\phi\partial^\mu\phi - \frac{1}{2}m_\phi^2\phi^2 - y_{\phi f_i f_i}\phi\bar{f}_i X f_i + y_{\phi WW}\phi W^\mu W_\mu + y_{\phi ZZ}\phi Z^\mu Z_\mu \\ &- \frac{1}{64\pi^2 M}\kappa_{\phi\gamma\gamma}\phi Y_{\mu\nu\sigma\tau}F^{\sigma\tau}F^{\mu\nu} - \frac{1}{32\pi^2 M}\kappa_{\phi\gamma Z}\phi Y_{\mu\nu\sigma\tau}F^{\sigma\tau}Z^{\mu\nu} - \frac{1}{64\pi^2 M}\kappa_{\phi gg}\phi Y_{\mu\nu\sigma\tau}G^{\sigma\tau}G^{\mu\nu} \\ &- \frac{1}{64\pi^2 M}\kappa_{\phi ZZ}\phi Y_{\mu\nu\sigma\tau}Z^{\sigma\tau}Z^{\mu\nu} - \frac{1}{32\pi^2 M}\kappa_{\phi WW}\phi Y_{\mu\nu\sigma\tau}W^{\sigma\tau}W^{\mu\nu},\end{aligned} \tag{A.1}$$

where $X = \gamma_5, Y_{\mu\nu\sigma\tau} = \epsilon_{\mu\nu\sigma\tau}$ for the CP-odd scalar, while $X = I$ (identity matrix), $Y_{\mu\nu\sigma\tau} = g_{\mu\sigma}g_{\nu\tau}$ for the CP-even scalar. Here $\kappa_{\phi ij}$ s contain other fermion and gauge boson loop contributions. Tree level scalar gauge boson couplings $y_{\phi ZZ}, y_{\phi WW}$ are zero for the A. The dimensionless effective couplings κ are created by pulling out a new-physics mass-scale M which is set as 1 TeV for numerical results. Although the effective couplings κ are defined by extracting a heavy new-physics mass scale M, SM fermion contributions are to be included when present. If SM fermions contribute and can go onshell, the κ are complex. In that case, the $\kappa_{\phi VV}$ that appear in this section should be read as $|\kappa_{\phi VV}|$. Eq. (A.1) is an effective Lagrangian at a scale just above m_ϕ.

The one-loop expressions for the ϕgg amplitudes $\kappa_{\phi gg}$, with $\phi = \{H, A\}$, as defined in Ref. [61] are given here. Defining $r_f = m_f^2/m_\phi^2$ and with f running over all colored fermion species with mass m_f and real Yukawa couplings $y_{\phi ff}$, and with the electric charge of the fermion (f) denoted by Q_f, the general expressions for $\kappa_{\phi gg}$ and $\kappa_{\phi\gamma\gamma}$ are given as

$$\begin{aligned} \kappa_{\phi gg} &= g_s^2 \sum_f y_{\phi ff} \frac{M}{m_f} F_{1/2}^{(1)}(r_f) \ , \\ \text{with} \quad F_{1/2}^{(1)}(r_f) &= 4 r_f \left(\int_0^1 dy \int_0^{1-y} dx \frac{g(x,y)}{(r_f - xy)} \right) \ , \end{aligned} \tag{A.2}$$

with $g(x, y) = (1 - 4xy)$ for the CP-even scalars (h, H) and 1 for the CP-odd scalar (A). These expressions are used for the LSS model discussed in the text.

Appendix B

Allowed Points

Nine representative points in the allowed parameter space are given in Table. B.1 and in Table. B.2.

Table B.1: The allowed parameter space after electroweak precision constraints.

Parameter	Pt-1	Pt-2	Pt-3	Pt-4	Pt-5	Pt-6	Pt-7	Pt-8	Pt-9
f	633.5	799.8	1096	1133	1133	1161	1207	1403	1429
g_1	0.657	0.655	0.688	0.901	0.851	0.675	0.852	0.679	0.705
$g_1^{'}$	0.567	2.869	1.6	2.809	1.448	1.23	1.449	1.161	1.376
y_1	1.985	2.774	1.664	2.276	1.568	2.305	1.583	2.763	2.607
y_2	1.342	1.422	1.199	1.343	1.257	1.475	1.271	2.525	2.82
y_3	2.372	1.964	2.691	2.082	2.391	2.027	2.393	2.113	2.234
y_4	0.165	0.358	0.843	0.533	0.798	0.485	0.800	1.64	2.048
y_5	2.076	1.185	2.706	1.977	2.602	1.887	2.612	1.464	1.507
c	1.33	1.325	1.51	0.775	0.805	1.169	0.808	1.587	1.558
c'	1.771	2.579	2.246	2.46	2.172	1.596	2.173	2.681	2.504
g_2	6.864	10.9	2.106	0.949	1.021	2.634	1.018	2.395	1.742
g_2'	0.465	0.363	0.369	0.363	0.371	0.376	0.371	0.378	0.373
t_β	0.73	0.73	0.6	0.74	0.95	0.88	0.97	1.79	1.9
λ_5'	0.568	0.566	0.666	0.561	0.513	0.509	0.517	0.713	0.751
M_s	5163	10220	3573	2719	2496	4039	2681	7283	7202
$M_{W'}$	3089	6177	1716	1048	1065	2231	1133	2470	1898
$M_{B'}$	328.6	1636	1272	2269	1198	1056	1276	1212	1440
m_h	124.8	124.7	124.7	124.5	124.4	124.1	125	125	124.1
m_H	1111	1666	1445	1901	1284	2020	1386	2075	1309
m_A	1118	1671	1450	1905	1290	2024	1392	2079	1315
$m_{H^\pm}$	1111	1666	1443	1901	1284	2020	1386	2074	1307
m_t	166.4	159.2	161.1	159.1	158.4	159.7	159.4	163.3	162.7

Table B.2: The allowed parameter space after electroweak precision constraints.

Parameter	Pt-1	Pt-2	Pt-3	Pt-4	Pt-5	Pt-6	Pt-7	Pt-8	Pt-9
M_{t2}	1218	2376	2037	2537	1987	2626	2134	4402	4707
M_{t3}	1794	1823	3246	2935	3078	3036	3287	4748	5191
M_{b2}	1315	947.5	2965	2239	2949	2190	3152	2055	2153
M_{b3}	1727	1928	3228	2806	3061	2910	3271	4620	5141
κ_{htt}	-1.007	-0.987	-1.011	-0.98	-0.969	-0.977	-0.974	-0.998	-1.011
$s_{\beta-\alpha}$	-1	-1	-1	-1	-1	-1	-1	-1	-1

Bibliography

[1] G. Aad *et al.* [ATLAS Collaboration], Phys. Lett. B **716**, 1 (2012) [arXiv:1207.7214 [hep-ex]].

[2] S. Chatrchyan *et al.* [CMS Collaboration], Phys. Lett. B **716**, 30 (2012) [arXiv:1207.7235 [hep-ex]].

[3] G. 't Hooft, NATO Adv. Study Inst. Ser. B Phys. **59**, 135 (1980).

[4] R. K. Kaul, arXiv:0803.0381 [hep-ph];

[5] G. Bhattacharyya, Rept. Prog. Phys. **74**, 026201 (2011) [arXiv:0910.5095 [hep-ph]].

[6] R. N. Mohapatra and J. W. F. Valle, Phys. Rev. D **34**, 1642 (1986). doi:10.1103/PhysRevD.34.1642

[7] V. A. Kuzmin, V. A. Rubakov and M. E. Shaposhnikov, Phys. Lett. B **155**, 36 (1985). doi:10.1016/0370-2693(85)91028-7

[8] The ATLAS collaboration, ATLAS-CONF-2015-081.

[9] CMS Collaboration [CMS Collaboration], CMS-PAS-EXO-15-004.

[10] The ATLAS collaboration [ATLAS Collaboration], ATLAS-CONF-2016-059.

[11] CMS Collaboration [CMS Collaboration], CMS-PAS-EXO-16-027.

[12] S. Gopalakrishna, T. S. Mukherjee and S. Sadhukhan, Phys. Rev. D **94**, no. 1, 015034 (2016) doi:10.1103/PhysRevD.94.015034 [arXiv:1512.05731 [hep-ph]].

[13] T. Modak, S. Sadhukhan and R. Srivastava, Phys. Lett. B **756**, 405 (2016) arXiv:1601.00836 [hep-ph].

[14] H. Georgi and S. L. Glashow, Phys. Rev. Lett. **32**, 438 (1974). doi:10.1103/PhysRevLett.32.438

[15] H. Georgi, H. R. Quinn and S. Weinberg, Phys. Rev. Lett. **33**, 451 (1974). doi:10.1103/PhysRevLett.33.451

[16] A. J. Buras, J. R. Ellis, M. K. Gaillard and D. V. Nanopoulos, Nucl. Phys. B **135**, 66 (1978). doi:10.1016/0550-3213(78)90214-6

[17] N. Arkani-Hamed, A. G. Cohen and H. Georgi, Phys. Lett. B **513**, 232 (2001) [hep-ph/0105239].

[18] M. Schmaltz and D. Tucker-Smith, Ann. Rev. Nucl. Part. Sci. **55**, 229 (2005) [hep-ph/0502182].

[19] M. Perelstein, Prog. Part. Nucl. Phys. **58**, 247 (2007) [hep-ph/0512128].

[20] G. Senjanovic and R. N. Mohapatra, Phys. Rev. D **12**, 1502 (1975). doi:10.1103/PhysRevD.12.1502

[21] A. Maiezza, M. Nemevsek, F. Nesti and G. Senjanovic, Phys. Rev. D **82**, 055022 (2010) doi:10.1103/PhysRevD.82.055022 [arXiv:1005.5160 [hep-ph]].

[22] N. G. Deshpande, J. F. Gunion, B. Kayser and F. I. Olness, Phys. Rev. D **44**, 837 (1991). doi:10.1103/PhysRevD.44.837

[23] W. A. Ponce, Y. Giraldo and L. A. Sanchez, Phys. Rev. D **67**, 075001 (2003) doi:10.1103/PhysRevD.67.075001 [hep-ph/0210026].

[24] J. C. Montero, V. Pleitez and M. C. Rodriguez, Phys. Rev. D **65**, 035006 (2002) doi:10.1103/PhysRevD.65.035006 [hep-ph/0012178].

[25] A. G. Dias, C. A. de S.Pires and P. S. Rodrigues da Silva, Phys. Lett. B **628**, 85 (2005) doi:10.1016/j.physletb.2005.09.028 [hep-ph/0508186].

[26] P. V. Dong, D. T. Huong, F. S. Queiroz and N. T. Thuy, Phys. Rev. D **90**, no. 7, 075021 (2014) doi:10.1103/PhysRevD.90.075021 [arXiv:1405.2591 [hep-ph]].

[27] M. Carena, A. Daleo, B. A. Dobrescu and T. M. P. Tait, Phys. Rev. D **70**, 093009 (2004) doi:10.1103/PhysRevD.70.093009 [hep-ph/0408098].

[28] S. Iso, N. Okada and Y. Orikasa, Phys. Rev. D **80**, 115007 (2009) doi:10.1103/PhysRevD.80.115007 [arXiv:0909.0128 [hep-ph]].

[29] T. Appelquist, B. A. Dobrescu and A. R. Hopper, Phys. Rev. D **68**, 035012 (2003) doi:10.1103/PhysRevD.68.035012 [hep-ph/0212073].

[30] L. Basso, A. Belyaev, S. Moretti and C. H. Shepherd-Themistocleous, Phys. Rev. D **80**, 055030 (2009) doi:10.1103/PhysRevD.80.055030 [arXiv:0812.4313 [hep-ph]].

[31] I. Low, W. Skiba and D. Tucker-Smith, Phys. Rev. D **66**, 072001 (2002) [hep-ph/0207243].

[32] N. Arkani-Hamed, A. G. Cohen, E. Katz and A. E. Nelson, JHEP **0207**, 034 (2002) [hep-ph/0206021].

[33] H. C. Cheng and I. Low, JHEP **0408**, 061 (2004) [hep-ph/0405243].

[34] I. Low, JHEP **0410**, 067 (2004) [hep-ph/0409025].

[35] S. Chang, JHEP **0312**, 057 (2003) doi:10.1088/1126-6708/2003/12/057 [hep-ph/0306034].

[36] C. Csaki, J. Hubisz, G. D. Kribs, P. Meade and J. Terning, Phys. Rev. D **68**, 035009 (2003) doi:10.1103/PhysRevD.68.035009 [hep-ph/0303236].

[37] D. E. Kaplan and M. Schmaltz, JHEP **0310**, 039 (2003) [hep-ph/0302049].

[38] J. Reuter and M. Tonini, JHEP **1302**, 077 (2013) doi:10.1007/JHEP02(2013)077 [arXiv:1212.5930 [hep-ph]];

[39] J. Reuter, M. Tonini and M. de Vries, JHEP **1402**, 053 (2014) doi:10.1007/JHEP02(2014)053 [arXiv:1310.2918 [hep-ph]];

[40] X. F. Han, L. Wang, J. M. Yang and J. Zhu, Phys. Rev. D **87**, no. 5, 055004 (2013) doi:10.1103/PhysRevD.87.055004 [arXiv:1301.0090];

[41] P. Kalyniak, T. Martin and K. Moats, Phys. Rev. D **91**, no. 1, 013010 (2015) doi:10.1103/PhysRevD.91.013010 [arXiv:1310.5130 [hep-ph]];

[42] C. Han, A. Kobakhidze, N. Liu, L. Wu and B. Yang, Nucl. Phys. B **890**, 388 (2014) doi:10.1016/j.nuclphysb.2014.11.021 [arXiv:1405.1498 [hep-ph]];

[43] J. Berger, J. Hubisz and M. Perelstein, JHEP **1207**, 016 (2012) doi:10.1007/JHEP07(2012)016 [arXiv:1205.0013 [hep-ph]];

[44] J. L. Hewett, F. J. Petriello and T. G. Rizzo, JHEP **0310**, 062 (2003) doi:10.1088/1126-6708/2003/10/062 [hep-ph/0211218].

[45] C. Csaki, J. Hubisz, G. D. Kribs, P. Meade and J. Terning, Phys. Rev. D **67**, 115002 (2003) doi:10.1103/PhysRevD.67.115002 [hep-ph/0211124].

[46] T. Han, H. E. Logan, B. McElrath and L. T. Wang, Phys. Rev. D **67**, 095004 (2003) doi:10.1103/PhysRevD.67.095004 [hep-ph/0301040];

[47] T. Han, H. E. Logan and L. T. Wang, JHEP **0601**, 099 (2006) doi:10.1088/1126-6708/2006/01/099 [hep-ph/0506313];

[48] J. Hubisz and P. Meade, Phys. Rev. D **71**, 035016 (2005) doi:10.1103/PhysRevD.71.035016 [hep-ph/0411264];

[49] E. Ma and R. Srivastava, Mod. Phys. Lett. A **30**, no. 26, 1530020 (2015) doi:10.1142/S0217732315300207 [arXiv:1504.00111 [hep-ph]].

[50] E. Ma and R. Srivastava, Phys. Lett. B **741**, 217 (2015) arXiv:1411.5042 [hep-ph].

[51] S. Kanemura, T. Nabeshima and H. Sugiyama, Phys. Rev. D **85**, 033004 (2012) doi:10.1103/PhysRevD.85.033004 [arXiv:1111.0599 [hep-ph]].

[52] S. Kanemura, T. Matsui and H. Sugiyama, Phys. Rev. D **90**, 013001 (2014) doi:10.1103/PhysRevD.90.013001 [arXiv:1405.1935 [hep-ph]].

[53] S. Khalil, Phys. Rev. D **82**, 077702 (2010) doi:10.1103/PhysRevD.82.077702 [arXiv:1004.0013 [hep-ph]].

[54] S. Iso, N. Okada and Y. Orikasa, Phys. Lett. B **676**, 81 (2009) doi:10.1016/j.physletb.2009.04.046 [arXiv:0902.4050 [hep-ph]].

[55] L. Basso, arXiv:1106.4462 [hep-ph].

[56] K. Huitu, S. Khalil, H. Okada and S. K. Rai, Phys. Rev. Lett. **101**, 181802 (2008) doi:10.1103/PhysRevLett.101.181802 [arXiv:0803.2799 [hep-ph]].

[57] R. Contino, arXiv:1005.4269 [hep-ph].

[58] H. Davoudiasl, S. Gopalakrishna, E. Ponton and J. Santiago, New J. Phys. **12**, 075011 (2010) [arXiv:0908.1968 [hep-ph]].

[59] H. C. Cheng and I. Low, JHEP **0309**, 051 (2003) [hep-ph/0308199].

[60] N. Arkani-Hamed, A. G. Cohen, E. Katz, A. E. Nelson, T. Gregoire and J. G. Wacker, JHEP **0208**, 021 (2002) [hep-ph/0206020].

[61] S. Gopalakrishna, T. S. Mukherjee and S. Sadhukhan, Phys. Rev. D **93**, no. 5, 055004 (2016) doi:10.1103/PhysRevD.93.055004 [arXiv:1504.01074 [hep-ph]].

[62] S. L. Glashow and S. Weinberg, Phys. Rev. D **15**, 1958 (1977).

[63] G. C. Branco, P. M. Ferreira, L. Lavoura, M. N. Rebelo, M. Sher and J. P. Silva, Phys. Rept. **516**, 1 (2012) [arXiv:1106.0034 [hep-ph]].

[64] B. Dumont, J. F. Gunion, Y. Jiang and S. Kraml, arXiv:1409.4088 [hep-ph].

[65] B. Dumont, J. F. Gunion, Y. Jiang and S. Kraml, Phys. Rev. D **90**, 035021 (2014) [arXiv:1405.3584 [hep-ph]].

[66] S. Chatrchyan *et al.* [CMS Collaboration], Eur. Phys. J. C **73**, 2469 (2013) doi:10.1140/epjc/s10052-013-2469-8 [arXiv:1304.0213 [hep-ex]].

[67] A. Djouadi, Phys. Rept. **459**, 1 (2008) doi:10.1016/j.physrep.2007.10.005 [hep-ph/0503173].

[68] B. Dumont, J. F. Gunion, Y. Jiang and S. Kraml, Phys. Rev. D **90**, 035021 (2014) doi:10.1103/PhysRevD.90.035021 [arXiv:1405.3584 [hep-ph]]; B. Dumont, J. F. Gunion, Y. Jiang and S. Kraml, arXiv:1409.4088 [hep-ph]; A. Broggio, E. J. Chun, M. Passera, K. M. Patel and S. K. Vempati, JHEP **1411**, 058 (2014) doi:10.1007/JHEP11(2014)058 [arXiv:1409.3199 [hep-ph]].

[69] A. Djouadi and A. Lenz, Phys. Lett. B **715**, 310 (2012) doi:10.1016/j.physletb.2012.07.060 [arXiv:1204.1252 [hep-ph]].

[70] S. Dawson and E. Furlan, Phys. Rev. D **86**, 015021 (2012) [arXiv:1205.4733 [hep-ph]].

[71] N. Vignaroli, JHEP **1207**, 158 (2012) doi:10.1007/JHEP07(2012)158 [arXiv:1204.0468 [hep-ph]].

[72] A. De Simone, O. Matsedonskyi, R. Rattazzi and A. Wulzer, JHEP **1304**, 004 (2013) doi:10.1007/JHEP04(2013)004 [arXiv:1211.5663 [hep-ph]].

[73] P. W. Graham, A. Ismail, S. Rajendran and P. Saraswat, Phys. Rev. D **81**, 055016 (2010) doi:10.1103/PhysRevD.81.055016 [arXiv:0910.3020 [hep-ph]].

[74] S. P. Martin, Phys. Rev. D **82**, 055019 (2010) doi:10.1103/PhysRevD.82.055019 [arXiv:1006.4186 [hep-ph]].

[75] S. Gopalakrishna, T. Mandal, S. Mitra and R. Tibrewala, Phys. Rev. D **84**, 055001 (2011) [arXiv:1107.4306 [hep-ph]].

[76] S. Gopalakrishna, T. Mandal, S. Mitra and G. Moreau, JHEP **1408**, 079 (2014) [arXiv:1306.2656 [hep-ph]].

[77] S. A. R. Ellis, R. M. Godbole, S. Gopalakrishna and J. D. Wells, JHEP **1409**, 130 (2014) [arXiv:1404.4398 [hep-ph]].

[78] K. Agashe, H. Davoudiasl, S. Gopalakrishna, T. Han, G. Y. Huang, G. Perez, Z. G. Si and A. Soni, Phys. Rev. D **76**, 115015 (2007) doi:10.1103/PhysRevD.76.115015 [arXiv:0709.0007 [hep-ph]];

[79] K. Agashe, S. Gopalakrishna, T. Han, G. Y. Huang and A. Soni, Phys. Rev. D **80**, 075007 (2009) doi:10.1103/PhysRevD.80.075007 [arXiv:0810.1497 [hep-ph]];

[80] S. Gopalakrishna, T. Han, I. Lewis, Z. g. Si and Y. F. Zhou, Phys. Rev. D **82**, 115020 (2010) doi:10.1103/PhysRevD.82.115020 [arXiv:1008.3508 [hep-ph]].

[81] S. Alekhin, A. Djouadi and S. Moch, Phys. Lett. B **716**, 214 (2012) [arXiv:1207.0980 [hep-ph]].

[82] G. Aad *et al.* [ATLAS and CMS Collaborations], Phys. Rev. Lett. **114**, 191803 (2015) [arXiv:1503.07589 [hep-ex]].

[83] The ATLAS and CMS Collaborations, ATLAS-CONF-2015-044.

[84] The ATLAS collaboration [ATLAS Collaboration], ATLAS-CONF-2013-056.

[85] The ATLAS collaboration [ATLAS Collaboration], ATLAS-CONF-2013-060.

[86] J. F. Gunion and H. E. Haber, Phys. Rev. D **67**, 075019 (2003) [hep-ph/0207010].

[87] G. Bhattacharyya and D. Das, arXiv:1507.06424 [hep-ph].

[88] T. Gregoire, D. Tucker-Smith and J. G. Wacker, Phys. Rev. D **69**, 115008 (2004) [hep-ph/0305275].

[89] Z. Han and W. Skiba, Phys. Rev. D **72**, 035005 (2005) [hep-ph/0506206].

[90] A. Crivellin, A. Kokulu and C. Greub, Phys. Rev. D **87**, no. 9, 094031 (2013) doi:10.1103/PhysRevD.87.094031 [arXiv:1303.5877 [hep-ph]].

[91] J. F. Gunion, H. E. Haber, G. L. Kane and S. Dawson, Front. Phys. **80**, 1 (2000).

[92] G. Aad *et al.* [ATLAS Collaboration], JHEP **1503**, 088 (2015) doi:10.1007/JHEP03(2015)088 [arXiv:1412.6663 [hep-ex]].

[93] V. Khachatryan *et al.* [CMS Collaboration], JHEP **1511**, 018 (2015) doi:10.1007/JHEP11(2015)018 [arXiv:1508.07774 [hep-ex]]; G. Aad *et al.* [ATLAS Collaboration], arXiv:1512.03704 [hep-ex].

[94] L. Basso, A. Lipniacka, F. Mahmoudi, S. Moretti, P. Osland, G. M. Pruna and M. Purmohammadi, JHEP **1211**, 011 (2012) doi:10.1007/JHEP11(2012)011 [arXiv:1205.6569 [hep-ph]].

[95] J. Hernandez-Sanchez, S. Moretti, R. Noriega-Papaqui and A. Rosado, JHEP **1307**, 044 (2013) doi:10.1007/JHEP07(2013)044 [arXiv:1212.6818];

[96] R. Barbieri and G. F. Giudice, Nucl. Phys. B **306**, 63 (1988).

[97] J. C. Montero and V. Pleitez, Phys. Lett. B **675**, 64 (2009) doi:10.1016/j.physletb.2009.03.065 [arXiv:0706.0473 [hep-ph]].

[98] A. Davidson, Phys. Rev. D **20**, 776 (1979). doi:10.1103/PhysRevD.20.776

[99] R. E. Marshak and R. N. Mohapatra, Phys. Lett. B **91**, 222 (1980). doi:10.1016/0370-2693(80)90436-0

[100] M. Auger *et al.* [EXO-200 Collaboration], Phys. Rev. Lett. **109**, 032505 (2012) doi:10.1103/PhysRevLett.109.032505 [arXiv:1205.5608 [hep-ex]].

[101] M. Agostini *et al.* [GERDA Collaboration], Phys. Rev. Lett. **111**, no. 12, 122503 (2013) doi:10.1103/PhysRevLett.111.122503 [arXiv:1307.4720 [nucl-ex]].

[102] A. Gando *et al.* [KamLAND-Zen Collaboration], Phys. Rev. Lett. **110**, no. 6, 062502 (2013) doi:10.1103/PhysRevLett.110.062502 [arXiv:1211.3863 [hep-ex]].

[103] A. C. B. Machado and V. Pleitez, Phys. Lett. B **698**, 128 (2011) doi:10.1016/j.physletb.2011.02.051 [arXiv:1008.4572 [hep-ph]].

[104] A. C. B. Machado and V. Pleitez, J. Phys. G **40**, 035002 (2013) doi:10.1088/0954-3899/40/3/035002 [arXiv:1105.6064 [hep-ph]].

[105] P. Roy and O. U. Shanker, Phys. Rev. Lett. **52**, 713 (1984) Erratum: [Phys. Rev. Lett. **52**, 2190 (1984)] doi:10.1103/PhysRevLett.52.713.

[106] E. Ma, N. Pollard, R. Srivastava and M. Zakeri, Phys. Lett. B **750**, 135 (2015) [arXiv:1507.03943 [hep-ph]].

[107] D. S. Akerib *et al.* [LUX Collaboration], Phys. Rev. Lett. **112**, 091303 (2014) [arXiv:1310.8214 [astro-ph.CO]].

[108] G. Aad *et al.* [ATLAS Collaboration], arXiv:1507.04548 [hep-ex].

[109] R. Franceschini *et al.*, arXiv:1512.04933 [hep-ph].

[110] G. Aad *et al.* [ATLAS Collaboration], Phys. Lett. B **738**, 428 (2014) [arXiv:1407.8150 [hep-ex]]; G. Aad *et al.* [ATLAS Collaboration], arXiv:1507.05930 [hep-ex]; G. Aad *et al.* [ATLAS Collaboration], arXiv:1509.00389 [hep-ex]; V. Khachatryan *et al.* [CMS Collaboration], Eur. Phys. J. C **75**, no. 5, 235 (2015) [arXiv:1408.3583 [hep-ex]];
G. Aad *et al.* [ATLAS Collaboration], Phys. Rev. D **91**, no. 5, 052007 (2015) [arXiv:1407.1376 [hep-ex]];
CMS Collaboration [CMS Collaboration], CMS-PAS-EXO-14-005.

[111] ATLAS and CMS physics results from Run 2, talks by Marumi Kado and Jim Olsen, CERN, 15 December 2015

[112] ATLAS Collaboration, Search for resonances decaying to photon pairs in 3.2 fb^{-1} of pp collisions at $\sqrt{s} = 13$ TeV with the ATLAS detector, ATLAS-CONF-2015-081

[113] CMS Collaboration, Search for new physics in high mass diphoton events in proton-proton collisions at 13 TeV, CMS-PAS-EXO-15-004

[114] E. Ma, arXiv:1512.09159 [hep-ph]; E. Ma, arXiv:1601.01400 [hep-ph]; S. Gopalakrishna, T. S. Mukherjee and S. Sadhukhan, arXiv:1504.01074 [hep-ph]; S. Gopalakrishna, T. S. Mukherjee and S. Sadhukhan, arXiv:1512.05731 [hep-ph]; Y. Mambrini, G. Arcadi and A. Djouadi, arXiv:1512.04913 [hep-ph]; O. Antipin, M. Mojaza and F. Sannino, arXiv:1512.06708 [hep-ph]; S. K. Kang and J. Song, arXiv:1512.08963 [hep-ph]; K. Harigaya and Y. Nomura, arXiv:1512.04850 [hep-ph]; J. Ellis, S. A. R. Ellis, J. Quevillon, V. Sanz and T. You, arXiv:1512.05327 [hep-ph]; Y. Jiang, Y. Y. Li and T. Liu, arXiv:1512.09127 [hep-ph]; Y. J. Zhang, B. B. Zhou and J. J. Sun, arXiv:1602.05539 [hep-ph]; U. K. Dey, S. Mohanty and G. Tomar, arXiv:1512.07212 [hep-ph]; A. Angelescu, A. Djouadi and G. Moreau, arXiv:1512.04921 [hep-ph]; B. Dutta, Y. Gao, T. Ghosh, I. Gogoladze and T. Li, arXiv:1512.05439 [hep-ph]; S. Ghosh, A. Kundu and S. Ray, arXiv:1512.05786 [hep-ph]; M. Bauer and M. Neubert, arXiv:1512.06828 [hep-ph]; D. Bardhan, D. Bhatia, A. Chakraborty, U. Maitra, S. Raychaudhuri and T. Samui, arXiv:1512.06674 [hep-ph]; S. Chakraborty, A. Chakraborty and S. Raychaudhuri, arXiv:1512.07527 [hep-ph]; S. Kanemura, N. Machida, S. Odori and T. Shindou, arXiv:1512.09053 [hep-ph]; K. Das and S. K. Rai, arXiv:1512.07789 [hep-ph]; A. E. C. Hernandez and I. Nisandzic, arXiv:1512.07165 [hep-ph]; R. Benbrik, C. H. Chen and T. Nomura, arXiv:1512.06028 [hep-ph]; A. Falkowski, O. Slone and T. Volansky, arXiv:1512.05777 [hep-ph]; H. Han, S. Wang and S. Zheng, arXiv:1512.07992 [hep-ph]; A. Ahmed, B. M. Dillon, B. Grzadkowski, J. F. Gunion and Y. Jiang, arXiv:1512.05771 [hep-ph]; W. C. Huang, Y. L. S. Tsai and T. C. Yuan, arXiv:1512.07268 [hep-ph]; A. E. C. HernÃąndez, arXiv:1512.09092 [hep-ph]; Y. Nakai, R. Sato and K. Tobioka, arXiv:1512.04924

[hep-ph]; X. F. Han, L. Wang, L. Wu, J. M. Yang and M. Zhang, arXiv:1601.00534 [hep-ph]; F. Wang, W. Wang, L. Wu, J. M. Yang and M. Zhang, arXiv:1512.08434 [hep-ph]; P. S. B. Dev, R. N. Mohapatra and Y. Zhang, arXiv:1512.08507 [hep-ph];

[115] L. D. Landau, Dokl. Akad. Nauk Ser. Fiz. **60**, 207 (1948).

[116] C. -N. Yang, Phys. Rev. **77**, 242 (1950).

[117] J. Alwall *et al.*, JHEP **1407**, 079 (2014) [arXiv:1405.0301 [hep-ph]].

[118] R. D. Ball *et al.* [NNPDF Collaboration], Nucl. Phys. B **877**, 290 (2013) [arXiv:1308.0598 [hep-ph]].

[119] J. M. Cline and Z. Liu, arXiv:1512.06827 [hep-ph].

[120] G. Aad *et al.* [ATLAS Collaboration], Phys. Rev. D **90**, no. 5, 052005 (2014) [arXiv:1405.4123 [hep-ex]]; G. Aad *et al.* [ATLAS Collaboration], JHEP **1411**, 056 (2014) [arXiv:1409.6064 [hep-ex]]; S. Chatrchyan *et al.* [CMS Collaboration], [arXiv:1309.2030 [hep-ex]];

[121] The ATLAS collaboration [ATLAS Collaboration], ATLAS-CONF-2014-005.